

# **44th Condensed Matter and Materials Meeting**



Holiday Inn, Rotorua, New Zealand  
4-7 February 2020



## Organizing Committee

Dr Philip Brydon, University of Otago (chair)

Prof. Tilo Söhnel, University of Auckland

Dr Ben Mallett, University of Auckland

# Contents

Sponsors .....	3
General Information .....	4
Program at a glance .....	5
Program .....	6
Posters .....	10
Memories of Wagga 2014 .....	13
Talk Abstracts .....	14
Poster Abstracts .....	55
Participant List .....	89

# Sponsors

We gratefully acknowledge the support of the following:



## General Information

### **Scientific program:**

The conference will take place at the Holiday Inn Rotorua. All lectures will be held in the Totara room. Session chairs and speakers are asked to adhere closely to the schedule for the oral program. A laptop, data projector, laser pointer and microphone will be available. Please check as early as possible the compatibility with the computer facilities provided. Posters should be mounted on Tuesday evening or Wednesday morning in the allocated space in the Kauri room (please refer to the number of your poster). Please remove all posters by Thursday night or Friday morning.

### **Administration:**

Please wear your name tag at all times. Registration desk will be open from 3pm - 7pm on Tuesday for delegate registration and other matters regarding the conference. Questions or problems regarding the accommodation, please contact the hotel reception. Wireless internet access is available in the hotel. Please make sure to pay for any additional costs charged by you on your room number before your departure.

### **Meals and refreshments:**

Lunch and dinner will be served in the Pohutu In room. Lunch will be served according to the program on Wednesday through Friday. Dinner will begin each night at 7:30pm. Morning and afternoon tea will be available in the conference room.

### **Contact information:**

Holiday Inn Rotorua: 10 Tryon St, Whakarewarewa, Rotorua 3043

+64 7 348 1189

Organizing committee: Philip Brydon

+64 21 088 73495

## Program at a glance

	Tuesday	Wednesday	Thursday	Friday
8:50		Opening		
9:00		Grochala	Schwerdtfeger	Fehske
		Rachel	Novelli	O'Brien
		Menke	Jayalatharachchi	Bonca
		Jovic	Goodacre	Nawaz
10:30		Morning Tea	Morning Tea	Morning Tea
11:00		Karel	Knibbe	Granville
		Ulrich	Tallon	Maekawa
		Tretiakov	Storey	Kammermeier
12:00		Spasovski	Chan	Keser
		Lunch	Lunch	Prizes and closing
13:30		Ling	Nielsen	Lunch
		Narayanan	Culcer	
		Yick	Lewis	
		Prelovsek	Park	
15:00		Afternoon Tea	Photo	
15:30		Acharya	Afternoon Tea	
		Henkel	Trodahl	
		Christopher	Holmes-Hewett	
17:00		Jacobson	Anton	
		Posters	Tribute	
		Posters	Posters	
19:30	Dinner	Dinner	Conference Dinner	
		Quiz		

# Program

## Tuesday, 4<sup>th</sup> February 2020

15:00 – 19:00 Registration

19:00 Dinner

## Wednesday, 5<sup>th</sup> February 2020

08:50 – 09:00 *Opening*  
Philip Brydon, University of Otago, New Zealand

Session chair: Chris Ling (University of Sydney)

09:00 – 09:30 *Remarkable fluoroargentates(II) - the ultimate siblings of oxocuprate materials*  
**(invited)** Wojciech Grochala, University of Warsaw, Poland

09:30 – 09:50 *High-Temperature Majorana Fermions in Magnet-Superconductor Hybrid Systems*  
Stephan Rachel, University of Melbourne, Australia

09:50 – 10:10 *Stabilizing even-parity chiral superconductivity in  $Sr_2RuO_4$*   
Henri Menke, University of Otago, New Zealand

10:10 – 10:30 *Dirac nodal lines and flat-band surface state in the functional oxide  $RuO_2$*   
Vedran Jovic, GNS Science, New Zealand

10:30 – 11:00 Morning Tea

Session Chair: Dimitrie Culcer (University of NSW)

11:00 – 11:30 *The Anomalous Hall Effect of Antiferromagnetic  $Mn_3Ge$  and Amorphous Ferromagnetic  $Fe_xSi_{1-x}$  and  $Fe_yCo_{1-y}Si$*   
**(invited)** Julie Karel, Monash University, Australia

11:30 – 11:50 *Increase of the stability range of the skyrmion phase in doped  $Cu_2OSeO_3$*   
Clemens Ulrich, University of New South Wales, Australia

11:50 – 12:10 *Tuning Skyrmion Hall effect via Engineering of Spin-orbit Interaction*  
Oleg Tretiakov, University of New South Wales, Australia

12:10 – 12:30 *Tuning Magnetic Frustration in Bixbyites*  
Martin Spasovski, University of Auckland, New Zealand

12:30 – 13:30 Lunch

Session Chair: Stephan Rachel (University of Melbourne)

13:30 – 14:00  *$FeMn_3Ge_2Sn_7O_{16}$  : a Spin-liquid Candidate with a Perfectly Isotropic 2-D Kagome Lattice*  
**(invited)** Chris Ling, University of Sydney, Australia

- 14:00 – 14:20 *Symmetry analysis of the ferroic transitions in the coupled honeycomb system (Fe, Co, Mn)<sub>4</sub>Ta<sub>2</sub>O<sub>9</sub>*  
Narendirakumar Narayanan, Australian National University, Australia
- 14:20 – 14:40 *Neutron Study of Magnetic Phase Transition in SrCoO<sub>3</sub> Thin Films*  
Samuel Yick, University of New South Wales, Australia
- 14:40 – 15:10 *Spin-liquid state in planar Heisenberg models*  
**(invited)** Peter Prelovsek, Jozef Stefan Institute, Slovenia
- 15:10 – 15:40 Afternoon tea
- Session chair: Ben Mallett (University of Auckland)
- 15:40 – 16:00 *Avalanches, Criticality and Correlations in Self-Organised Nanoscale Networks*  
Susant Acharya, University of Canterbury, New Zealand
- 16:00 – 16:20 *Investigation of lithium-vacancy diffusion in lithium titanate: A FPMD simulation study*  
Pascal Henkel, Julius Liebig University Geissen, Germany
- 16:20 – 16:40 *Exploring the novel garnet system of Li<sub>6.75-3x</sub>Ga<sub>x</sub>La<sub>3</sub>Zr<sub>1.75</sub>Ta<sub>0.25</sub>O<sub>12</sub>*  
Timothy Daniel Christopher, University of Auckland, New Zealand
- 16:40 – 17:00 *Scanning Tunnelling Spectroscopy of the Indium Oxide (111) Surface*  
Peter Jacobson, University of Queensland, Australia
- 17:00 – 19:00 Poster session
- 19:30 – 20:30 Dinner
- 20:30 Quiz

### Thursday, 6<sup>th</sup> February 2020

Session Chair: Holger Fehske (University of Greifswald)

- 09:00 – 09:30 *From Sticky Hard Spheres to Lennard-Jones potentials and many-body expansions for rare gas solids*  
**(invited)** Peter Schwerdtfeger, Massey University, New Zealand
- 09:30 – 09:50 *Carbon molecules in space: a thermal Equation of State study of solid hexamethylenetetramine*  
Giulia Novelli, Australian Nuclear Science and Technology Organization, Australia
- 09:50 – 10:10 *Monodisperse Silver Clusters Stabilized by an Organic Network*  
Vishakya Jayalatharachchi, Queensland University of Technology, Australia
- 10:10 – 10:30 *X-ray photoelectron studies of vanadium oxide surfaces in the presence of water*  
Dana Goodacre, University of Auckland, New Zealand
- 10:30 – 11:00 Morning Tea



Session Chair: Eva Anton (Victoria University of Wellington)

- 11:00 – 11:30 *Electron Holography of high temperature superconductors*  
**(invited)** Ruth Knibbe, University of Queensland, Australia
- 11:30 – 11:50 *NMR and thermodynamic studies of cuprate high-T<sub>c</sub> superconductors*  
Jeff Tallon, Victoria University of Wellington, New Zealand
- 11:50 – 12:20 *Towards a single-model description of cuprates in the pseudogap state*  
**(invited)** James Storey, Victoria University of Wellington, New Zealand
- 12:20 – 12:40 *Magnetic Ordering in Superconducting Sandwiches*  
Andrew Chan, University of Auckland, New Zealand
- 12:40 – 13:40 Lunch

Session Chair: Tilo Söhnle (University of Auckland)

- 13:40 – 14:00 *Demonstrating the Hot Carrier Solar Cell Through Broadband Absorption and Resonant Carrier Extraction*  
Michael Nielsen, University of New South Wales, Australia
- 14:00 – 14:20 *Resonant Photovoltaic Effect in Doped Magnetic Topological Materials*  
Dmitrie Culcer, University of New South Wales, Australia
- 14:20 – 14:40 *Condensed Matter Terahertz Interactions*  
Roger Lewis, University of Wollongong, Australia
- 14:40 – 15:00 *Realization of an Acoustic Supercoupler using Density-Near-Zero Metamaterial*  
Choon Mahn Park, Dong-A University, Korea
- 15:00 – 15:10 *Photo*
- 15:10 – 15:30 *Afternoon tea*

Session Chair: Ruth Knibbe (University of Queensland)

- 15:30 – 16:00 *Rare-earth nitrides: Mixed valence, strongly correlated heavy Fermions*  
**(invited)** Joe Trodahl, Victoria University of Wellington, New Zealand
- 16:00 – 16:20 *4f Conduction in Rare Earth Nitrides*  
William Holmes-Hewett, Victoria University of Wellington, New Zealand
- 16:20 – 16:50 *Superconducting computing memory using rare-earth nitrides*  
**(invited)** Eva Anton, Victoria University of Wellington, New Zealand
- 16:50 – 17:00 *Tribute: Ralph Severin (Sev) Crisp, Eric Raymond (Lou) Vance, and Geoff Wilson*  
Trevor Finlayson, University of Melbourne, Australia  
Dan Gregg, Australian Nuclear Science and Technology Organization, Australia  
Glen Stewart, University of New South Wales, Canberra, Australia
- 17:10 – 19:00 Poster session
- 19:30 Conference dinner

**Friday, 7<sup>th</sup> February 2020**

Session Chair: Philip Brydon (University of Otago)

09:00 – 09:30 *Exotic criticality and symmetry-protected topological states in dimerised fermion, boson and spin chain models*  
**(invited)**  
Holger Fehske, University of Greifswald, Germany

09:30 – 9:50 *Anomalous Spectral Broadening from an Infrared Catastrophe in 2D Quantum Antiferromagnets*  
Matthew O'Brien, University of New South Wales, Australia

9:50 – 10:20 *Spectral Function of the Holstein Polaron at Finite Temperature*  
**(invited)**  
Janez Bonca, Jozef Stefan Institute, Slovenia

10:20 – 10:40 *Ferromagnetic Ni<sub>1-x</sub>Fe<sub>x</sub> nanofibers produced by electrospinning*  
Tehreema Nawaz, Victoria University of Wellington, New Zealand

10:40 – 11:00 Morning Tea

Session Chair: Julie Karel (Monash University)

11:00 – 11:30 *Topological electronic transport properties of magnetic Weyl semi-metal Co<sub>2</sub>MnGa*  
**(invited)**  
Simon Granville, Victoria University of Wellington, New Zealand

11:30 – 11:50 *Spin Mechatronics in Spintronics*  
Sadamichi Maekawa, RIKEN, Japan

11:50 – 12:10 *Inplane magnetoelectric response in bilayer graphene*  
Michael Kammermeier, Victoria University of Wellington, New Zealand

12:10 – 12:30 *Hydrodynamic electron flow in 2D semiconductor heterostructures*  
Aydin Cem Keser, University of New South Wales, Australia

12:30 – 12:40 *Presentations and closing*  
Philip Brydon, University of Otago, New Zealand  
Ben Mallett, University of Auckland, New Zealand

12:40 – 13:40 Lunch

## Posters

All posters will be displayed in the Kauri room for the duration of the conference.

1. *Topology from Interactions: Haldane-like Phase in the Extended Hubbard Model*  
Roman Rausch, Kyoto University, Japan
2. *New on the Physics Menu: Superconducting Sandwiches!*  
Andrew Chan, University of Auckland, New Zealand
3. *Control of the persistent spin helix lifetime by crystal orientation*  
Daisuke Iizasa, Tohoku University, Japan
4. *Magnetism in alloys of the rare-earth nitrides*  
Jackson Miller, Victoria University of Wellington, New Zealand
5. *High Magnetic Saturation Holmium-Terbium Thin-Films Alloys; Application in High- $T_c$  machines*  
Tane James Butler, Victoria University of Wellington, New Zealand
6. *Topological superconductivity from the 2D Hubbard model*  
Sebastian Wolf, University of Melbourne, Australia
7. *Delocalisation of d-electrons within Transition Metal Doped Clusters: Pushing the Limits of the Superatom Model*  
James Gilmour, Victoria University of Wellington, New Zealand
8. *Development of a spin-injection field effect transistor utilizing Rare-earth Nitrides*  
Kira Pitman, Victoria University of Wellington, New Zealand
9. *Carbon-fibre incorporated  $\text{CoSb}_3$  based skutterudite facilitating colossal electrical conductivity fabricated by Field Assisted Sintering Method.*  
Ridwone Hossain, University of Wollongong, Australia
10. *Preparation and structural characterisation of pure and Te-doped  $\text{Cu}_2\text{OSeO}_3$*   
Rosanna Roy, University of Auckland, New Zealand
11. *Exploring the Pyrophosphate Series  $\text{K}_2\text{Cu}_{1-x}\text{Fe}_x\text{P}_2\text{O}_7$*   
Ryan Silk, University of Auckland, New Zealand
12. *Development of whitlockite  $\beta\text{-Ca}_3(\text{PO}_4)_2$  phosphors*  
Huihua Zhou, University of Auckland, New Zealand

13. *Crystal structure and thermoelectric properties of n-type Bi<sub>2-x</sub>Ce<sub>x</sub>O<sub>2</sub>Se ceramics*  
Kyeongsoon Park, Sejong University, Korea
14. *Exploring the Novel Pyrovanadate Series K<sub>2</sub>Mn<sub>1-x</sub>CoV<sub>2</sub>O<sub>7</sub>*  
Mark Smith, University of Auckland, New Zealand
15. *Computational and Spectroscopic Studies on Magnetically Frustrated M'M''<sub>3</sub>Si<sub>2</sub>Sn<sub>7</sub>O<sub>16</sub> (M' = Fe, Co; M'' = Fe, Mn) Structures*  
Joseph Vella, University of Auckland, New Zealand
16. *Magnonic Crystals: A Bottom-up Fabrication Approach Utilizing Polymer and Supramolecular Chemistry*  
Daniel Clyde, University of Auckland, New Zealand
17. *Temperature dependent terahertz spectra for glycine single crystal*  
Jackson Allen, University of Wollongong, Australia
18. *Temperature Dependence of Electron Delocalization in Mixed Valence Freudenbergit*  
John Cashion, Monash University, Australia
19. *Intrinsic Anomalous Hall Effect in Chiral D<sub>4h</sub> Superconductors*  
Mathew Denys, University of Otago, New Zealand
20. *A menagerie of strongly correlated phases on the decorated honeycomb lattice*  
Henry Nourse, University of Queensland, Australia
21. *Substitutional Doping of Trirutiline Phases, AB<sub>2</sub>O<sub>6</sub>*  
Sneh Patel, University of Auckland, New Zealand
22. *Robustness of unconventional s-wave superconducting states against disorder*  
David Cavanagh, University of Otago, New Zealand
23. *Deformation Studies of Mg-PSZ under Compressive Loading*  
Trevor Finlayson, University of Melbourne, Australia
24. *Reinterpretation of physical property data for TmV<sub>2</sub>Al<sub>20</sub>*  
Wayne Hutchison, University of New South Wales, Canberra, Australia
25. *Modelling 1D and 2D High-Temperature Superconducting Quantum Interference Filters*  
Marc A. Gali Labarias, CSIRO Manufacturing, Australia
26. *Bulk Currents in Artificial Graphene with a Magnetic Field*  
Zeb Krix, University of New South Wales, Australia

27. *Characterising the local crystal field interaction for  $RFeO_3$  ( $R = Er, Ho$ )*  
Glen Stewart, University of New South Wales, Canberra, Australia
28. *Quantum size effects in topological-insulator nanostructures*  
Ulrich Zuelicke, Victoria University of Wellington, New Zealand
29. *Prediction of the spin triplet two-electron quantum dots in Si: towards controlled quantum simulations of magnetic systems*  
Oleg Sushkov, University of New South Wales, Australia
30. *Photoluminescence of *Coscinodiscus* sp. Diatoms*  
Jiazun Wu, Victoria University of Wellington, New Zealand
31. *Low-energy electron beam induced damage to organic molecules – limits to IPES application on organic molecules*  
Gabriele Motta, Queensland University of Technology, Australia
32. *Nonlinear optical response of the  $\alpha$ - $T_3$  model due to the nontrivial topology of the dispersion*  
Jack Zuber, University of Wollongong, Australia
33. *Magnonic Hydrogen Gas Sensing*  
Mikhael Kostylev, University of Western Australia, Australia
34. *Surveying the higher dimensions of the aperiodic composite nonadecane/urea*  
Garry McIntyre, Australian Nuclear Science and Technology Organization, Australia

# Memories of Wagga 2014

Waiheke Island, New Zealand, 4-7 February 2014

(thanks to Garry McIntyre)



# Talk Abstracts

## Avalanches, Criticality and Correlations in Self-Organised Nanoscale Networks

Susant K. Acharya<sup>1</sup>, Joshua Brian Mallinson<sup>1</sup>, Shota Shirai<sup>1</sup>, Saurabh K. Bose<sup>1</sup>, Matthew D. Pike<sup>2</sup>, Edoardo Galli<sup>1</sup>, Matthew D. Arnold<sup>3</sup>, and Simon A. Brown<sup>1</sup>

<sup>1</sup> *MacDiarmid Institute for Advanced Materials and Nanotechnology, School of Physical and Chemical Sciences, University of Canterbury, 8140, Christchurch, New Zealand;*

<sup>2</sup> *Electrical and Electronics Engineering, University of Canterbury, Private Bag 4800, Christchurch 8140, New Zealand;*

<sup>3</sup> *School of Mathematical and Physical Sciences, University of Technology Sydney, Australia*

Neuronal avalanches are one of the key characteristic features of signal propagation in the brain. [1] These avalanches originate from the complexity of the network of neurons and synapses, which are widely believed to form a self-organised critical system. Criticality is hypothesised to be intimately linked to the brain's computational power [2] but efforts to achieve neuromorphic computation have so far focused on highly organised architectures, such as integrated circuits and regular arrays of memristor. To date, little attention has been given to developing complex network architectures that exhibit criticality and thereby maximize computational performance. We show here, using methods developed by the neuroscience community, that electrical signals from self-organised percolating networks of nanoparticles exhibit brain-like correlations and criticality. [3] Specifically, the sizes and durations of avalanches of switching events are power-law distributed, and the power-law exponents satisfy rigorous criteria for criticality. Additionally we show that both the networks and their dynamics are scale-free. These networks provide a low-cost platform for computational approaches that rely on spatiotemporal correlations, such as reservoir computing, and are a significant step towards creating neuromorphic device architectures.

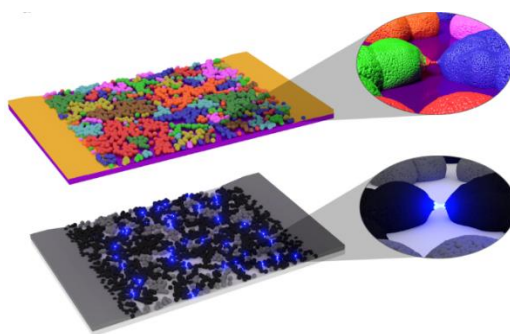


**Fig. 1:** *The percolating network of nanoparticles in a simple two-terminal contact geometry. The different colours represent groups of particles that are in contact with one another. The zoomed region shows a schematic of the growth of an atomic filament within a tunnel gap (a switching event, that can be seen as synapse-like) when a voltage is applied. Bottom: The same network schematic presented so as to show the conducting pathways (black) which result from atomic filament formation within the gaps between groups. When the applied potential causes one tunnel gap between groups to be bridged by a conducting filament, the electric field across other tunnel gaps is intensified, leading to avalanches of switching events.*

### References

- [1] Beggs, J. M. *et al.*, *J. Neurosci.* **23**, 11167 (2003).
- [2] Munoz, M. A. *Rev. Mod. Phy.* **90**, 031001 (2018).
- [3] Mallinson, J. B. *et al.* *Sci. Adv.* **11**, eaaw8438 (2019).



## **Superconducting computing memory using rare-earth nitrides**

E.-M. Anton, S. Devese, J. Miller, F. Ullstad, B. J. Ruck, H. J. Trodahl, F. Natali

*The MacDiarmid Institute for Advanced Materials and Nanotechnology, School of Chemical and Physical Sciences, Victoria University of Wellington, PO Box 600, Wellington, New Zealand*

Data centers are at the core of infrastructure providing internet, cloud computing and data storage. Their size and power consumption are growing rapidly to meet demand, and will become unsustainable within the next decade without breakthrough technologies or radical change in consumer behaviour. Data centers are predicted to use 5 -15 % of the global electricity and to exceed the carbon footprint of air travel as early as 2025, even when factoring in improvements in efficiency based on current semiconductor technology.

Superconducting computing is a potential pathway to reduce energy consumption of data centers by a factor of 100, even taking into account the power needed for cryogenic cooling. On-going research efforts have made much progress in developing superconducting processors, but finding a compatible memory remains challenging.

We are developing magnetic memory devices that are compatible with the cryogenic temperatures at which superconducting computers operate. The rare-earth nitrides are a promising group of materials for this task, as many are intrinsic ferromagnetic semiconductors with low Curie temperatures and they provide a range of different magnetic properties. Among them are hard and soft ferromagnets, a strong ferromagnet with near-zero magnetic moment and a superconductor itself, and they can be stacked easily in devices due to similar chemistry and lattice constants. This talk will present the current status of research on rare-earth nitrides for memory devices, and give an outlook to future applications.

## Spectral Function of the Holstein Polaron at Finite Temperature

J. Bonča,<sup>1,2</sup> S. A. Trugman,<sup>3</sup> M. Berçiu<sup>4</sup>

<sup>1</sup> *Faculty of Mathematics and Physics, University of Ljubljana, SI-1000 Ljubljana, Slovenia*

<sup>2</sup> *J. Stefan Institute, SI-1000 Ljubljana, Slovenia*

<sup>3</sup> *Los Alamos National Institute, 87544 Los Alamos, NM*

<sup>4</sup> *Department of Physics and Astronomy, University of British Columbia, Vancouver, BC, Canada, V6T 1Z1*

I will present the Holstein polaron spectral function on a one dimensional ring obtained using the finite-temperature (T) Lanczos method. After a brief introduction in to basic properties of the model I will present most important features of the electron spectral function. With increasing T additional features in the spectral function emerge even at temperatures below the phonon frequency. We observe a substantial spread of the spectral weight towards lower frequencies and the broadening of the quasiparticle (QP) peak. In the weak coupling regime the QP peak merges with the continuum in the high-T limit. In the strong coupling regime the main features of the low-T spectral function remain detectable up to the highest T used in our calculations. The effective polaron mass shows a non-monotonic behavior as a function of T at small phonon frequency but increases with T at larger frequencies. The self energy remains k-independent even at elevated T in the frequency range corresponding to the polaron band while at higher frequencies it develops a distinguishable k-dependence. Analytical expressions for the first few frequency moments are derived and they agree well with those extracted from numerical calculations in a wide-T regime. Finally, I will also discuss some relaxation properties of the electron coupled to various bosonic excitations [2].

### References

- [1] J. Bonča, S. A. Trugman, and M. Berçiu, Phys. Rev. B 100, 094307 (2019).
- [2] J. Kogoj, M. Mierzejewski and J. Bonča, Phys. Rev. Lett., 117, 227002 (2016).

## Magnetic Ordering in Superconducting Sandwiches

A. Chan<sup>1,2,4,5</sup>, N.J. van der Heijden<sup>2,4</sup>, T. Söhnel<sup>2,4</sup>, M.C. Simpson<sup>1,2,3,4,5</sup>, K.C. Rule<sup>6</sup>,  
G.L. Causer<sup>6</sup>, W.-T. Lee<sup>6</sup>, C. Bernhard<sup>7</sup>, B.P.P. Mallett<sup>1,2,4,5</sup>

<sup>1</sup>The Photon Factory, The University of Auckland, New Zealand

<sup>2</sup>School of Chemical Sciences, The University of Auckland, New Zealand

<sup>3</sup>Department of Physics, The University of Auckland, New Zealand

<sup>4</sup>The MacDiarmid Institute for Advanced Materials and Nanotechnology, New Zealand

<sup>5</sup>The Dodd-Walls Centre for Photonic and Quantum Technologies, New Zealand

<sup>6</sup>Australian Nuclear Science and Technology Organization, Lucas Heights, Sydney, Australia

<sup>7</sup>Department of Physics, University of Fribourg, Switzerland

Our cuprate-manganite ‘superconducting sandwich’ multilayers exhibit a highly unusual magnetic-field induced insulating-to-superconducting transition, contrary to the commonly held understanding that magnetic fields are detrimental to superconductivity [1, 2]. This new behaviour is a result of the specific magnetic and electronic properties of the manganite coupling with the cuprate (YBa<sub>2</sub>Cu<sub>3</sub>O<sub>7- $\delta$</sub> , YBCO). Due to the specific manganite composition, Nd<sub>0.65</sub>(Ca<sub>0.7</sub>Sr<sub>0.3</sub>)<sub>0.35</sub>MnO<sub>3</sub> (NCSMO), we hypothesize the behaviour to originate from CE-type antiferromagnetic ordering as well as charge and orbital ordering [3]. Zero-field cooled polarized neutron reflectometry (PNR) data in Fig 1(A) shows a sizable spin-flip (R<sup>+</sup>) signal which may result from disordered ferromagnetic domains which sum to give a vanishing macroscopic magnetization. Initial elastic neutron scattering measurements performed on 100 nm thin film NCSMO display signatures of magnetic ordering (Fig 1(B)). Future neutron scattering measurements will look at the modification of magnetic order in a superlattice to better understand the relationship between NCSMO magnetization and our newly discovered insulating-to-superconducting transition.

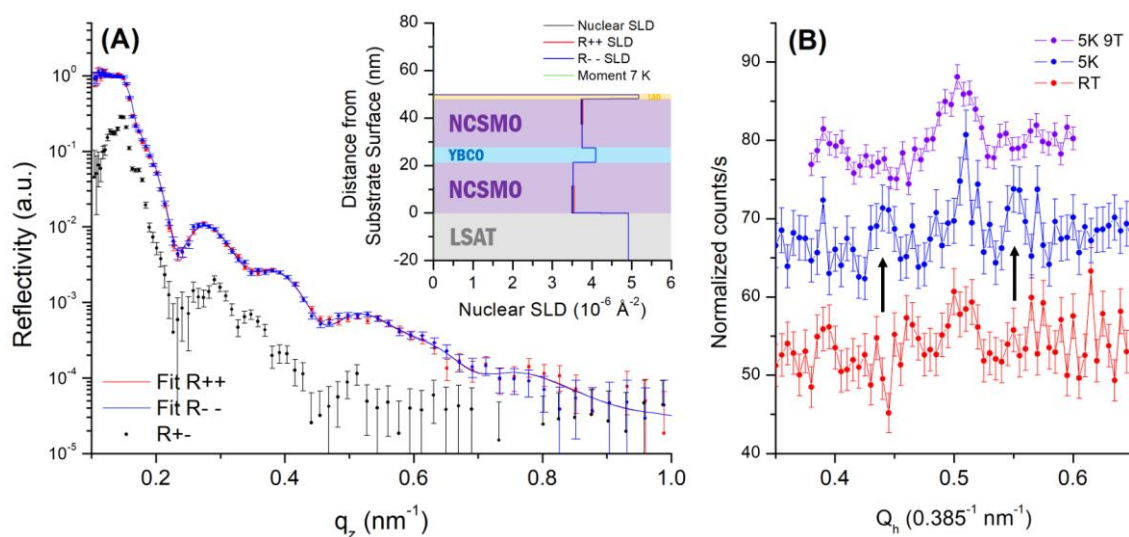


**Fig. 1:** (A) PNR profiles for a NCSMO<sub>20nm</sub>-YBCO<sub>7nm</sub>/NCSMO<sub>20nm</sub> trilayer after zero-field cooling to 7 K. Inset show corresponding nuclear and magnetic scattering length densities (SLDs) obtained from best fits to the data in (A). Plot (B) show zero-field cooled elastic neutron scattering data along the  $[h02]$  direction for a 100 nm thin film NCSMO. Black arrows indicate incommensurate satellite peaks.

### References

- [1] B. Mallett et al. *Phys. Rev. B*. **94**, 180503(R) (2016)
- [2] E. Perret et al. *Comms. Phys.* **45**, 1-10 (2018)
- [3] Y. Tokura. *Rep. Prog. Phys.* **69**, 797-851 (2006).

## Exploring the novel garnet system of $\text{Li}_{6.75-3x}\text{Ga}_x\text{La}_3\text{Zr}_{1.75}\text{Ta}_{0.25}\text{O}_{12}$

Timothy Christopher<sup>1,2</sup>, Saifang Huang<sup>3</sup>, Peng Cao<sup>3</sup>, Tilo Söhnlel<sup>1,2</sup>

<sup>1</sup> School of Chemical Sciences & Centre of Green Chemical Science, University of Auckland, Auckland, New Zealand

<sup>2</sup> MacDiarmid Institute for Advanced Materials and Nanotechnology, Victoria University of Wellington, New Zealand

<sup>3</sup> Department of Chemical and Materials Engineering, University of Auckland, Auckland, New Zealand

Lithium garnet oxides have been put forward as a solid-state alternative for Li-ion electrolytes since the  $\text{Li}^+$  conducting abilities of  $\text{Li}_7\text{La}_3\text{M}_2\text{O}_{12}$  ( $\text{M} = \text{Ta}, \text{Nb}$ ) was discovered in 2003. [1] These solid-state materials exhibit physical and chemical properties desired for more efficient and safer Li-ion battery electrolytes. [2] Lithium garnet oxides can exist in tetragonal and cubic phase isomorphs with the latter exhibiting higher conductivities.  $\text{Li}_7\text{La}_3\text{Zr}_2\text{O}_{12}$  undergoes a phase transition from cubic to tetragonal due to the thermodynamic unstable nature of the cubic arrangement. [3] Ionic conductivities of up to  $1 \times 10^{-3} \text{ S cm}^{-1}$  have been reported for cubic phase garnet materials of  $\text{Li}_{6.4}\text{La}_3\text{Zr}_{1.4}\text{Ta}_{0.6}\text{O}_{12}$ . [4] Here we present a dual doped garnet series of  $\text{Li}_{6.75-3x}\text{Ga}_x\text{La}_3\text{Zr}_{1.75}\text{Ta}_{0.25}\text{O}_{12}$  and attempt to mimic the high conductivities seen in that  $\text{Li}_{6.4}\text{La}_3\text{Zr}_{1.4}\text{Ta}_{0.6}\text{O}_{12}$ . Successful synthesis of the proposed series was achieved via standard solid-state sintering from gallium doping up to  $x = 0.5$ . The garnet structure of  $x = 0.1$  is shown in Figure 1. X-ray and neutron source diffraction characterisation revealed Ga has a preference to occupy the Li tetrahedral (Li24d) site over the octahedral (Li96h) site. High-temperature neutron diffraction studies show the relationship between temperature, Ga content and Li displacement between the Li24d and Li96h sites. With increasing temperature and increasing Ga content, the Li96h site occupancy increased with Li24d site decreasing. Ionic conductivity is shown to be dependent on the Ga/Li content within the garnet.

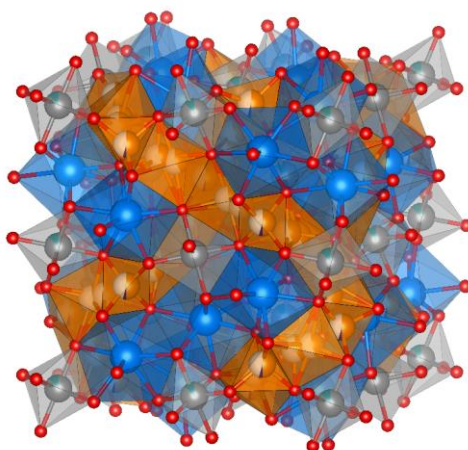


**Fig. 1:** Proposed crystal structure of cubic phase  $\text{Li}_{6.45}\text{Ga}_{0.1}\text{La}_3\text{Zr}_{1.75}\text{Ta}_{0.25}\text{O}_{12}$  refined from neutron powder diffraction data. Li - orange, Ga - purple, La - blue, Zr - grey, Ta - cyan, O - red.

### References

- [1]. V. Thangadurai, *et al.*, *Journal of the American Ceramic Society*, 2003, **86**, 437-440.
- [2]. V. Thangadurai, *et al.*, *Chemical Society Reviews*, 2014, **43**, 4714-4727.
- [3]. G. Larraz, *et al.*, *Journal of Materials Chemistry A*, 2013, **1**, 11419-11428.

## Resonant photovoltaic effect in doped magnetic topological materials

Pankaj Bhalla<sup>1,2</sup>, Allan H. MacDonald<sup>3</sup>, Dimitrie Culcer<sup>2,4</sup>

<sup>1</sup>*Beijing Computational Science Research Center, Beijing 100193, China*

<sup>2</sup>*ARC Centre of Excellence for Future Low-Energy Electronics Technologies, UNSW Node, Sydney 2052, Australia*

<sup>3</sup>*Department of Physics, The University of Texas at Austin, Austin TX78712, USA*

<sup>4</sup>*School of Physics, The University of New South Wales, Sydney 2052, Australia*

The non-linear optical response of clean undoped semiconductors contains a static intrinsic term - the shift current. We have recently shown that when Kramers degeneracy is lifted, the second order dc response of doped topological materials and semimetals to an ac electric field becomes large at the interband absorption threshold in clean nearly isotropic materials.

We refer to this effect, which results from an interesting interplay between inter-band coherence and intra-band occupation number response, as the resonant photovoltaic effect (RPE). We evaluate the RPE for a model of the surface states of Bi<sub>2</sub>Te<sub>3</sub> coupled to in-plane magnetic order due to either bulk doping or proximity coupling [1].

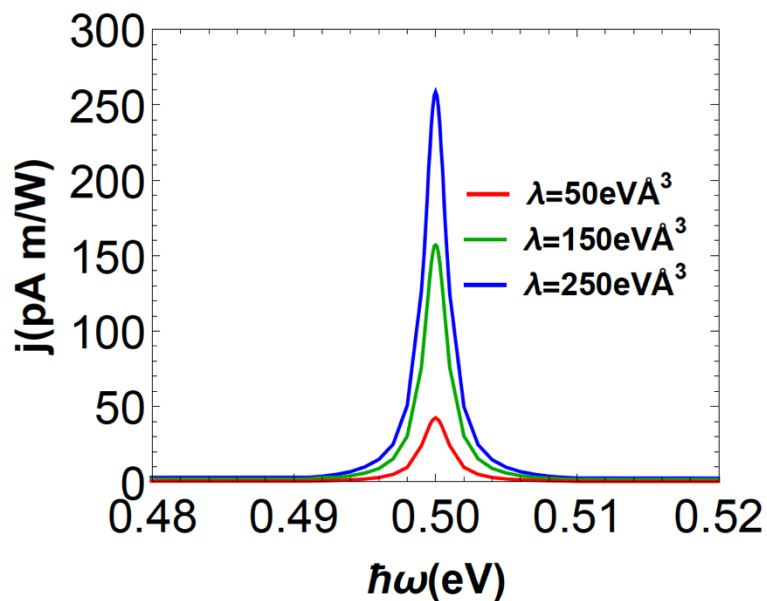


**Fig. 1:** RPE due to magnetized TI surface states with different values of the warping coefficient  $\lambda$ . Blue curve: experimental value of  $\lambda$  for Bi<sub>2</sub>Te<sub>3</sub>.

### References

- [1] P. Bhalla, A. H. MacDonald, and D. Culcer, arXiv:1910:06570.

## Exotic criticality and symmetry-protected topological states in dimerised fermion, boson and spin chain models

S. Ejima<sup>1</sup>, F. Essler<sup>2</sup>, F. Lange<sup>1</sup>, Y. Ohta<sup>3</sup>, K. Sugimoto<sup>3</sup>, T. Yamaguchi<sup>3</sup>, H. Fehske<sup>1</sup>

<sup>1</sup>*Institute of Physics, University Greifswald, 17489 Greifswald, German*

<sup>2</sup>*Rudolf Peierls Centre for Theoretical Physics, Oxford University, Oxford OX1 3NP,*

<sup>3</sup>*Center for Frontier Science, Chiba University, Chiba 263-8522, Japan*

Combining numerical density-matrix renormalisation group techniques and field theory we analyse the ground-state properties of several paradigmatic dimerised quantum lattice models in one dimension. First, we explore the quantum phase transition (QPT) between Peierls and density-wave (DW) states in the half-filled, extended Hubbard model with explicit bond dimerisation. We show that the critical line of the continuous Ising transition terminates at a tricritical point, belonging to the universality class of the tricritical Ising model with central charge  $c=7/10$ . Above this point, the QPT becomes first order. The entanglement spectrum shows that dimerised Peierls insulator is a symmetry-protected topological (SPT) state. By means of bosonisation we describe the transition region in terms of a triple sine-Gordon model. The field theory predictions for the power-law (exponential) decay of the density-density (spin-spin) and bond-order-wave correlation functions are in excellent agreement with our numerical data. Secondly, we consider the dimerised extended Bose-Hubbard model and show that an SPT Haldane insulator appears between dimerised Mott and DW insulating phases, at weak Coulomb interactions, for filling factor one. Analysing the critical behaviour of the model, we prove that the phase boundaries of the Haldane phase to Mott insulator and DW states belong to the Gaussian and Ising universality classes with  $c=1$  and  $c=1/2$ , respectively, and merge in a tricritical point. Furthermore, we demonstrate a direct Ising QPT between the dimerised Mott and DW phases above the tricritical point. Thirdly, we demonstrate that a nontrivial SPT Haldane phase also exists in dimerised spin-1 XXZ chain with single-ion anisotropy  $D$ , up to a critical dimerisation above which the Haldane phase disappears. In addition, the ground-state phase diagram exhibits large- $D$  and antiferromagnetically ordered phases. Again, for weak dimerisation, the phases are separated by Gaussian and Ising QPTs. One of the Ising transitions terminates in a critical point in the universality class of the dilute Ising model. We comment on the relevance of our results to experiments on quasi-one-dimensional anisotropic spin-1 quantum magnets.

### References

- [1] S. Ejima, F. H. L. Essler, F. Lange, and H. Fehske, *Phys. Rev. B* **93**, 235118 (2016).
- [2] S. Ejima, T. Yamaguchi, F. H. L. Essler, F. Lange, Y. Ohta, and H. Fehske, *SciPost Phys.* **5**, 059 (2018).
- [3] K. Sugimoto, S. Ejima, F. Lange, and Fehske, *Physical Review A* **99**, 012122 (2019).

## X-ray photoelectron studies of vanadium oxide surfaces in the presence of water

Dana Goodacre<sup>1,2</sup>, Hendrik Bluhm<sup>3</sup>, Monika Blum<sup>3</sup>, Tilo Söhnle<sup>1,2</sup>, Kevin Smith<sup>4</sup>

<sup>1</sup> School of Chemical Sciences, The University of Auckland, Auckland 1010, New Zealand.

<sup>2</sup> The MacDiarmid Institute for Advanced Materials and Nanotechnology, Wellington 6140, New Zealand.

<sup>3</sup> Chemical Science Division, Lawrence Berkeley National Laboratory, Berkeley, California 94720, USA.

<sup>4</sup> Department of Physics, Boston University, Boston, Massachusetts 02215, USA.

Surface science experiments where chemical species are quantified typically rely on ultra-high vacuum conditions, which do not closely mimic the conditions present in catalytic or environmental processes. Ambient pressure X-ray photoelectron spectroscopy (AP-XPS) is a technique that has allowed researchers to bridge this pressure gap and investigate what happens when the first few monolayers of water adsorb on various metal oxide materials.<sup>1</sup> Here, it is applied to vanadium oxides, which are extensively used as industrial catalysts. The wide variety of oxidation states available in vanadium oxides makes them valuable for oxygen transfer reactions, where water may be present as an intermediate and in the atmosphere as the reaction is carried out.<sup>2</sup> Using the beamline 11.0.2. AP-XPS system at the Advanced Light Source in Berkeley California, several oriented VO<sub>2</sub> films with various substrates and surface compositions have been investigated, at catalytically relevant temperatures up to 400 °C and water vapour pressures up to 2 Torr. The AP-XPS spectra have been fit with peaks corresponding to adsorbed hydroxide and molecular water (Fig. 1), and the coverage as a function of relative humidity has been determined. The trends observed give further insights into the fundamental behaviour of oxides in the presence of water.

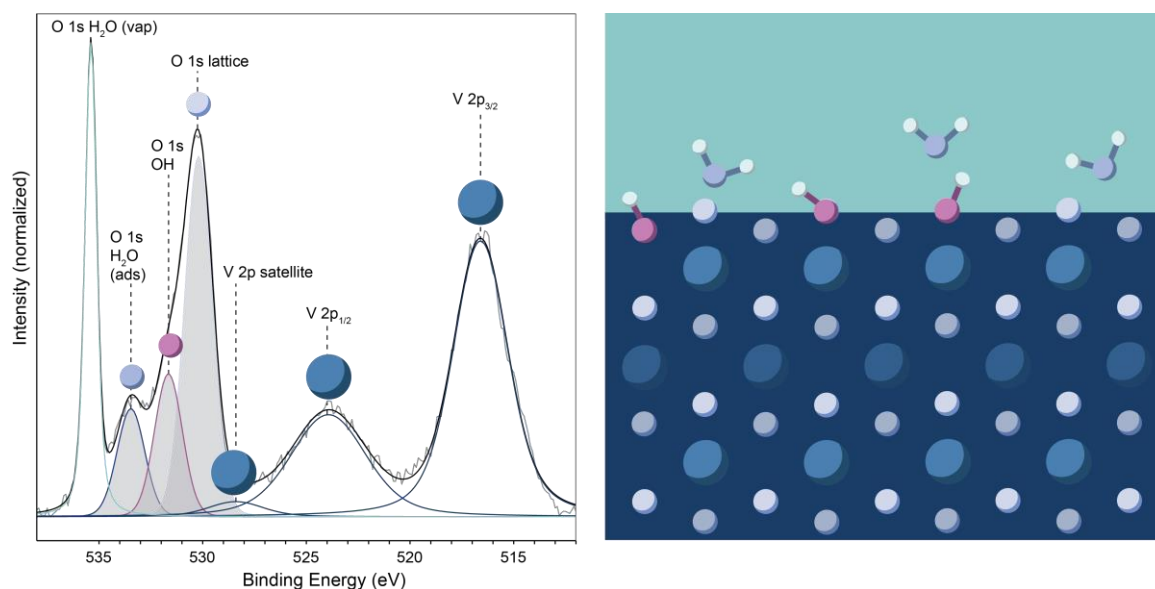


**Fig. 1:** Representative fit of O 1s and V 2p region (left) and graphical representation (right) of a vanadium oxide surface in the presence of water.

### References

- (1) Starr, D. E.; Liu, Z.; Havecker, M.; Knop-Gericke, A.; Bluhm, H. Investigation of Solid/Vapor Interfaces Using Ambient Pressure X-Ray Photoelectron Spectroscopy. *Chem. Soc. Rev.* **2013**, 42 (13), 5833–5857. <https://doi.org/10.1039/C3CS60057B>.
- (2) Surnev, S.; Ramsey, M. G.; Netzer, F. P. Vanadium Oxide Surface Studies. *Prog. Surf. Sci.* **2003**, 73 (4), 117–165. <https://doi.org/https://doi.org/10.1016/j.progsurf.2003.09.001>.



# Topological electronic transport properties of magnetic Weyl semi-metal Co<sub>2</sub>MnGa

S. Granville<sup>1,2</sup>, Y. Zhang<sup>1,2</sup>, T. Butler<sup>1</sup>, G. Dubuis<sup>1,2</sup>

<sup>1</sup>Robinson Research Institute, Victoria University of Wellington, Wellington, New Zealand

<sup>2</sup>MacDiarmid Institute for Advanced Materials and Nanotechnology, Wellington, New Zealand

Topologically interesting materials that are also magnetic are expected to be particularly important for the study of novel topological phases in condensed matter. The coupling of magnetic and transport properties in such materials could allow for spin topotronic devices, that take advantage simultaneously of the magnetic and topological physics. For instance, there are claims that ferromagnetic topological materials may allow the quantum anomalous Hall effect state, normally only seen below 10 K, to persist to room temperature.

Excitingly, very recent results indicate that Heusler alloy Co<sub>2</sub>MnGa could be a room-temperature ferromagnetic Weyl semi-metal, a material with protected electronic states due to a topological band structure [1-3]. In this presentation I will show the signatures of these topological states are visible in magnetoelectric and magneto-thermoelectric measurements in thin films of Co<sub>2</sub>MnGa. Thin films of Co<sub>2</sub>MnGa set new room temperature records of the anomalous Hall and anomalous Nernst effects. For thinner films, the anomalous Hall effect weakens, and we discuss the implications of this for exploiting the Weyl-like characteristics of Co<sub>2</sub>MnGa in thin film devices.

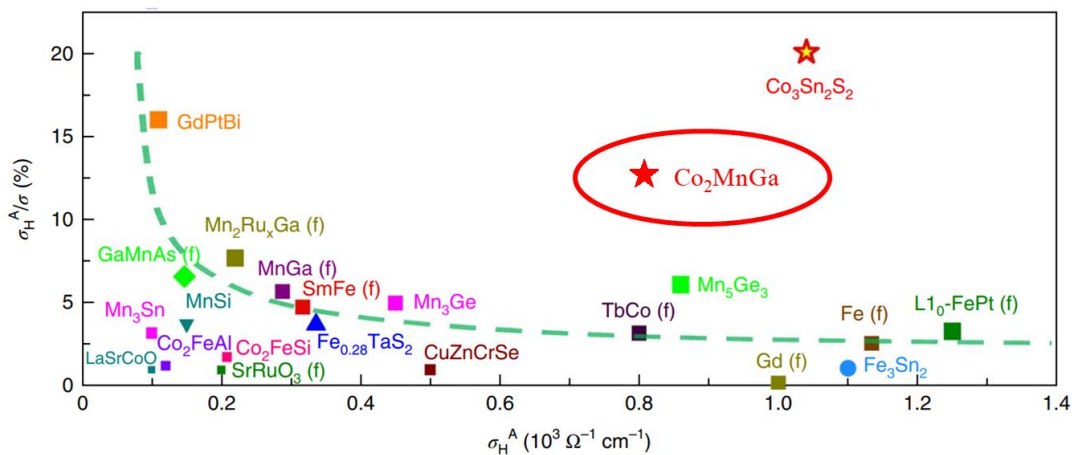


**Fig. 1:** Anomalous Hall angle vs anomalous Hall conductivity of magnetic materials, highlighting Weyl semi-metals, including Co<sub>2</sub>MnGa. Adapted from *Nat. Phys.* **14**, 1125 (2018).

## References

- [1] A. Sakai *et al.*, *Nature Physics* **14**, 1119–1124 (2018)
- [2] K. Manna *et al.*, *Phys. Rev. X* **8**, 041045 (2018)
- [3] I. Belopolski *et al.*, *Science* **365**, 1278–1281 (2019)
- [4] J. Kübler *et al.*, *Europhys. Lett.* **114**, 47005 (2016)
- [5] G. Chang *et al.*, *Phys. Rev. Lett.* **119**, 156401 (2017)



## Remarkable fluoroargentates(II) - the ultimate siblings of oxocuprate materials

W. Grochala<sup>1</sup>

<sup>1</sup> *University of Warsaw, CeNT, Zwirki i Wigury 93, 02089 Warsaw Poland*

Coinage group metals differ considerably from each other in terms of chemistry and physics. One particularly interesting manifestation of differences is offered by divalent state, which is enormously common and well-studied for copper, much less so for silver, while it is represented by only a handful of stoichiometries for gold. Here I will focus on compounds of divalent silver, notably fluorides. There are over a hundred of distinct stoichiometries known, most of them featuring magnetically isolated Ag(II) centers. However, some are known bearing direct Ag-F-Ag linkers (mostly in one dimension, seldom in two), which favour transmission of strong superexchange interactions. Here, I will discuss uniqueness of the crystal, electronic and magnetic structures as well as high pressure behavior of these compounds. Ultimately I will show what similarities and differences exist between them and undoped copper(II) oxides – precursors of the family of high- $T_C$  superconductors [1-9]. The prospect for achieving extremely strong antiferromagnetic superexchange in 2D [10] and 1D materials [7], as exemplified by  $\text{AgF}_2$  and  $\text{AgFBF}_4$ , respectively, will be discussed. The former compound shows profound similarities to  $\text{La}_2\text{CuO}_4$ , with magnetic superexchange constant reaching 70 meV (2/3 of that for the copper compound). On the other hand,  $\text{AgFBF}_4$  features straight 1D [ $\text{AgF}^+$ ] chains with magnetic superexchange constant exceeding 300 meV. This value is second to none amongst all chemical systems explored so far, and it is followed by 241 meV observed previously for  $\text{Sr}_2\text{CuO}_3$  cuprate. Simultaneously,  $\text{AgFBF}_4$  exhibits magnetic anisotropy which is 2 orders of magnitude higher than that for its oxocuprate rival, rendering the former the reference 1D antiferromagnet.

### References

- [1] ANGEW CHEM INT ED ENGL 40(15): 2742-2781 2001
- [2] CHEMPHYSCHEM 4(9): 997-1001 2003
- [3] NATURE MATER 5(7): 513-514 2006
- [4] PHYS STAT SOL RRL 2(2): 71-73 2008
- [5] ANGEW CHEM INT ED ENGL 49(9): 1683-1686 2010
- [6] CHEM COMMUN 49(56): 6262-6264 2013
- [7] ANGEW CHEM INT ED ENGL 56(34): 10114–10117 2017
- [8] PHYS REV B 96(15): 155140 2017
- [9] INORG CHEM 56(23): 14651–14661 2017
- [10] PNAS 116(5): 1495–1500 2019

## Investigation of lithium-vacancy diffusion in lithium titanate: A FPMD simulation study

P. Henkel<sup>1,2</sup>, D. Mollenhauer<sup>1,2</sup>

<sup>1</sup>*Institute of Physical Chemistry, Justus Liebig University Giessen, Giessen, Germany*

<sup>2</sup>*Center of Materials Research (LaMa), Justus Liebig University Giessen, Giessen, Germany*

The requirements to mobile devices are constantly increasing. A limiting factor is the energy supply. Over the last decades, lithium-ion batteries (*LIBs*) have emerged as a promising key technology for these. The ion transport through cathode, electrolyte and anode is an essential factor for the performance of an *LIB*. Therefore lithium titanate (*LTO*) is an auspicious anode material [1]. Essential properties of *LTO* are its chemical stability against metallic Li and its small volume-change during the Li-uptake, for which a phase transformation takes place from the Li-poor ( $\text{Li}_4\text{Ti}_5\text{O}_{12}$ ) to the Li-rich ( $\text{Li}_7\text{Ti}_5\text{O}_{12}$ ) phase [2]. The Li-ions occupy in the lithium-poor phase all *8a*- and 5/6 of the *16d*-Wyckoff positions. For a more precise understanding of lithium vacancy transport in *LTO*, we considered in our calculations a vacancy defect concentration of about 10% in the lithium-poor phase and investigated the Li-ion transport in the temperature range of 800K - 1000K using *first principles* molecular dynamic simulations (*FPMD*). Our simulations indicate that the lithium vacancy diffusion can take place via two diffusion paths: I) from an *8a*- to an *8a*-position – which is more efficient from an energetic point of view [4] – and II) from an *8a*- to a *16d*-position (see Fig 1).

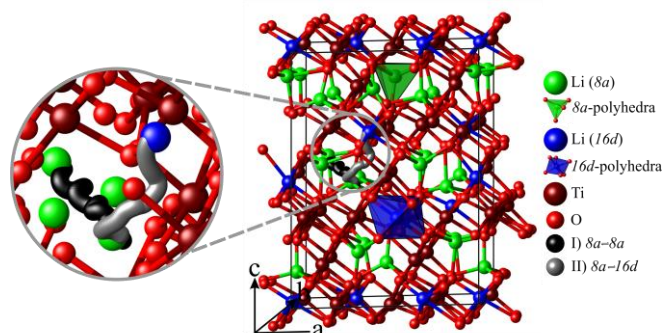


**Fig. 1:** Lithium-vacancy diffusion paths I)  $8a \rightleftharpoons 8a$  and II)  $8a \rightleftharpoons 16d$  within the Li-poor *LTO* structure.

The aim of our *FPMD* simulation is to characterize the lithium vacancy diffusion paths more precisely by considering several vacancies and their interaction. Firstly, the simulations give evidence that the ion transport mainly takes place via the  $8a \rightleftharpoons 8a$  path. Secondly, after a short simulation time, two out of three lithium vacancies are trapped in a *16d*-position. Therefore, the vacancy interaction and their orientation to each other is essential. Also, a back diffusion of path I) is determined, which occurs by a factor of 1:2 to path I) and does not contribute to the Li-ion transport [4].

### References

- [1]. M. Gockeln *et al.*, *Nano Energy* **49**, 464-573 (2018).
- [2]. T. Ohzuku, A. Ueda, and N. Yamamoto, *J. Electrochem. Soc.* **142**, 1431 (1995).
- [3]. M. Wagemaker *et al.*, *J. Phys. Chem. B* **113**, 224-230 (2009).
- [4]. P. Henkel, J. Janek, D. Mollenhauer, Manuscript to be submitted.

## 4f Conduction in Rare Earth Nitrides

W. F. Holmes-Hewett<sup>1</sup>, R. G. Buckley<sup>2</sup>, B. J. Ruck<sup>1</sup>, F. Natali<sup>1</sup> and H. J. Trodahl<sup>1</sup>

<sup>1</sup>The MacDiarmid Institute for Advanced Materials and Nanotechnology and The School of Chemical and Physical Sciences, Victoria University of Wellington

<sup>2</sup>The MacDiarmid Institute for Advanced Materials and Nanotechnology and Robinson Research Institute, Victoria University of Wellington

The influence of the 4f band on electrical transport in SmN and NdN promises a new class of simply structured NaCl materials, the rare earth nitrides, in which to investigate heavy Fermion systems. The 4f levels of the semiconducting rare earth nitrides span the conduction band and along with the control of carrier concentration, via doping with nitrogen vacancies, gives the potential for the Fermi energy to be tuned into the 4f band. SmN and NdN stand out with 4f bands predicted to meet the 5d, near the conduction band minimum [1]. Measurements of an enhanced anomalous Hall effect in each material give clear evidence for mobile electrons in the 4f band [2,3]. Optical measurements have now located the 4f bands as forming the conduction band minimum in both SmN and NdN, in close proximity to the 5d band [3,4]. Transport measurements will be presented of an enhanced anomalous Hall effect showing evidence of conduction in the 4f band (Figure 1) and optical spectroscopy that places the 4f band at the conduction band minimum in SmN and NdN. The role played by the 4f band on conduction in SmN and NdN indicates the rare earth nitrides present a series of simply structured materials ideally suited for the study of heavy Fermion systems.

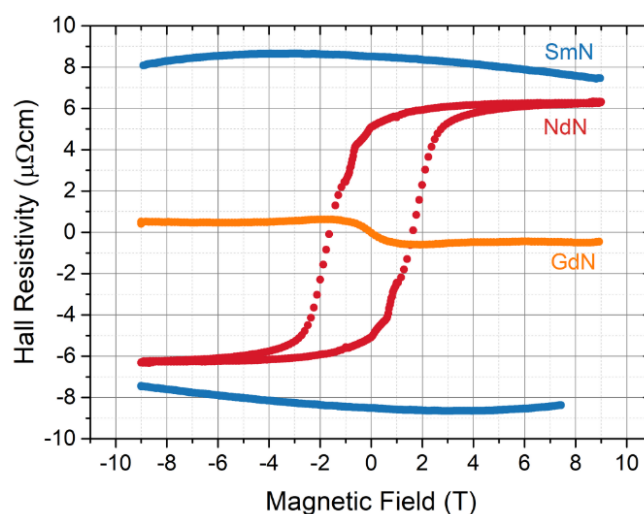


**Fig. 1:** Measurements of the Hall resistivity in SmN (blue), NdN (red), and GdN (orange).

### References

- [1] P. Larson, Walter R. L. Lambrecht, Athanasios Chantis, and Mark van Schilfhaarde, Phys. Rev. B **75**, 045114 (2007).
- [2] W. F. Holmes-Hewett, F. H. Ullstad, B. J. Ruck, F. Natali and H. J. Trodahl, Phys. Rev. B **98**, 235201 (2018).
- [3] W. F. Holmes-Hewett, R. G. Buckley, B. J. Ruck, F. Natali and H. J. Trodahl, Phys. Rev. B, **100**, 195119 (2019).
- [4] W. F. Holmes-Hewett, R. G. Buckley, B. J. Ruck, F. Natali and H. J. Trodahl, Phys. Rev. B, **99**, 205131 (2019).

## Scanning Tunnelling Spectroscopy of the Indium Oxide (111) Surface

Peter Jacobson<sup>1</sup>, Margareta Wagner<sup>2</sup>, Martin Setvin<sup>2</sup>, Michael Schmid<sup>2</sup>, Ulrike Diebold<sup>2</sup>

<sup>1</sup>*School of Mathematics and Physics, The University of Queensland, QLD 4072, Brisbane, Australia*

<sup>2</sup>*Institute of Applied Physics, TU Wien, 1040 Vienna, Austria*

Indium oxide ( $\text{In}_2\text{O}_3$ ) is a ubiquitous material in consumer electronic displays and photovoltaics due to an ideally matched optical transmission window and, unusual for a wide bandgap semiconductor, metallic conduction at room temperature. The exceptional functionality of many  $\text{In}_2\text{O}_3$  devices stems from the presence of a near surface electron accumulation layer and the formation of a two-dimensional electron gas (2DEG) decoupled from the bulk electronic states. When  $\text{In}_2\text{O}_3$  is paired with organic materials, a near universal fabrication step is the introduction of a thin organic buffer layer to improve the charge injection efficiency from the 2DEG to the organic active layer. Using a combination of atomic force microscopy and scanning tunnelling spectroscopy, we probe the structure and density of states (DOS) at the prototypical copper phthalocyanine (CuPc) -  $\text{In}_2\text{O}_3$  interface. Differential conductance ( $dI/dV$ ) measurements show that, in some instances, narrow gaps form at the Fermi level. This talk will discuss the possible origin of these gaps and the relevance to devices.

## Monodisperse Silver Clusters Stabilized by an Organic Network

V. Jayalatharachchi<sup>1</sup>, J. MacLeod<sup>1</sup>, J. Lipton-Duffin<sup>1,2</sup>

<sup>1</sup> School of Chemistry Physics and Mechanical Engineering, Queensland University of Technology, Brisbane, 4001-Australia

<sup>2</sup> Institute for Future Environments, Queensland University of Technology, Brisbane, 4001 QLD, Australia

In this study, we investigate 7-atom metal clusters coordinated by deprotonated carboxylic acid molecules on Ag(111) [1, 2]. The chemical and spatial precision of these types of monodisperse clusters of atoms have important implications for catalysis and energy production [3]. Deprotonation was examined by X-ray photoemission spectroscopy (XPS) and scanning tunnelling microscopy (STM), Fig.1 (a), while changes in the valence band region were interrogated by ultraviolet photoelectron spectroscopy (UPS). We used near edge X-ray absorption fine structure spectroscopy (NEXAFS), Fig.1 (b) in these experiments to confirm that the molecular core remains planar after deprotonation of the carboxylic/carboxylate groups via C-K edge/ O-K edge measurements.

Careful study of the chemical and electronic structure of these clusters will allow us to better understand how to use organic molecules to engineer arrays of single-atom catalysts on surfaces, with the goal of tailoring these 2D materials systems for reactivity and selectivity in targeted catalysed reaction.

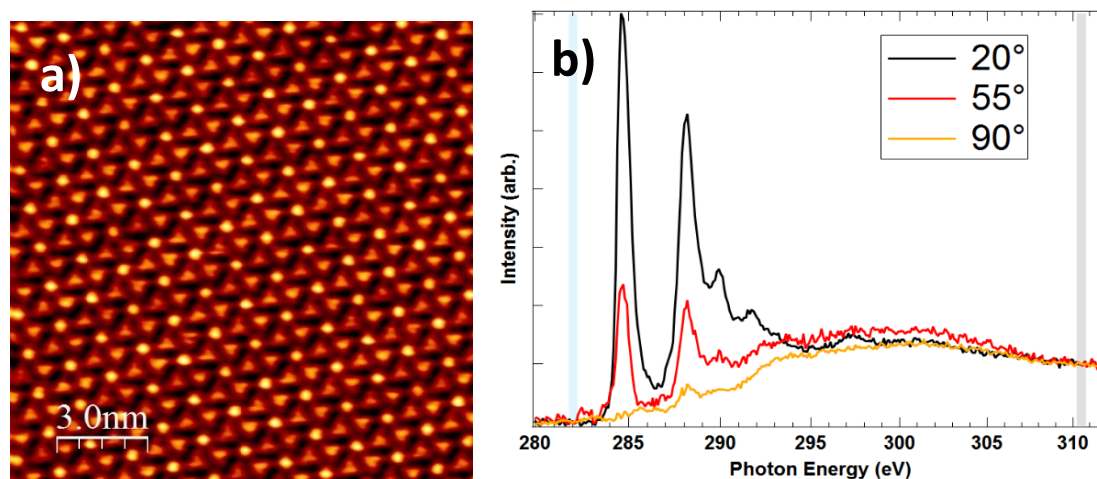


**Fig. 1:** a) STM image of periodic metal-coordinated structure b) C K-edge NEXAFS data of fully deprotonated surface

### References

- [1]. Svane, K.L., *et al.*, The Journal of Chemical Physics, (2018).
- [2]. Lipton-Duffin, J., M. Abyazisani, and J., MacLeod, *et al.*, Chemical Communications, (2018).
- [3]. Svane, K. L., Babiloliaei, M. S., Hammer, B., & Diekhöner, L., *et al.*, The Journal of Chemical Physics, (2018).

## **Dirac nodal lines and flat-band surface state in the functional oxide RuO<sub>2</sub>**

Vedran Jovic,<sup>1,2</sup> Roland J. Koch,<sup>1</sup> Swarup K. Panda,<sup>3</sup> Helmuth Berger,<sup>4</sup> Philippe Bugnon,<sup>4</sup> Arnaud Magrez,<sup>4</sup> Kevin E. Smith,<sup>2,5</sup> Silke Biermann,<sup>3,6</sup> Chris Jozwiak,<sup>1</sup> Aaron Bostwick,<sup>1</sup> Eli Rotenberg,<sup>1</sup> and Simon Moser<sup>1,7,\*</sup>

<sup>1</sup>*Advanced Light Source, E. O. Lawrence Berkeley National Laboratory, Berkeley, California 94720, USA*

<sup>2</sup>*School of Chemical Sciences and Centre for Green Chemical Sciences, University of Auckland, Auckland 1142, New Zealand*

<sup>3</sup>*Centre de Physique Théorique, Ecole Polytechnique, CNRS-UMR7644, Université Paris-Saclay, 91128 Palaiseau, France*

<sup>4</sup>*Institute of Physics, Ecole Polytechnique Fédérale de Lausanne (EPFL), CH-1015 Lausanne, Switzerland*

<sup>5</sup>*Department of Physics, Boston University, Boston, Massachusetts 02215, USA*

<sup>6</sup>*Collège de France, 11 place Marcelin Berthelot, 75005 Paris, France*

<sup>7</sup>*Physikalisches Institut, Universität Würzburg, D-97074 Würzburg, Germany*

The efficiency and stability of RuO<sub>2</sub> in various applications has made this material a subject of intense fundamental and industrial interest. The surface functionality is rooted in its electronic and magnetic properties, determined by a complex interplay of lattice-, spin-rotational, and time-reversal symmetries, as well as the competition between Coulomb and kinetic energies. This interplay was predicted to produce a network of Dirac nodal lines (DNLs), where the valence and conduction bands touch along continuous lines in momentum space. Here we uncover direct evidence for three DNLs in RuO<sub>2</sub> by angle-resolved photoemission spectroscopy. These DNLs give rise to a flat-band surface state that is readily tuned by the electrostatic environment, and that presents an intriguing platform for exotic correlation phenomena. Our findings support high spin-Hall conductivities and bulk magnetism in RuO<sub>2</sub> and are likely related to its functional properties.

## Inplane magnetoelectric response in bilayer graphene

M. Kammermeier<sup>1</sup>, P. Wenk<sup>2</sup>, U. Zuelicke<sup>1</sup>

<sup>1</sup>*School of Chemical and Physical Sciences an MacDiarmid Institute for Advanced Materials and Nanotechnology, Victoria University of Wellington,, New Zealand*

<sup>2</sup>*Department of Theoretical Physics, University of Regensburg, Germany*

A graphene bilayer shows an unusual magnetoelectric response whose magnitude is controlled by the valley-isospin density, making it possible to link magnetoelectric behaviour to valleytronics. Complementary to previous studies, we consider the effect of static homogeneous electric and magnetic fields that are oriented parallel to the bilayer's plane. Starting from a tight-binding description and using quasidegenerate perturbation theory, the low-energy Hamiltonian is derived, including all relevant magnetoelectric terms whose prefactors are expressed in terms of tight-binding parameters. We confirm the existence of an expected axion-type pseudoscalar term, which turns out to have the same sign and about twice the magnitude of the previously obtained out-of-plane counterpart. Additionally, small anisotropic corrections to the magnetoelectric tensor are found that are fundamentally related to the skew interlayer hopping parameter  $\gamma_4$ . We discuss possible ways to identify magnetoelectric effects by distinctive features in the optical conductivity.

### References

[1]. M. Kammermeier, Phys. Rev. B. **100**, 075421 (2019).

## The Anomalous Hall Effect of Antiferromagnetic Mn<sub>3</sub>Ge and Amorphous Ferromagnetic Fe<sub>x</sub>Si<sub>1-x</sub> and Fe<sub>y</sub>Co<sub>1-y</sub>Si

J. Karel<sup>1,2</sup>

<sup>1</sup> Department of Materials Science and Engineering, Monash University, Melbourne, Australia

<sup>2</sup> ARC Centre of Excellence in Future Low-Energy Electronics Technologies, Monash University, Melbourne, Australia

Magnetoresistive random access memory (MRAM) utilizing spin orbit torque (SOT) based switching has emerged as a promising non-volatile memory candidate, and amorphous materials offer a unique prospect with respect to this technology. They lack long range order, and theory has predicted that disorder may lead to an enhancement in spin orbit torques.<sup>1,2</sup> Moreover, amorphous materials are extremely tolerant to defects, meaning less stringent manufacturing requirements and thus lower costs.

The mechanisms used to describe the spin Hall effect (SHE) borrow directly from the physics of the AHE; therefore, a large AHE may point to a large SHE and a potential application in SOT-MRAM. The first part of this talk will present a study of the anomalous Hall effect (AHE) in a series of amorphous Fe<sub>x</sub>Si<sub>1-x</sub> and Fe<sub>1-y</sub>Co<sub>y</sub>Si (0<y<1) thin films. A large AHE was found in the amorphous thin films. The magnitude of the Hall resistivity is larger than previously reported in the bulk crystalline analog (e.g. Fe<sub>0.9</sub>Co<sub>0.1</sub>Si ~2μΩcm at 5K).<sup>3</sup> This large effect persists up to room temperature. The magnetic moment is also larger than previously reported in bulk crystalline Fe<sub>1-y</sub>Co<sub>y</sub>Si (e.g. y=0.1 M<sub>s</sub> ~50 emu/cm<sup>3</sup>).<sup>3</sup> Similar enhancements in magnetization have been reported in amorphous Fe<sub>x</sub>Si<sub>1-x</sub> (0.45<x<0.65) thin films in comparison to the crystalline analogue.<sup>4</sup> The origins of this large AHE will be discussed. Specifically, we will show that the results suggest the intrinsic mechanism (e.g. non-zero Berry curvature) may play an important role.<sup>5</sup> In these amorphous materials, the possible dependence of the AHE on the intrinsic mechanism is remarkable because it indicates a local atomic level description of a Berry phase in a system that lacks lattice periodicity. The second part of the talk will discuss the emergence of the AHE in the noncollinear antiferromagnet, Mn<sub>3</sub>Ge.<sup>6</sup> The AHE in ferromagnets generally scales with the magnetization, meaning that an antiferromagnet with no net magnetization should not exhibit an AHE. It will be shown that not only does Mn<sub>3</sub>Ge exhibit an AHE but one that is comparable to that of ferromagnetic metals. Theoretical calculations will demonstrate that this effect originates from a non-vanishing Berry curvature, arising from the chiral spin structure.

### References

<sup>1</sup> I. A. Ado, O. A. Tretiakov, *et al.*, *Phys. Rev B* **95**, 094401 (2017)

<sup>2</sup> O. A. Tretiakov, *et al.*, *Phys. Rev Lett* **119**, 077203 (2017)

<sup>3</sup> N. Manyala, *et al.*, *Nature Materials* **3** 255 (2004)

<sup>4</sup> J. Karel *et al.*, *Materials Research Express* **1** 026102 (2014)

<sup>5</sup> J. Karel, *et al.*, *Europhysics Letters* **114** 57004 (2016)

<sup>6</sup> Nayak *et al.*, *Science Advances* **2**, e1501870 (2016)



## **Hydrodynamic electron flow in 2D semiconductor heterostructures**

A. C. Keser<sup>1,2</sup>, D. Q. Wang<sup>1,2</sup>, O. Klochan<sup>3,2</sup>, D. Y. H. Ho<sup>4</sup>, S. Adam<sup>4</sup>, D. Culcer<sup>1,2</sup>,  
A. Hamilton<sup>1,2</sup>, O. P. Sushkov<sup>1,2</sup>

<sup>1</sup>*School of Physics, University of New South Wales, Kensington, NSW 2052, Australia*

<sup>2</sup>*Australian Research Council Centre of Excellence in Low-Energy Electronics Technologies, The  
University of New South Wales, Sydney 2052, Australia*

<sup>3</sup>*UNSW Canberra at the Australian Defence Force Academy*

<sup>4</sup>*Department of Physics, Faculty of Science National University of Singapore, Science Drive  
3, Singapore 117551*

We propose to experimentally study the hydrodynamic flow of two-dimensional electron gas by longitudinal resistance measurements. There are two major differences compared to previous works: (i) The electron mobility in semiconductor heterostructures is about  $10^7$  cm<sup>2</sup>/Vs, hence the electron mean free path with respect to scattering from impurities,

$l_i = 70\mu\text{m}$ , is comparable with the system size. (ii) The "pipe" system formed by electrostatic gates provides the perfect slip boundary condition at walls. Hence, only the internal friction dictated by geometry of the pipe system determines the effective resistance disregarding the scattering from phonons. To investigate phonon scattering we measure the temperature dependence of the resistance of a prototypical GaAs hydrodynamics device. This measurement demonstrates that at temperature 20-30 K phonons do not destroy the hydrodynamic flow. The optimal device for studies of the hydrodynamic flow must provide maximal internal friction. In the present work we optimise the device by numerically solving the Navier-Stokes equation for different pipe geometries.

## Electron holography of high temperature superconductors

Ruth Knibbe<sup>1</sup>, Anne-Helene Puichaud<sup>2</sup> and Stuart Wimbush<sup>2</sup>

<sup>1</sup>*School of Mechanical and Mining Engineering, University of Queensland, Brisbane, Australia.*

<sup>2</sup>*Robinson Research Institute, Victoria University of Wellington, Wellington, New Zealand.*

Medium resolution electron holography is a transmission electron microscopy (TEM) technique which can be used to study magnetic and electric fields. This technique has been used by researchers to study magnetic vortex formation and migration in type-II superconductors with mixed success. The understanding of magnetic vortex migration and the pinning of vortices by microstructural defects is important as it is the principal mechanism which defines the superconductor wire's current-carrying capacity [1].

Two electron holography techniques can be used to study the magnetic vortices: off-axis or in-line electron holography. Quantitative information about magnetic and electric fields can be obtained from the off-axis technique, whereas with in-line electron holography, or coherent beam Lorentz microscopy, vortex migration can be observed. Previous work has been done by Tonomura and co-workers on YBa<sub>2</sub>Cu<sub>3</sub>O<sub>7- $\delta$</sub>  (YBCO) single crystals [2] using the 1 MeV transmission electron microscope they developed [3].

In this current project, we used in-line electron holography, with a 300 keV probe-corrected FEI Titan, to study magnetic vortices in a YBCO crystal. Many challenges have been encountered including sample inhomogeneity, geometry and preparation. In particular, the observation of magnetic vortices in-situ requires that the sample be cooled with liquid helium, presenting further experimental restraints. In this presentation, I will present the progress we have made with vortex imaging of YBCO using Lorentz microscopy with a TEM operated at 300 keV, and discuss the experimental challenges.

### References

- [1] X Obradors *et al*, "Growth, nanostructure and vortex pinning in superconducting YBa<sub>2</sub>Cu<sub>3</sub>O<sub>7</sub> thin films based on trifluoroacetate solutions", *Supercond. Sci. Technol*, 25 (2012) Art. No. 123001.
- [2] A Tonomura, *et al*, "Observation of Structure Chain Vortices Inside Anisotropic High-Tc Superconductors", *Phys. Rev. Lett*, 88 (2002) Art. No 237001.
- [3] T Kawasaki *et al*, "Fine crystal lattice fringes observed using a transmission electron microscope with 1 MeV coherent electron waves", *Applied Physics Letters*, 76 (2000) Art. No 1342.

### Acknowledgements:

This work was financed by the Royal Society of New Zealand with a Marsden Fund. We would like to acknowledge Dr James Loudon for the useful discussions regarding this work.

## Condensed Matter Terahertz Interactions

R. A. Lewis

*Institute of Superconducting and Electronic Materials and School of Physics,  
University of Wollongong, Wollongong NSW 2522 Australia*

The terahertz-frequency region of the electromagnetic spectrum, lying between the microwaves and visible radiation, is often described as being scientifically rich, but relatively unexplored. The reason for this is that sources for producing, components for manipulating, and detectors for sensing terahertz radiation are less developed than those for the electronic and optical regions that bracket it. This dearth of technological tools has led to the rise of the concept of the “terahertz gap”. Yet the situation has changed in recent years, especially with the development of terahertz time-domain spectroscopy [1].

Condensed matter physics plays a central role in terahertz science and technology. Many of the sources that generate terahertz radiation are based on solid-state devices, such as photoconductive antennas fabricated on semiconductor surfaces or electro-optic crystals allowing optical rectification [2]. Likewise, many applications of terahertz radiation concern condensed matter, ranging from fundamental physics to cultural heritage applications, such as analyzing historical and synthetic paint pigments [3].

The present work is concerned with solid-state devices being employed as sensors of terahertz radiation [4]. There are five main mechanisms by which terahertz radiation may be detected: heating a material and producing a change in a physical property; interacting with the collective motion of electrons; inducing an electronic transition; mixing with reference radiation in a non-linear medium and interacting with ultrashort optical pulses. In each case, the study of solid-state interactions, typically semiconducting, superconducting or electro-optic, has not only led to technological improvements, but advanced fundamental physics.

### References

- [1] R. A. Lewis, *Terahertz Physics* (Cambridge: Cambridge University Press, 2012).
- [2] R. A. Lewis, “A review of terahertz sources”, *J. Phys. D: Appl. Phys.* **47**, 374001 (2014).
- [3] A. D. Squires and R. A. Lewis, “Terahertz analysis of phthalocyanine pigments”, *J. Infrared Millim. THz Waves* **40**, 738 (2019).
- [4] R. A. Lewis, “A review of terahertz detectors”, *J. Phys. D: Appl. Phys.* **52**, 433001 (2019).

## **FeMn<sub>3</sub>Ge<sub>2</sub>Sn<sub>7</sub>O<sub>16</sub> : a Spin-liquid Candidate with a Perfectly Isotropic 2-D Kagomé Lattice**

M.C. Allison<sup>1,2</sup>, S. Wurmehl<sup>2</sup>, B. Büchner<sup>2</sup>, J. Valla<sup>3</sup>, T. Söhnel<sup>3</sup>, M. Avdeev<sup>1,4</sup>, S. Schmid<sup>1</sup>, C.D. Ling<sup>1</sup>

<sup>1</sup> *School of Chemistry, The University of Sydney, Sydney, Australia.*

<sup>2</sup> *Leibniz IFW Dresden, Institute for Solid State Research, Dresden, Germany.*

<sup>3</sup> *School of Chemical Sciences, University of Auckland, Auckland, New Zealand.*

<sup>4</sup> *Australian Centre for Neutron Scattering, ANSTO, Menai, Australia*

The compound Fe<sub>4</sub>Si<sub>2</sub>Sn<sub>7</sub>O<sub>16</sub> has a hitherto unique crystal structure, consisting of ionic oxide layers based on edge-sharing FeO<sub>6</sub> and Sn<sup>4+</sup>O<sub>6</sub> octahedra alternating with layers of intermetallic character based on FeSn<sup>2+</sup><sub>6</sub> octahedra, separated by covalent SiO<sub>4</sub> tetrahedra. [1,2] The ionic layers contain kagomé lattices of magnetic Fe<sup>2+</sup> cations (octahedral crystal field, high-spin [HS] d<sup>6</sup>, S = 2) with perfect trigonal symmetry; while the intermetallic layers are non-magnetic because the Fe<sup>2+</sup> is in the low-spin (S = 0) state. The formula is more correctly written as Fe<sub>4</sub>Si<sub>2</sub>Sn<sub>7</sub>O<sub>16</sub> to differentiate the one LS-Fe<sup>2+</sup> per formula unit in the intermetallic layer from the three HS-Fe<sup>2+</sup> per formula unit in the kagomé oxide layer.

Fe<sub>4</sub>Si<sub>2</sub>Sn<sub>7</sub>O<sub>16</sub> also has a unique magnetic ground state below a Néel ordering temperature T<sub>N</sub> = 3.5 K, in which the spins on 2/3 of the Fe<sup>2+</sup> sites in the kagomé oxide layers order antiferromagnetically, while 1/3 remain disordered and fluctuating down to at least 0.1 K. [3] The nature and origin of this unique “striped” partial spin-liquid state is unclear. The fact that it breaks trigonal symmetry, which the more conventional q = 0 or √3×√3 kagomé states would not, raises the possibility that the anisotropic distribution of the 6 unpaired spins on HS-Fe<sup>2+</sup> (t<sub>2g</sub><sup>4</sup>e<sub>g</sub><sup>2</sup>) plays a role. To test this possibility, we have now synthesised an isotropic analogue with a kagomé lattice of HS Mn<sup>2+</sup> (t<sub>2g</sub><sup>3</sup>e<sub>g</sub><sup>2</sup>), by co-substituting Ge<sup>4+</sup> for Si<sup>4+</sup> in the bridging/stannite layers to match the lattice dimensions between layers.

We found that FeMn<sub>3</sub>Ge<sub>2</sub>Sn<sub>7</sub>O<sub>16</sub> has the same “striped” magnetic ground state as Fe<sub>4</sub>Si<sub>2</sub>Sn<sub>7</sub>O<sub>16</sub>, in the same temperature range, ruling out this explanation. However, the zero-field striped structure is collinear for FeMn<sub>3</sub>Ge<sub>2</sub>Sn<sub>7</sub>O<sub>16</sub> vs. non-collinear for Fe<sub>4</sub>Si<sub>2</sub>Sn<sub>7</sub>O<sub>16</sub>, which may indeed be a consequence of the change in anisotropy on the magnetic kagomé site, and suggests that FeMn<sub>3</sub>Ge<sub>2</sub>Sn<sub>7</sub>O<sub>16</sub> is an even more ideal spin-liquid candidate than Fe<sub>4</sub>Si<sub>2</sub>Sn<sub>7</sub>O<sub>16</sub>. We also found that an external applied magnetic field lifts the degeneracy on the disordered site, giving rise to another ordered magnetic structure never before observed nor predicted on a kagomé lattice.

### References

- [1] Söhnel, T., et al., *Z. Anorg. und Allg. Chemie* **624**, 708–714 (1998).
- [2] Allison, M.C., et al., *Dalton Trans.* **45**, 9689–9694 (2016).
- [3] Ling, C.D., et al., *Phys. Rev. B* **9**, 180410 (2017).

## Spin Mechatronics in Spintronics

Sadamichi Maekawa<sup>1,2</sup>

<sup>1</sup>*RIKEN Center for Emergent Matter Science (CEMS), Wako, 351-0198, Japan*

<sup>2</sup>*Kavli ITS at University of Chinese Academy of Sciences, Beijing, China*

Albert Einstein together with de Haas showed the equivalence of magnetism and mechanical rotation in 1915 [1]. In the same year, Barnett found that mechanical rotation can generate a magnetic field even in a body with no electric charge [2]. The year, 1915, was that of the discovery of the general relativity by A. Einstein. These phenomena are caused by the angular momentum conservation between electron spin and mechanical rotation, which is proved in the general relativistic quantum mechanics [3].

The recent progress of nano-technology has made it possible to extend the coupling of electron spin and mechanical motion to Spintronics. We examine a variety of novel spintronics phenomena due to mechanical motion. In particular, we find that the angular momentum compensation in ferrimagnets may be detected by the mechanical rotation [4]. We show the generation of spin current by the flow of liquid metals [5], that of liquid <sup>3</sup>He [6], and by the rotating surface acoustic waves [7]. The reverse effect, namely, the mechanical force due to spin current is also observed [8]. The mechanical generation of spin current opens a door from "Spintronics" to "Spin-Mechatronics" [9].

### References

- [1] A.Einstein and W.J.de Haas, *Verhandl.Deut.Physik.Ges.*, **17**,154 (1915).
- [2] S.J.Bernett, *Phys. Rev.* **6**, 239 (1915).
- [3] See, for example, M.Matuo, J.Ieda and S.Maekawa, *Phys. Rev. Lett.* **106**, 076601 (2011).
- [4] M.Imai, S.Maekawa, et al., *Appl. Phys. Lett.*, **114**, 162402 (2019).
- [5] R.Takahashi, M.Ono, K.Harii, S.Okayasu, M.Matsuo, J.Ieda, S.Takahashi, S.Maekawa and E.Saitoh, *Nature Phys.* **12**, 52 (2015).
- [6] Y. Tsutsumi and S.Maekawa, to be published in *J. Low Temp. Phys.*
- [7] D.Kobayashi, M.Matsuo, S.Maekawa, Y.Nozaiki, et al., *Phys. Rev. Lett.* **119**, 077202 (2017).
- [8] K.Harii, M.Matsuo, S.Maekawa, E.Saitoh, et al., *Nature Commun.* **10**, 2616 (2019).
- [9] *Spin Current (Second Edition)*, eds. S. Maekawa *et al.* (Oxford University Press, 2017).

## Stabilizing even-parity chiral superconductivity in Sr<sub>2</sub>RuO<sub>4</sub>

Han Gyeol Suh<sup>1</sup>, Henri Menke<sup>2</sup>, P. M. R. Brydon<sup>2</sup>, Carsten Timm<sup>3</sup>, Aline Ramires<sup>4,5,6</sup>,  
and Daniel F. Agterberg<sup>1</sup>

<sup>1</sup>*Department of Physics, University of Wisconsin, Milwaukee, WI 53201, USA*

<sup>2</sup>*Department of Physics and MacDiarmid Institute for Advanced Materials and Nanotechnology, University of Otago, P.O. Box 56, Dunedin 9054, New Zealand*

<sup>3</sup>*Institute for Advanced Studies, Institute of Theoretical Physics, Technische Universität Dresden, 01062 Dresden, Germany*

<sup>4</sup>*Max Planck Institute for the Physics of Complex Systems, Dresden, 01187, Germany*

<sup>5</sup>*ICTP-SAIFR, International Centre for Theoretical Physics, South American Institute for Fundamental Research, São Paulo, SP, 01140-070, Brazil*

<sup>6</sup>*Instituto de Física Teórica, Universidade Estadual Paulista, São Paulo, SP, 01140-070, Brazil*

For a long time Sr<sub>2</sub>RuO<sub>4</sub> was believed to be a textbook example of an odd-parity *p*-wave superconductor. This view has recently been challenged after early Knight shift measurements have been revisited, revealing a suppression below  $T_c$  [1]. In this work we investigate the stability of alternative pairing states, in particular an even-parity chiral *d*-wave state, which is consistent with the observation of time-reversal symmetry breaking and a jump in the shear modulus  $c_{66}$ . To this end we decompose on-site interactions of the Hubbard-Kanamori type in the Cooper channel where the two-component nature of the order parameter is encoded in the orbital degree of freedom. An orbital-antisymmetric spin-singlet pairing state in the  $E_g$  irrep can be stabilized by momentum-dependent spin-orbit coupling, but only if the full three-dimensional bandstructure is taken into account [2], see Fig. 1.

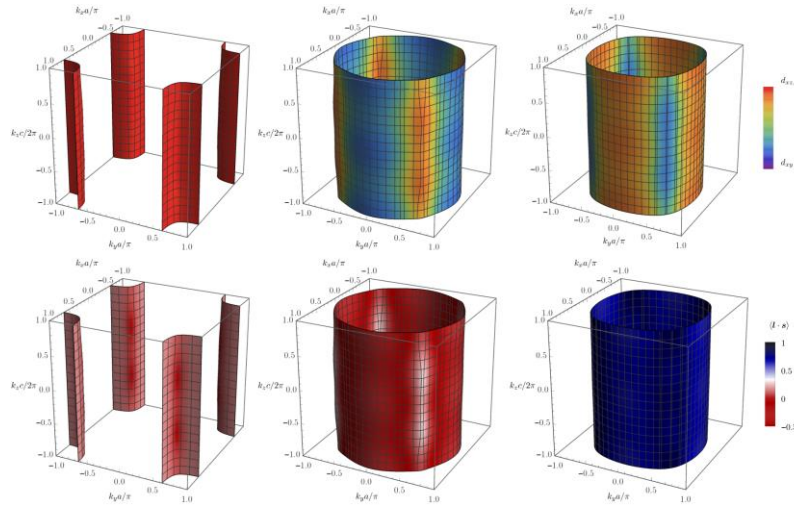


**Fig. 1:** Three-dimensional Fermi surface of Sr<sub>2</sub>RuO<sub>4</sub> obtained from fitting to a DFT model [2]. The color indicates the orbital (upper row) and spin polarization (lower row).

## References

- [1] A. Pustogow *et al.*, Nature **574**, 72–75 (2019).
- [2] C.N. Veenstra *et al.*, Phys. Rev. Lett. **112**, 127002 (2014).

## Symmetry analysis of the ferroic transitions in the coupled honeycomb system (Fe, Co, Mn)<sub>4</sub>Ta<sub>2</sub>O<sub>9</sub>

N. Narayanan<sup>1,2\*</sup>, T. Faske<sup>3</sup>, T. Lu<sup>1</sup>, Z. Liu<sup>1</sup>, M. Brennan<sup>1</sup>, J. Hester<sup>2</sup>, M. Avdeev<sup>2</sup>, A. Senyshyn<sup>4</sup>, D. Mikhailova<sup>5</sup>, H. Ehrenberg<sup>6</sup>, W. D. Hutchison<sup>7</sup>, R. Mole<sup>2</sup>, H. Fuess<sup>3</sup>, G. J. McIntyre<sup>2</sup>, Y. Liu<sup>1</sup>, and D. Yu<sup>2</sup>

<sup>1</sup>Research School of Chemistry, The Australian National University, ACT 2601, Australia.

<sup>2</sup>Australian Nuclear Science and Technology Organisation (ANSTO), Lucas Heights NSW 2234, Australia.

<sup>3</sup>Institute for Materials Science, Darmstadt University of Technology, 64287 Darmstadt,

<sup>4</sup>Heinz Maier-Leibnitz Zentrum (MLZ), 85748 Garching, Germany.

<sup>5</sup>Leibniz Institute for Solid State and Materials Research (IFW) Dresden, D-01069 Dresden, Germany.

<sup>6</sup>Institute for Applied Materials (IAM), Karlsruhe Institute of Technology (KIT), D-76344 Eggenstein-Leopoldshafen, Germany.

<sup>7</sup>School of PEMS, The University of New South Wales Canberra at ADFA, ACT 2600, Australia.

Exotic phenomena such as spin liquid, spin-orbital entities, magnetic order induced multiferroicity (type ii) or quantum criticality have recently triggered extensive research on the ground state properties of frustrated magnetic systems. The ground states of these compounds are determined by the coupling of the spin to the orbital, charge and lattice degrees of freedom. One of the extensively investigated lattices is the honeycomb lattice due to the development of the Kitaev model for quantum spin liquids [1-2]. In this work, we are interested in the coupled honeycomb system M<sub>4</sub>A<sub>2</sub>O<sub>9</sub> (M=Fe, Co and Mn and A=Nb, Ta). All members have two crystallographically distinct M sites, which are in the distorted octahedral oxygen cages. These cages form edge-shared coplanar and corner-shared buckled honeycombs respectively which are interconnected in the perpendicular direction leading to competing exchange paths. The M=Co and Mn members were magnetoelectrics, whereas Fe<sub>2</sub>Ta<sub>2</sub>O<sub>9</sub> was reported to exhibit both magnetoelectric and (type ii) multiferroic phases depending on the temperature [3-4]. Magnetoelectrics and multiferroics are technically highly relevant with a variety of applications such as MRAMs and field sensors. However, the coupling mechanism is very complicated [5]. Furthermore, due to the group properties of the symmetry analysis methods such as representation analysis and magnetic space groups, the magnetic structure of the Nb counterpart Co<sub>4</sub>Nb<sub>2</sub>O<sub>9</sub> is controversially discussed. It is therefore apparent that the above discussed diversities of the properties are determined by the magnetic structure and the closely related electronic structure. These can be elucidated by investigating the structure and dynamics of these compounds, which will help to understand the emergence of different ground states and the diverse phase transitions in this family of materials. In this work, we systematically investigate the magnetic and electronic structure of the (Fe, Co, Mn)<sub>4</sub>Ta<sub>2</sub>O<sub>9</sub> system. We combined several different techniques of neutron powder diffraction, inelastic neutron scattering, heat capacity, electronic band structure calculations and spin wave modeling based on linear spin wave theory.

### References

- [1] H. Tagaki et al., *Nat. Rev. Phys.* 1, 264 (2019).
- [2] Y. J. Choi et al., *PRL* 110, 157202 (2013)
- [3] N. D. Khanh et al., *PRB* 93, 075117 (2016)
- [4] A. Maignan et al., *PRM* 2, 091401(R) (2018).
- [5] S.-W. Cheong et al., *Nat. Mater.* 6, 13 (2007).

## Ferromagnetic Ni<sub>1-x</sub>Fe<sub>x</sub> nanofibers produced by electrospinning

Tehreema Nawaz<sup>1</sup>, Grant V.M. Williams<sup>1</sup>, Martyn P. Coles<sup>1</sup>, and Shen V. Chong<sup>2</sup>

<sup>1</sup>*School of Chemical and Physical Sciences, Victoria University of Wellington, PO Box 600, Wellington, New Zealand*

<sup>2</sup>*Robinson Research Institute, Victoria University of Wellington, PO Box 33436, Lower Hutt 5046, New Zealand*

Magnetic nanomaterials are well known for their intriguing properties such as superparamagnetism, enhanced coercivity and exchange bias that have been utilized in a variety of applications in drug delivery, magnetic memory devices, spintronic devices, and sensors etc.<sup>1, 2</sup> Bimetallic Ni<sub>1-x</sub>Fe<sub>x</sub> nanomaterials are particularly interesting because the bulk material has a very high magnetic permeability. They can also display a magnetoresistance from spin tunnelling between nanoparticles.<sup>3</sup> Recently, one dimensional nanofibers have gained popularity due to their uniaxial direction and narrow diameter that makes them favourable in nano-flux guiding and electromagnetic device systems.<sup>4</sup>

Herein, we report the fabrication of quasi-one-dimensional nanofibers with two different concentrations of x~0.1 and 0.2 using the electrospinning method. Both concentrations have shown nucleation of a bimodal nanoparticle size distribution (see Fig. 1 for x~0.1). There are smaller nanoparticles embedded within the fiber and larger nanoparticles on the surface. There are some structural differences e.g. more and larger surface nanoparticles for x~0.1. The saturation moment per gram of nanofibers (Fig. 1) is high for x~0.1 when compared with the bulk compound.

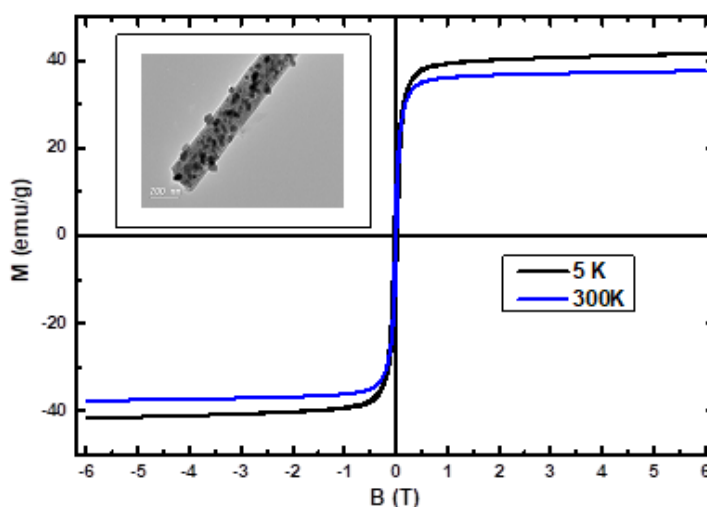


**Fig. 1:** Magnetic data from Ni<sub>0.9</sub>Fe<sub>0.1</sub> nanofiber. inset: TEM for x~0.1

### References

1. Williams, G. V. M.; Kennedy, J.; Murmu, P. P.; Rubanov, S. *Applied Surface Science* **2018**, 449, 399-404.
2. Williams, G. V. M.; Kennedy, J.; Murmu, P. P.; Rubanov, S.; Chong, S. V. *Journal of Magnetism and Magnetic Materials* **2019**, 473, 125-130.
3. Prakash, T.; Williams, G. V. M.; Kennedy, J.; Murmu, P. P.; Leveneur, J.; Chong, S. V.; Rubanov, S. *Journal of Alloys and Compounds* **2014**, 608, 153-157.
4. Bayat, M.; Yang, H.; Ko, F. K.; Michelson, D.; Mei, A. *Polymer* **2014**, 55, (3), 936-943.



## Demonstrating the Hot Carrier Solar Cell Through Broadband Absorption and Resonant Carrier Extraction

M. P. Nielsen<sup>1</sup>, J. A. R. Dimmock<sup>2,3</sup>, and N. J. Ekins-Daukes<sup>1</sup>

<sup>1</sup>*School of Photovoltaic and Renewable Energy Engineering, University of New South Wales, Sydney, NSW, 2052, Australia*

<sup>2</sup>*Quantum Motion Technologies, Leeds Innovation Centre, Leeds, LS2 9DF, UK*

<sup>3</sup>*Sharp Laboratories of Europe Ltd, Oxford, OX4 4GB, UK*

Conventional photovoltaics are ultimately limited in efficiency because a broad spectrum of light (and thus energies) is used to drive essentially a two-level system. Thus, the largest loss channel in conventional photovoltaic cells are thermalization losses as excited carriers with energy in excess of the absorber bandgap lose this excess energy to the lattice as heat before carriers are extracted at the conduction and valence band edge. In contrast, the hot carrier solar cell operates analogous to a heat engine by maintaining carriers in the absorber and collector at two different temperatures and allowing only energy selective extraction of carriers from the hotter region to the colder region. By utilizing the excess thermalization energy, the hot carrier cell has an extraordinary limiting efficiency of 85% [1]. To approach this limiting efficiency, a hot carrier solar cell must meet several criteria. Firstly, the absorber should have a high absorption coefficient across a broadband spectral range and slow electron-phonon interactions to enable efficient extraction before carrier thermalization with the lattice. Secondly, the carrier extraction must be done through energy selective contacts to enable recycling of excess carrier energy.

Here we present recent experimental demonstrations of hot carrier solar cells using both semiconductor [2-4] and metallic absorbers [5]. The use of a metallic absorber is of particular interest for next generation thin film solar cells as a metal layer on the order of 10nm can almost completely absorb broadband sunlight as previously demonstrated in the infrared [6]. By depositing a thin chromium absorber layer on an AlGaAs-based resonant tunnel diode as the selective energy contact a hot carrier photocurrent has been experimentally demonstrated. By comparing the IV characteristics of this structure against an equivalent Schottky diode formed of Cr/AlGaAs we demonstrate that the photocurrent arises from a hot carrier population as opposed to internal photoemission. This distinction is key to the demonstration of any hot carrier device as only the hot carrier device can attain high power conversion efficiency. Future improvements and study of this device through ultrafast spectroscopy will be discussed along with the potential for alternative applications such as photon energy resolving photodetection.

### References

- [1] R. T. Ross and A. J. Nozik, *J. Appl. Phys.* **53**, 3813-8 (1982).
- [2] L. C. Hirst et al, *Applied Physics Letters* **104**, 231115 (2014).
- [3] J. A. R. Dimmock et al, *Progress In Photovoltaics* **22**, 151–60 (2014).
- [4] J. A. R. Dimmock et al, *Journal of Optics* **18**, 074003 (2016).
- [5] J. A. R. Dimmock et al, *Semiconductor Science & Technology* (Special Issue on Hot Carrier Solar Cells), Submitted (2019).
- [6] C. Hilsum, *Journal of the Optical Society of America* **44**, 188–91 (1954).

## Carbon molecules in space: a thermal Equation of State study of solid hexamethylenetetramine

G. Novelli<sup>1,2</sup>, G. J. McIntyre<sup>2</sup>, H. E. Maynard-Casely<sup>2</sup>, W. G. Marshall<sup>3</sup>, K. V. Kamenev<sup>4</sup> and S. Parsons<sup>1</sup>

<sup>1</sup>*School of Chemistry, The University of Edinburgh, King's Buildings, Edinburgh, Scotland, United Kingdom*

<sup>2</sup>*Australian Nuclear Science and Technology Organisation, Lucas Heights, Sydney, New South Wales, Australia*

<sup>3</sup>*ISIS Pulsed Neutron and Muon Facility, STFC Rutherford Appleton Laboratory, Didcot, United Kingdom*

<sup>4</sup>*Centre for Science at Extreme Conditions and School of Engineering, The University of Edinburgh, King's Buildings, Edinburgh, Scotland, United Kingdom*

Properties such as compressibility, thermo-elasticity and the energy landscape remain unknown for many organic compounds under conditions encountered on extraterrestrial planets and moons and in space. In this study, a thermal Equation of State (EoS) for the crystalline solid hexamethylenetetramine was determined by neutron powder diffraction in the temperature and pressure ranges of 113–480 K and 0–5 GPa, respectively. The material was chosen as a molecular model for its high symmetry and its property of remaining in the same phase throughout the experimental conditions selected to simulate the planetary environments.

Equations of States (EoSs) show how the thermodynamic variables of temperature ( $T$ ), pressure ( $P$ ) and volume ( $V$ ) are inter-related. The ideal gas law,  $PV = nRT$ , is an example of an EoS which is used as a simple but effective model to explain the properties of gases. More complex EoSs, where the assumption of ideality is relaxed, can be applied to solids in order to describe how the geometry and energy transform when they experience dramatic changes in their environment. Such information acquires enormous importance in planetary materials science, where scientists are trying to understand the fate of carbon, the fourth most abundant element in our galaxy, in the context of the origin of life and planetary environments. Despite the large heterogeneity of galactic and interstellar regions, the organic chemistry of the universe seems to follow common pathways. Molecules of high astrobiological and astrophysical relevance such as amino acids,<sup>1</sup> polyaromatic hydrocarbons, and N-heterocycles<sup>2</sup> have been identified across the solar system, but how they behave under such varied conditions is a question yet to be answered.

Key to our approach was the determination of how the internal energy ( $U$ ), entropy ( $S$ ) and the Gibbs free energy ( $G$ ) vary with pressure not only computationally, but also, and for the first time, experimentally.<sup>3</sup> A new method has been developed, able to transform directly variable-PT crystallographic data into thermodynamic information. Although it is quite common to model thermal expansion at ambient pressure with a VT-EoS, and compression at ambient temperature using a PV-EoS, determinations of PVT-EoSs are much less common, particularly for organic materials.<sup>4</sup> This paucity of PTV-EoSs reflects the difficulty of varying pressure and temperature simultaneously in crystallographic experiments, especially at reduced temperatures. The task was addressed in this study by the variable-temperature insert for the Paris-Edinburgh press available on the PEARL instrument at the ISIS Neutron Spallation Source (UK).<sup>5</sup> The results were successfully combined with periodic DFT (Figure 1) and other semi-empirical calculations, where pressure and temperature can be included at little time cost, enabling the stability profile of the material to be understood, right down to the level of individual intermolecular interactions.

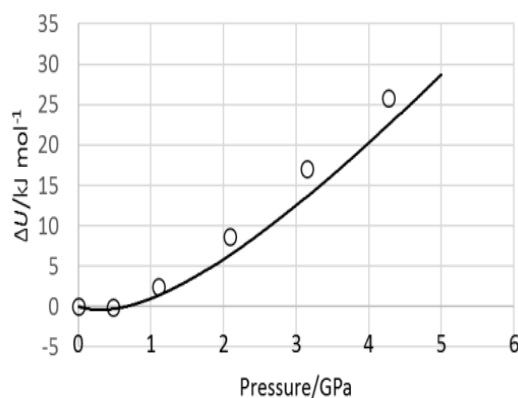


**Fig. 2:** Variation of internal energy with pressure for hexamethylenetetramine determined by periodic DFT (open circles) and experimentally from thermal equation of state measurements (solid line).

1. Elsilá, J. E. *et al. Meteoritics & Planetary Science* **44** (2009) 1323-1330
2. Ehrenfreund, P. *et al. Faraday Discussions* **133** (2006) 277-288
3. Novelli, G. *et al. In preparation* (2019). Poster MS15-Po3 ECM, Oviedo 2018. Winner, IUCr Applied Crystallography poster prize.
4. Likhacheva, A. Y. *et al. The Journal of Chemical Physics* **140** (2014) 164508
5. Bull, C. L. *et al. High Pressure Research* **36** (2016) 493-511

# Anomalous Spectral Broadening from an Infrared Catastrophe in 2D Quantum Antiferromagnets

Matthew C. O'Brien and Oleg P. Sushkov

*School of Physics, The University of New South Wales, Sydney, Australia*

Infrared divergences due to the emission of radiation by charged particles are well understood in particle physics. The gauge nature of massless force carriers allows infinitely many excitations with arbitrarily low energies to be produced during scattering events [1,2]. Similarly, in systems with a spontaneously broken continuous symmetry, the emergence of gapless Goldstone particles [3], ensures the relevance of infrared physics. Together with the enhancement of fluctuations in low spatial dimensions, this leads to considerable obstacles in developing accurate theoretical models of many-body systems, particularly in two dimensions, where exact methods are much rarer than in one dimension. This is the case for two-dimensional quantum antiferromagnets at finite temperature, which continue to challenge physicists despite decades of research [4-6]. In this talk, we report the first theoretical observation of the phenomenon of thermal *bremssstrahlung* in the context of easy-plane antiferromagnets. We present an exact solution of the response of this system to a scattered external probe, and demonstrate that not only is elastic scattering forbidden, but an infinite number of Goldstone quasiparticles are always excited in the process. We also propose a roadmap for understanding the behaviour of Heisenberg antiferromagnets, as well as electron-phonon interactions in graphene.

## References

- [1]. Bloch, F. & Nordsieck, A. Note on the Radiation Field of the Electron. *Phys. Rev.* **52**, 54-59 (1937).
- [2]. Weinberg, S. Infrared Photons and Gravitons. *Phys. Rev.* **140**, B516–B524 (1965).
- [3]. Goldstone, J., Salam, A. & Weinberg, S. Broken Symmetries. *Phys. Rev.* **127**, 965–970 (1962).
- [4]. Chakravarty, S., Halperin, B. I. & Nelson, D. R. Two-dimensional quantum Heisenberg antiferromagnet at low temperatures. *Phys. Rev. B* **39**, 2344–2371 (1989).
- [5]. Tyč, S. & Halperin, B. I. Damping of spin waves in a two-dimensional Heisenberg antiferromagnet at low temperatures. *Phys. Rev. B* **42**, 2096–2115 (1990).
- [6]. Chubukov, A. V, Sachdev, S. & Ye, J. Theory of two-dimensional quantum Heisenberg antiferromagnets with a nearly critical ground state. *Phys. Rev. B* **49**, 11919–11961 (1994).

## Realization of an Acoustic Supercoupler using Density-Near-Zero Metamaterial

Choon Mahn Park<sup>1</sup>, Sang Hun Lee<sup>2</sup>

<sup>1</sup>*Department of Materials Physics, Dong-A University, Saha-gu, Busan, 49315, Republic of Korea.*

<sup>2</sup>*Department of Physics, Sogang University, Mapo-gu, Seoul 04107, South Korea.*

When elastic membranes of mass  $M$  and cross-sectional area  $A_{ch}$  are installed periodically with distance of  $d$  as lumped elements within a one-dimensional acoustic wave guide filled with air, the motion of the membrane acts as a dynamic restoring force. As a result, the motion of the air with acceleration is affected, and the effective mass density of the medium is changed[1].

We made an acoustic metamaterial of density near zero with thin PVC membranes used as a lumped element. A sub-wavelength acoustic tunnel was created using this metamaterial. Even though this tunnel with diameter of  $\lambda/40$  has a cross sectional area only 2.25% of a normal wave guide, it acts as nearly perfect acoustic supercoupler by transmitting 95.1% of the acoustic energy without phase delay. This result could open new possibilities for developing various devices in the fields of noise control, signal processing and medical imaging that use acoustic waves.

### References

[1]. S. H. Lee. *et al.*, Phys. Lett. A 373, 4464 (2009).

## Spin-Liquid State in Planar Heisenberg Models

P. Prelovšek<sup>1,2</sup>

<sup>1</sup>*J. Stefan Institute, Ljubljana, Slovenia*

<sup>2</sup>*Faculty of Mathematics and Physics, University of Ljubljana, Ljubljana, Slovenia*

Motivated by recent experiments, revealing a spin liquid in layered 1T-TaS<sub>2</sub> [1], being a block-spin system on a triangular lattice, we consider several frustrated planar Heisenberg models and calculate their finite-temperature static and dynamical properties. Using mostly the numerical FTLM approach based on exact diagonalization of small clusters, we show that the frustration enables reliable results to considerably lower  $T$  relative to unfrustrated lattices [2]. The reduced-basis approach will be also presented, using the triangle as the basic unit, which allows for a unified treatment of Heisenberg models on triangular and kagome lattices and reveals the similarity of thermodynamic quantities on both lattices in their spin-liquid regimes [3]. The hallmark of the similarity of spin-liquid regimes, also in several other planar models, is the generalised Wilson ratio which vanishes at low temperatures, indicating the predominant role of low-lying singlet excitations over the triplet ones [4], which is in contrast to reference one-dimensional Heisenberg model. The relevance and comparison of theoretical results with the experimental ones on spin liquids in real materials, in particular those on kagome lattices, will be also discussed.

### References

- [1] M. Klanjšek et al., Nat. Phys. **13**, 1130 (2017).
- [2] P. Prelovšek and J. Kokalj, Phys. Rev. B **98**, 035107 (2018).
- [3] P. Prelovšek and J. Kokalj, arXiv:1906.11576 (2019).
- [4] P. Prelovšek, K. Morita, T. Tohyama, and J. Herbrych, in preparation.

## High-Temperature Majorana Fermions in Magnet-Superconductor Hybrid Systems

Daniel Crawford<sup>1</sup>, Eric Mascot<sup>2</sup>, Dirk K. Morr<sup>2</sup>, Stephan Rachel<sup>1</sup>

<sup>1</sup>*School of Physics, University of Melbourne, Parkville, VIC 3010 Australia*

<sup>2</sup>*University of Illinois at Chicago, Chicago, IL 60607, USA*

Magnet-superconductor hybrid structures represent one of the most promising platforms to realize, control and manipulate Majorana modes using scanning tunneling methods. By depositing either chains or islands of magnetic atoms on the surface of a conventional superconductor such as Pb or Re, topological superconducting phases can emerge. They feature either localised Majorana bound states at the chain ends or dispersing chiral Majorana modes at the island's boundary. Yet many of these experiments have not reached the spectral resolution to clearly distinguish between topological Majorana and trivial Shiba peaks due to tiny gap sizes in experiments performed at sub-Kelvin temperatures. Here we consider superconducting substrates with unconventional spin-singlet pairing, including high-temperature d-wave and extended s-wave superconductors. We derive topological phase diagrams and compute edge states for cylinder and island geometries and discuss their properties. Also various time-reversal invariant topological superconducting phases of the

Zhang-Kane-Mele type are found and discussed. Quite generally, we find that unconventional superconducting substrates work as well as the conventional s-wave substrates to realize topological phases. In particular, iron-based pnictide and chalcogenide superconductors are the most promising class of substrates for accessing Majorana modes in high-temperature magnet-superconductor hybrid systems.

## From Sticky Hard Spheres to Lennard-Jones potentials and many-body expansions for rare gas solids.

P. Schwerdtfeger<sup>1,2</sup>, L. Trombach<sup>1</sup>, O. Smits<sup>1</sup>, A. Burrows<sup>1</sup>

<sup>1</sup> Centre for Theoretical Chemistry and Physics, The New Zealand Institute for Advanced Study (NZIAS), Massey University, Auckland, New Zealand

<sup>2</sup> Centre for Advanced Study (CAS) at the Norwegian Academy of Science and Letters, Drammensveien 78, NO-0271 Oslo, Norway

The Lennard-Jones (LJ) potential is the most widely used interaction potential between atoms with widespread applications in physical, chemical and biological sciences. This simple potential also has the advantage that the cohesive energy, pressure and the bulk modulus of a simple solid (simple cubic, body-centered cubic, and face-centered cubic) can be expressed analytically as a function of volume using lattice sums in three dimensions, originally developed by Hund, Born and Lennard-Jones [1]. Changing the LJ parameter allows to study the limit towards sticky hard spheres extensively used in nucleation theory [2]. By doing this, we can show for the first time an exponential increase in the number of minima with number of atoms in a cluster. Moreover, through many-body expansions using computer intensive relativistic coupled cluster methods we can get the cohesive energy for solid argon accurate to within 1 J/mol and within experimental accuracy [3]. This allows for the accurate simulation of melting of the rare gas solids with an accuracy of a few Kelvin [4], and to predict that the heaviest element in the periodic table, the rare gas element oganesson, is indeed rare but not a gas.

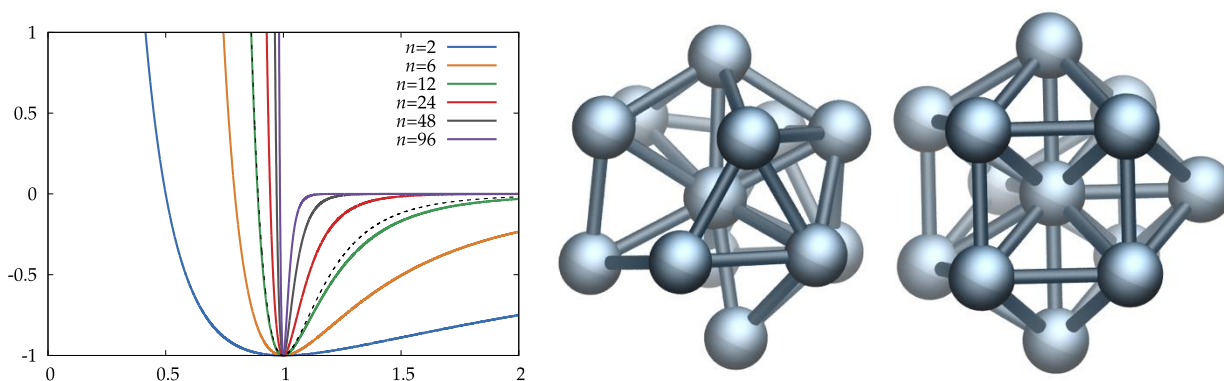


**Fig. 1:** From the Lennard-Jones potential to the limit of sticky hard spheres. If one allows for attractive interactions between hard spheres the ideal icosahedron will distort into 737 nonisomeric structures with two of them shown here.

$$V(r)/e = \left[ \left( \frac{r_e}{r} \right)^{2n} - 2 \left( \frac{r_e}{r} \right)^n \right]$$

### References

- [1] P. Schwerdtfeger *et al.*, Phys. Rev. B **73**, 064112 (2006).
- [2] L. Trombach *et al.*, Phys. Rev. E **97**, 043309 (2018).
- [3] P. Schwerdtfeger *et al.*, Angew. Chem. Int. Ed. **55**, 12200 (2016).
- [4] O. Smits *et al.*, Angew. Chem. Int. Ed. **57**, 9961 (2018).

## Tuning Magnetic Frustration in Bixbyites

M. Spasovski<sup>1,2</sup>, M. Avdeev<sup>3</sup>, T. Söhnel<sup>1,2</sup>

<sup>1</sup>*School of Chemical Sciences, University of Auckland, Auckland, New Zealand*

<sup>1</sup>*MacDiarmid Institute of Advanced Materials and Nanotechnology, Victoria University of Wellington, New Zealand*

<sup>3</sup>*Australian Nuclear and Science Technology Organisation (ANSTO), Australia*

The cubic bixbyite structure ( $\alpha$ - $\text{Mn}_2\text{O}_3$ ) has a deep history in solid-state chemistry, the first structural solution was completed by Zachariasen and later corrected by Pauling.[1] Related to the fluorite structure with  $\frac{1}{4}$  of the anions removed, these vacancies force the displacement of the remaining anions changing the coordination from cubic to strongly distorted octahedra. Today bixbyites are commonplace in every household found in everything from batteries, TV monitors and touch screens to industry catalysts.

The ternary oxide  $\text{Cu}_3\text{TeO}_6$  is an ordered bixbyite that has been the focus of intense study due to its interesting magnetic spin-web structure.[2-5] We have synthesized powders and single crystals from the solid solution  $\text{Cu}_{2.25+3x/4}\text{Sb}_{1-x}\text{Te}_x\text{O}_{4.75+5x/4}$ , Ga and Mn doped variants. Through single crystal, powder X-ray diffraction (XRD) and neutron diffraction (ND) we have seen that the bixbyite lattice can accommodate for a large variation of dopant pressure through site disorder and defects.[6] K and L-edge X-ray absorption spectroscopy has shown the bixbyite structure will also accommodate a large variation of charged species which when coupled with defects and site disorder manifests itself into interesting frustrated magnetic structures varying from canonical spin-glasses to complex anti-ferromagnetic order.

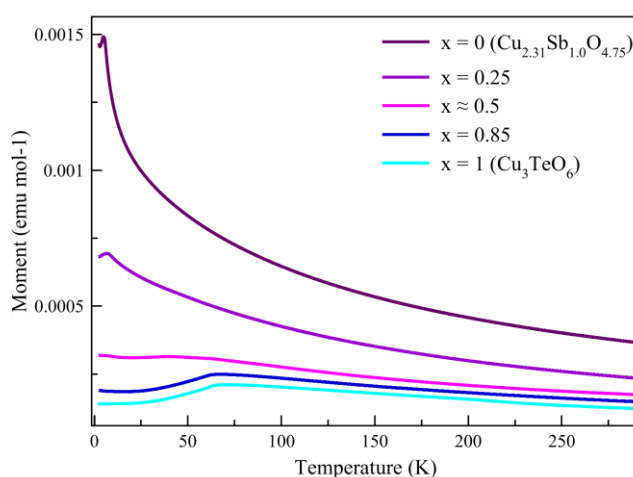


**Fig. 1:** Magnetic susceptibility for members of the  $\text{Cu}_{2.25+3x/4}\text{Sb}_{1-x}\text{Te}_x\text{O}_{4.75+5x/4}$  solid solution.

### References

- [1]. L. Pauling *et al.*, *Kristallogr. Cryst. Mater.* **1930**, 75, 128.
- [2]. L. Falck, O. Lindqvist *et al.*, *Acta Crystallog. B* **1978**, 34, 896 – 897.
- [3]. M. Herak *et al.*, *J. Phys. Cond. Mat.* **2005**, 17, 7667 – 7679.
- [4]. W. Yao *et al.*, *Nat. Phys.* **2018**, 14, 1011 – 1015.
- [5]. S. Bao *et al.*, *Nat. Comm.* **2018**, 9, 2591.
- [6]. M. Spasovski *et al.*, *Chem. Asian J.* **2019**, 14, 1286 – 1292.



## **Towards a single-model description of cuprates in the pseudogap state**

J.G. Storey<sup>1,2</sup>

<sup>1</sup>*Robinson Research Institute, Victoria University of Wellington, Wellington, New Zealand*

<sup>2</sup>*MacDiarmid Institute, Wellington, New Zealand*

Occupying a large tract of the phase diagram, the pseudogap is one of the most studied aspects of cuprate superconductors. For decades the most advanced techniques have been brought to bear on the pseudogap, and yet questions remain concerning its origin, and its relation to superconductivity as a collaborator, controller, competitor or cohabiter.

Understanding the vast amount of data gathered depends on the models used to interpret it. In this talk I will demonstrate how the observed electronic, thermodynamic, transport and spectroscopic properties lead us toward a Fermi surface reconstruction model for the pseudogap state. The implications and remaining knowledge gaps will be discussed.

## NMR and thermodynamic studies of cuprate high- $T_c$ superconductors

J. L. Tallon<sup>1</sup>

<sup>1</sup>Robinson Research Institute, Victoria University of Wellington,  
PO Box 33436, Lower Hutt 5046, New Zealand

NMR Knight shift and electronic specific heat measurements are presented for  $\text{YBa}_2\text{Cu}_3\text{O}_{7-d}$  and  $\text{YBa}_2\text{Cu}_4\text{O}_8$  along with several other cuprates, both underdoped and overdoped. The remarkable quantitative correspondence between the spin susceptibility and the entropy shows that the thermodynamic properties are those of a weakly interacting Fermion system despite the obvious presence of strong correlations and other competing correlations such as the pseudogap and charge order. This places strong constraints on the as-yet unresolved theory of cuprate superconductivity. These measurements enable the phase diagram to be mapped in considerable detail and the features that emerge play an exceedingly important role in practical applications.

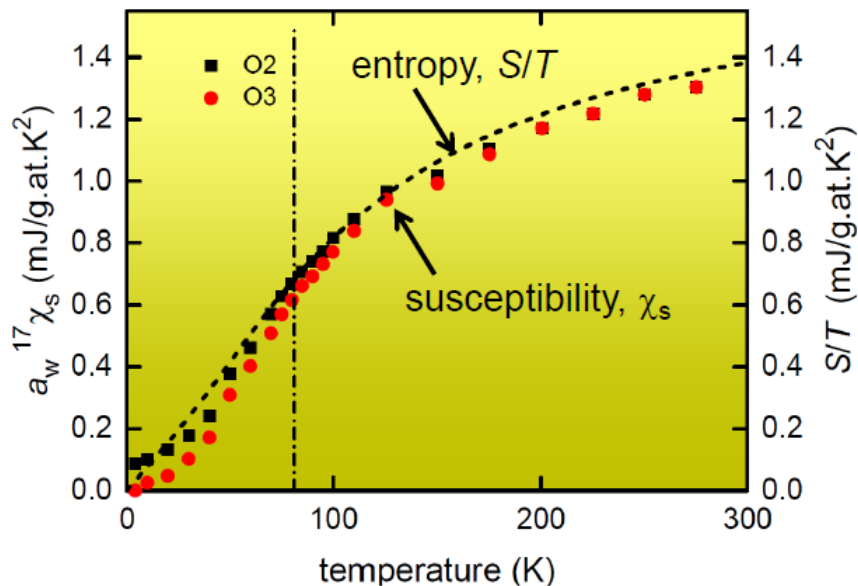


**Fig. 1:** The spin susceptibility derived from  $^{17}\text{O}$  Knight shift [1] in entropy units (red and black symbols) plotted along with the normal-state electronic entropy,  $S/T$ , for the archetypal underdoped cuprate superconductor  $\text{YBa}_2\text{Cu}_4\text{O}_8$ . The two quantities are quantitatively related by the Wilson ratio,  $a_w$ , a combination of fundamental constants. The suppression with decreasing temperature is due to the pseudogap, present in all underdoped cuprates. The splitting in the Knight shift below 200 K reveals the onset of electronic nematicity within the pseudogap state.

### References

- [1]. I. Tomeno *et al.*, Phys. Rev. B **49**, 15327 (1994).

## Tuning Skyrmion Hall effect via Engineering of Spin-orbit Interaction

C.A. Akosa<sup>1</sup>, H. Li<sup>2</sup>, G. Tatara<sup>1</sup>, O.A. Tretiakov<sup>3</sup>

<sup>1</sup>*RIKEN Center for Emergent Matter Science, Wako, Japan*

<sup>2</sup>*School of Physics and Electronics, Henan University, Kaifeng, China*

<sup>3</sup>*School of Physics, University of New South Wales, Sydney, Australia*

We demonstrate that the Magnus force acting on magnetic skyrmions can be efficiently tuned via modulation of the strength of spin-orbit interaction [1]. We show that the skyrmion Hall effect [2], which is a direct consequence of the non-vanishing Magnus force on the magnetic structure can be suppressed in certain limits. Our calculations show that the emergent magnetic fields in the presence of spin-orbit coupling (SOC) renormalize the Lorentz force on itinerant electrons and thus influence the topological transport. In particular, we show that for a Neel-type skyrmion and Bloch-type antiskyrmion, the skyrmion Hall effect (SkHE) can vanish by tuning appropriately the strength of Rashba and Dresselhaus SOCs, respectively. Our results open up alternative directions to explore in a bid to overcome the parasitic and undesirable SkHE for spintronic applications.

### References

- [1]. C. A. Akosa, H. Li, G. Tatara, and O. A. Tretiakov, *Phys. Rev. Appl.* **12**, 054032 (2019).
- [2]. K. Litzius, O. A. Tretiakov, *et al.*, *Nature Phys.* **13**, 170 (2017).

## Rare-earth nitrides: Mixed valence, strongly correlated heavy Fermions

Joe Trodahl<sup>1</sup>, Will Holmes-Hewett<sup>1</sup>, Ben Ruck<sup>1</sup>, Franck Natali<sup>1</sup>, Bob Buckley<sup>2</sup>

<sup>1</sup>*School of Chemical and Physical Sciences, Victoria University of Wellington, New Zealand*

<sup>2</sup>*Robinson Research Institute, Victoria University of Wellington, New Zealand*

Most mononitrides of the lanthanides (LN) are *intrinsic* ferromagnetic semiconductors; they form the only epitaxy-compatible series to populate this exceedingly rare material class. We have grown them as films for fifteen years, with the aim of developing devices, particularly MRAM for cloud computing centres. Along the way we have unravelled much concerning their outrageous coupled electronic/magnetic behaviour: strongly correlated electrons, strong spin-orbit interactions, orbital contributions to their ferromagnetic states, a zero-magnetisation ferromagnetic material. They offer exciting opportunities to investigate strongly correlated electrons and their heavy Fermion states.

The LN adopt a strongly ionic ( $L^{+3}$  and  $N^{-3}$ ) rock-salt structure. The  $5d$  conduction and  $2p$  valence bands are the full story in the end members (LaN, LuN) and in GdN, with its half-filled  $4f$  band, but the rest of the fourteen LN have very narrow  $4f$  bands threading through and hybridising with the more mobile  $5d$  and  $2p$  bands, exactly the heavy Fermion states that have attracted a great deal of mostly theoretical interest. They permit exploration of strong correlation and heavy Fermion physics, with in addition the potential, in these semiconductors, to dope into and across the hybridisation gap. We have now advanced to be able to identify several among the light rare-earth nitrides that show exactly heavy-Fermion promise. I will discuss the experiments that have opened the heavy-Fermion box, with a focus on EuN, SmN and NdN.

## Increase of the stability range of the skyrmion phase in doped $\text{Cu}_2\text{OSeO}_3$

J. Saucedo Flores<sup>1</sup>, R. Rov<sup>2</sup>, L. Camacho<sup>2</sup>, M. Spasovski<sup>2</sup>, J. Vella<sup>2</sup>, S. Yick<sup>1</sup>, E. Gilbert<sup>3</sup>, M.G. Han<sup>4</sup>, Y. Zhu<sup>4</sup>, J. Seidel<sup>5</sup>, Y. Kharkov<sup>1</sup>, O. Sushkov<sup>1</sup>, T. Söhnel<sup>2</sup>, and C. Ulrich<sup>1</sup>

<sup>1</sup>*School of Physics, UNSW Sydney, Sydney NSW 2052, Australia*

<sup>2</sup>*School of Chemical Sciences, University of Auckland, Auckland 1142, New Zealand*

<sup>3</sup>*Australian Centre for Neutron Scattering, ANSTO, Lucas Heights, NSW 2234, Australia*

<sup>4</sup>*Condensed Matter Physics and Materials Sciences Department, Brookhaven National Laboratory, Upton, NY, 11973, USA*

<sup>5</sup>*School of Materials Science and Engineering, UNSW Sydney, Sydney NSW 2052, Australia*

A skyrmion is a topological stable particle-like object comparable to a spin vortex at the nanometre scale. It consists of an about 50 nm large spin rotation and its spin winding number is quantized. Once formed, the skyrmions order in a two dimensional, typically hexagonal superstructure perpendicular to an applied external magnetic field (see Fig. 1). Its dynamics has links to flux line vortices as in high temperature superconductors.

$\text{Cu}_2\text{OSeO}_3$  is a unique case of a multiferroic materials where the skyrmion dynamics could be controlled through the application of an external electric field. The direct control of the skyrmion dynamics through a non-dissipative method would offer technological benefits and unique possibilities for testing fundamental theories also related to the Higgs Boson whose theoretical description has similarities to skyrmions.

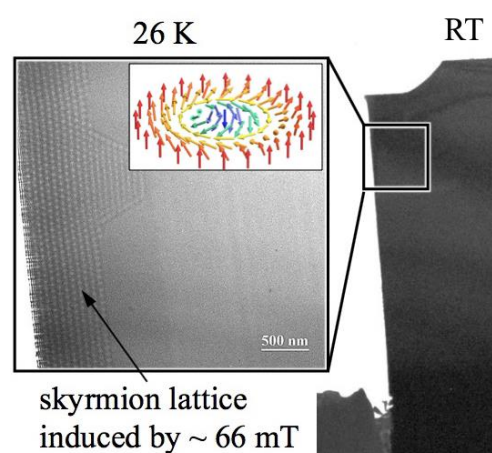


Figure 1: Skyrmion formation in our  $\text{Cu}_3\text{OSe}_{1-x}\text{Te}_x\text{O}_3$  single crystals measured by Lorentz force electron microscopy (in collaboration with the Brookhaven National Laboratory, USA).

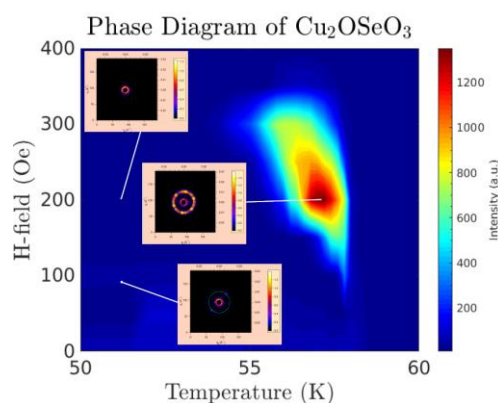


Figure 2: Stability range of the skyrmion phase of pure  $\text{Cu}_2\text{OSeO}_3$  determined on the SANS instrument QUOKKA/ANSTO.

Important for technological applications is a stability range of the skyrmion phase up to room temperature. While room temperature skyrmion materials exist,  $\text{Cu}_2\text{OSeO}_3$  orders magnetically below 58 K. Our combined small angle neutron scattering (see Fig. 2), SQUID magnetization measurements and electron microscopy investigations did provide direct evidence that the stability range of the skyrmion phase can be extended in Te-doped  $\text{Cu}_2\text{OSeO}_3$ . The understanding of this effect will help to obtain deeper insights in the magnetic correlations in charge of the skyrmion formation and will thus help to systematically search for skyrmion materials with phase transition temperatures towards room temperature.

## Neutron Study of Magnetic Phase Transition in SrCoO<sub>3</sub> Thin Films

S. Yick<sup>1,2</sup>, M. F. Peroz<sup>1</sup>, V. Nagarajan<sup>3</sup>, F. Klose<sup>2,4</sup>, and J. Seidel<sup>3</sup>, and C. Ulrich<sup>1,2</sup>

<sup>1</sup>*School of Physics, The University of New South Wales, Sydney, NSW 2052, Australia*

<sup>2</sup>*Australian Nuclear Science and Technology Organization,  
Lucas Heights, NSW 2234, Australia*

<sup>3</sup>*School of Materials Science and Engineering, The University of New South Wales,  
Sydney, NSW 2052, Australia*

<sup>4</sup>*Department of Physics and Materials Science, City University of Hong Kong,  
Hong Kong SAR, China*

Transition metal oxides represent a wide set of materials with a broad range of functionalities which can be tuned by the careful choice of parameters such as strain, oxygen content, and applied electric or magnetic fields. When the material exhibits more than one primary ferroic ordering- ferromagnetism, ferroelectricity, ferroelasticity or ferrotoridicity in the same phase, it becomes multiferroic. Such class of materials are of immense technological interest as magnetic and electric transitions can be driven through external factors. This opens new avenues for fundamental research and technical applications in spintronic or magnonic devices. Here, we present results we obtained from neutron-based techniques to investigate the magnetic properties of SrCoO<sub>3</sub> and similar thin films.

SrCoO<sub>3</sub> provides a particularly interesting system for these investigations. Lee and Rabe have simulated the effect of strain and have predicted that the magnetic state can be tuned through compressive or tensile strain with a ferromagnetic-antiferromagnetic phase transition [1,2]. Such a phase transition would be accompanied by a metal-to-insulator phase transition and a transition to a ferroelectric polarized state.

By using different substrates, we investigated the effect different epitaxial strain has on SrCoO<sub>3</sub> thin films. Previously, our neutron diffraction experiments on these 40 nm thin films have confirmed the predicted but hitherto unobserved phase transition from ferromagnetism to G-type antiferromagnetism when the film was grown on SrTiO<sub>3</sub> and DyScO<sub>3</sub> substrate respectively [3]. As such, SrCoO<sub>3</sub> would constitute a new class of multiferroic material where magnetic and electric polarizations can be driven through external strain. This tunability makes them ideal candidate materials for use in developing novel information and energy technologies.

## References

- [1] J.H. Lee and K.M. Rabe, *Phys. Rev. Lett.* **107**, 067601 (2011).
- [2] J.H. Lee and K.M. Rabe, *Phys. Rev. B* **84**, 104440 (2011).
- [3] S.J. Callori, S. Hu, J. Bertinshaw, Z. Yue, S. Danilkin, X.L. Wang, V. Nagarajan, F. Klose, and J. Seidel, and C. Ulrich, submitted to *Phys. Rev. B, Rapid. Com.* (2014).

## **Tributes to Three “Wagga” Scientists**

T.R. Finlayson<sup>1</sup>, D.J. Gregg<sup>2</sup> and G.A. Stewart<sup>3</sup>

*<sup>1</sup>The University of Melbourne, Melbourne, Victoria, 3010, Australia*

*<sup>2</sup>Australian Nuclear Science and Technology Organisation, Kirrawee DC, N.S.W., 2232, Australia*

*<sup>3</sup>UNSW at the Australian Defence Force Academy, Canberra BC 2610, Australia*

Ralph Severin (Sev) Crisp, Eric Raymond (Lou) Vance and Geoffrey Victor Herbert Wilson AM, all of whom passed away during 2019, were strong supporters of the “Wagga” Conference. Therefore, it is fitting that these tributes should be presented to outline their respective contributions to the field of “Condensed Matter and Materials”, now the accepted name for the conference. In this presentation their respective contributions to this conference will be summarized and set in the context of their broader contributions to Australian and International Condensed Matter Physics. We shall not only celebrate their scientific contributions, but also their extremely giving natures which have seen them share their lifelong knowledge with our community.

# Poster Abstracts



## Temperature dependent terahertz spectra for glycine single crystal

J. L. Allen, T. J. Sanders, J. Horvat, R. A. Lewis

*Institute for Superconducting and Electronic Materials and School of Physics,  
The University of Wollongong, Wollongong, 2522 Australia*

For the first time, large single crystals of the simplest amino acid, glycine, have been used to measure the temperature dependence of its terahertz spectrum. Use of the single crystal morphology at cryogenic temperatures has allowed for particularly high-quality spectra with very sharp absorption features in the terahertz region. A solution of 30mL of distilled water and 7g of glycine was heated to 50°C while being continuously stirred until all the solvent was dissolved, following the solvent evaporation method for crystals [1]. Crystals were allowed to grow in the solution at room temperature over three days, resulting in a 10×5mm crystal for spectroscopy.

Previous studies such as [2], and the references therein, have used pelletised blends. The single crystal approach of this work removes the potential of observing extrinsic interactions caused by these pelletised binding media.

The spectra have been measured using Fourier transform spectroscopy (FTS: Bomem DA8) in the range 30-250cm<sup>-1</sup>, and terahertz time-domain spectroscopy (THz-TDS: TeraView TeraPulse 4000) for validation of the range 20-100cm<sup>-1</sup>. This was done over a temperature range of 290-20K. Spectra below 150K were taken while warming the sample, and spectra above 150K were taken while cooling. The results in Fig. 1 show 7 total absorption bands. The first 3 absorption bands observed with both instruments red-shift with increasing temperature. These are seen at 50cm<sup>-1</sup> (shifting by 3.1cm<sup>-1</sup> from 20-216K), 69cm<sup>-1</sup> (shifting by 0.3cm<sup>-1</sup> from 20-235K), and at 92cm<sup>-1</sup> with a weak shoulder. A further 4 absorption bands are seen with the FTS system but are too absorptive to precisely locate the peak positions. Approximate peaks are at 145cm<sup>-1</sup>, 150cm<sup>-1</sup>, 185cm<sup>-1</sup>, and 222cm<sup>-1</sup>. The use of a single crystal sample, with purity validated by X-ray diffraction, accurately gives the intrinsic terahertz spectral features of glycine, and their temperature dependences.

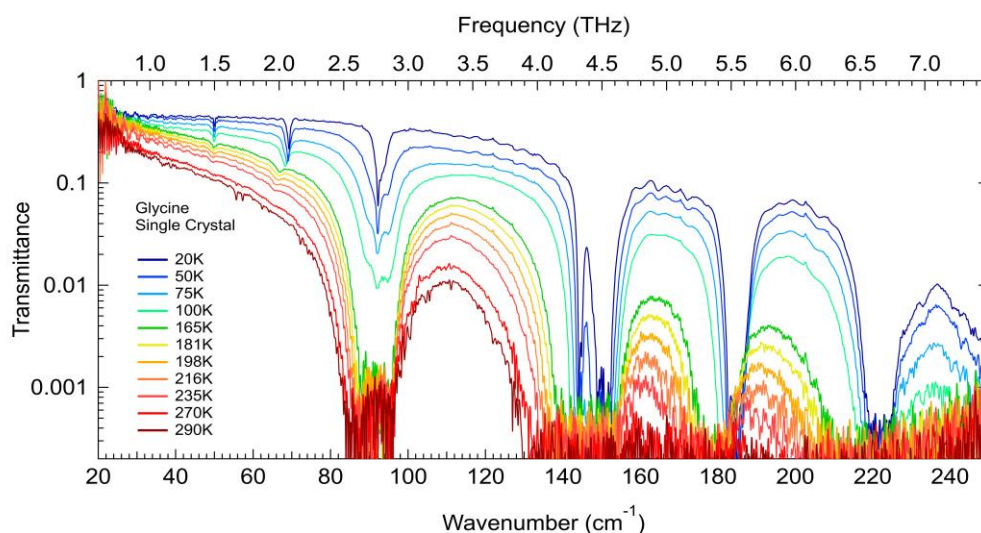


Fig. 1: Temperature dependent terahertz transmittance spectra of glycine using FTS.

### References

- [1]. T.P. Srinivasan *et al.*, J. Cryst. Growth. 318, 762 (2011)
- [2]. W. Yi *et al.*, Instr. Sci. Technol. 45, 423 (2017)

## High Magnetic Saturation Holmium-Terbium Thin-Films Alloys: Application in High- $T_c$ machines

T. Butler<sup>2,3</sup>, R. G. Buckley<sup>1,3</sup>, S. Granville<sup>1,3</sup>

<sup>1</sup>*Robinson Research Institute, Victoria University of Wellington, Lower Hutt, New Zealand*

<sup>2</sup>*School of Chemical and Physical Sciences, Victoria University of Wellington, Wellington, New Zealand*

<sup>3</sup>*MacDiarmid Institute for Advanced Materials and Nanotechnology, New Zealand*

The heavy rare-earth metals, holmium and terbium, are promising materials for application in high- $T_c$  superconducting (HTS) machines due to their high magnetic saturation ( $\mu_0M_s$ )<sup>1</sup> within the machine operating range (20-50 K). Bulk single-crystal holmium is particularly interesting as it is predicted to have a magnetic saturation as high as  $\sim 3.8$  T although exhibiting a low Curie temperature of  $\sim 20$  K<sup>2</sup>. On the other hand, single-crystal terbium offers a much higher Curie temperature of  $\sim 230$  K and a similar  $\mu_0M_s$  (3.4 T) to Holmium. The complexity arises due to competing non-ferromagnetic phases and the significant crystallographic and magnetic anisotropy in the predicted magnetic properties<sup>1</sup>.

We report the optimization of the growth of thin film alloys of these rare-earth metals with the purpose of identifying a composition exhibiting both a  $T_c$  in the 20-50 K range with a maximum  $\mu_0M_s$ . Thin films of holmium, terbium and their alloys were grown *by* DC magnetron sputtering. Microstructure and magnetic properties of holmium and terbium metal were measured as a function of nominal deposition rate ( $\zeta = 1, 2, 3 \text{ \AA s}^{-1}$ ), and deposition and ex situ annealing temperatures.

XRD measurements of both holmium and terbium films revealed that higher deposition rates promote the ferromagnetic hexagonal-close-packed (hcp) phase required to achieve high  $M_s$ , instead of the paramagnetic fcc phase.  $Ho_xTb_{1-x}$  alloys  $x = (0.25, 0.5, 0.75)$  were co-sputtered at  $\zeta = 2 \text{ \AA s}^{-1}$ ,  $350^\circ\text{C}$ .  $Ho_{0.5}Tb_{0.5}$  exhibits a  $\mu_0M_s \approx 2.5T$  at 10K and showed a strong hcp c-axis texturing characteristic of ferromagnetic rare-earth phase. The results clearly indicated that increasing nominal growth deposition rate and substrate temperature optimize the crystallographic microstructure required to achieve a high  $\mu_0M_s$  in  $Ho_{0.5}Tb_{0.5}$ .

### References

1. Scheunert, G., Heinonen, O., Hardeman, R., Lapicki, A., Gubbins, M., & Bowman, R. M. *A review of high magnetic moment thin films for microscale and nanotechnology applications*. Appl. Phys. Rev., 3, 011301 (2016)
2. W. C. Koehler J. W. Cable, H. R. Child, M. K. Wilkinson and E. O. Wollan, *Magnetic Structures of Holmium. II. The Magnetization Process*, Phys. Rev. 158, 450 (1967)
3. D. E. Hegland, S. Legvold and F. H. Spedding, *Magnetization and Electrical Resistivity of single Crystals of Terbium*, Phys. Rev. 131, 158 (1963)
4. F. H. Spedding, R. G. Jordan, and R. W. Williams, *Magnetic Properties of Tb-Ho Single-Crystal Alloys. I. Magnetization Measurements*, J. Chem. Phys., 51, 509 (1969)

## Temperature Dependence of Electron Delocalization in Mixed Valence Freudenbergitte

J.D.Cashion<sup>1</sup>, E.R. Vance<sup>2</sup>, D.H. Ryan<sup>3</sup>

<sup>1</sup>*School of Physics and Astronomy, Monash University, Melbourne, Vic 3800, Australia*

<sup>2</sup>*Deceased. Formerly: Australian Nuclear Science and Technology Organisation,  
Menai, NSW 2234, Australia*

<sup>3</sup>*Physics Department and Centre for the Physics of Materials, McGill University,  
3600 University Street, Montreal, Quebec, H3A 2T8, Canada.*

Since our last reports, we have carried out further experiments on the mixed valence sodium iron-titanate freudenbergitte [1, 2]. Freudenbergitte has the nominal formula  $\text{Na}_2\text{Fe}_x\text{Ti}_{8-x}\text{O}_{16}$ , with  $x = 1$  being ferrous and  $x = 2$  being ferric. However, a ferrous composition sample, calcined in air, became mixed valence with a closely 50:50 valence split. It is normally considered that the Fe and Ti ions are randomly distributed in the two (Fe,Ti) $\text{O}_6$  octahedra. However neutron diffraction showed that the Ti:Fe ratio was 0.82:0.18 in the larger M(1) site and 0.93:0.07 in the smaller M(2) site compared to the average 0.875:0.125. It is expected that all the iron in the smaller M(2) site will be ferric.

The sample turned out to have very unusual Mössbauer spectra as the temperature was varied. At low temperatures, well resolved ferric and ferrous doublets were observed. But as the temperature was increased, the ferrous doublet slowly collapsed and had to be fitted with up to three doublets to match the envelope. The ferric doublet remained unchanged in intensity and hyperfine parameters. The collapse of the ferrous spectrum is due to a thermally driven electron delocalisation of the sixth d-electron. The electric field gradient in ferrous materials is mainly due to this electron and its removal causes the quadrupole splitting to more closely resemble that of the ferric ions, which is due entirely to the lattice.

We have tried unsuccessfully to manufacture more of these electron mobile samples with various compositions and calcining in air and argon. However, pure ferrous and pure ferric samples do not display any dynamic behaviour, and even a ferrous sample with 3% ferric iron did not display any dynamics [2]. Spectra of the present sample taken at 6K and 10 K showed evidence of broadening, presumably due to the onset of magnetic ordering. However, it was not clear whether both ions were ordering or only one. There is no record of a magnetic ordering temperature for freudenbergitte in the literature, and any such observation will undoubtedly be strongly sample dependent.

The electron dynamics can be caused by intervalence charge transfer between ions or by crystal field effects or electron delocalisation in single ions, and are the primary cause of the colour in popular minerals. Other Fe-Ti minerals which exhibit such behaviour in the Mössbauer spectra include sapphire, kyanite, fassaite, omphacite, aenigmatite, and Ti andradite.

### References

- [1] Cashion, J. D. et al., *Hyperfine Interact.*, **226**, 579-583 (2014).
- [2] Cashion, J. D. et al., *Proc. 38th A&NZ CMM Meeting, Waiheke 2014*, p10.

# Robustness of unconventional s-wave superconducting states against disorder

D. C. Cavanagh<sup>1</sup>, P. M. R. Brydon<sup>2</sup>

<sup>1</sup>*Department of Physics, University of Otago, Dunedin, New Zealand*

<sup>2</sup>*Department of Physics and MacDiarmid Institute for Advanced Materials and Nanotechnology, University of Otago, Dunedin, New Zealand*

Unconventional superconductors are infamously unstable against the presence of nonmagnetic disorder, while the critical temperature of a conventional superconductor is insensitive to such disorder, as encapsulated in Anderson's theorem. Generalisation of Anderson's theorem to superconductors with multiple bands has proven difficult. We investigate the robustness against disorder of superconductivity in systems with two bands [1]. In these multi-band systems, unconventional superconducting states are possible with momentum-independent (s-wave) pairing functions. We have developed a general framework, based on the self-consistent Born approximation, to understand the stability of orbitally non-trivial superconductors against disorder, and applied this framework to two candidate topological superconductors, YPtBi and  $\text{Cu}_x\text{Bi}_2\text{Se}_3$ . Unconventional s-wave states are found to be significantly more robust against disorder than the analogous single-band states. Additionally, superconductors with momentum-dependent gaps in multi-band systems inherit some robustness against disorder from the s-wave states with the same symmetry, in a significant deviation from the behaviour exhibited in single-band superconductors.

## References

[1] D. C. Cavanagh and P. M. R. Brydon, arXiv: 1908.09476 (2019)

## New on the Physics Menu: Superconducting Sandwiches!

A. Chan<sup>1,2,4,5</sup>, T. Söhnel<sup>2,4</sup>, M.C. Simpson<sup>1,2,3,4,5</sup>, J. Khmaladze<sup>6</sup>, C. Bernhard<sup>6</sup>,  
B.P.P. Mallett<sup>1,2,4,5</sup>

<sup>1</sup>*The Photon Factory, The University of Auckland, New Zealand*

<sup>2</sup>*School of Chemical Sciences, The University of Auckland, New Zealand*

<sup>3</sup>*Department of Physics, The University of Auckland, New Zealand*

<sup>4</sup>*The MacDiarmid Institute for Advanced Materials and Nanotechnology, New Zealand*

<sup>5</sup>*The Dodd-Walls Centre for Photonic and Quantum Technologies, New Zealand*

<sup>6</sup>*Department of Physics, University of Fribourg, Switzerland*

Between two pieces of bread is a world of unlimited possibilities to discover exciting new flavours. As scientists with access to advanced layering technologies, we procure our own sandwiches with atomic-level precision - combining mutually exclusive phenomenon such as superconductivity and magnetism to study their interplay [1]. Superconductors carry electrical current with zero resistance when cooled below its critical temperature ( $T_c$ ).

Near-universally, however, superconductivity is degraded by large magnetic fields or electric currents – a key performance limitation bottlenecking emerging superconductor technologies.

Recently, we discovered novel emergent properties in thin-film multilayers of a cuprate high-temperature superconductor ( $\text{YBa}_2\text{Cu}_3\text{O}_7$ , YBCO) and magnetic manganite ( $\text{Pr}_{0.5}\text{La}_{0.2}\text{Ca}_{0.3}\text{MnO}_3$ , PLCMO). At low temperatures, this ‘superconductor sandwich’ hosts an exotic granular superconducting state characterized by a phase-pinned superconducting condensate and an unusually high resistance [2]. Surprisingly, the customary superconducting state is recovered in a large magnetic field and/or current, making our sandwiches one of just four systems exhibiting magnetic field and electric current induced superconductivity. As interesting as these sandwiches are, they are unfortunately unsuitable for human consumption. Rather, once we gain a better understanding of their novel physics, they may be destined as components in future electronic devices.

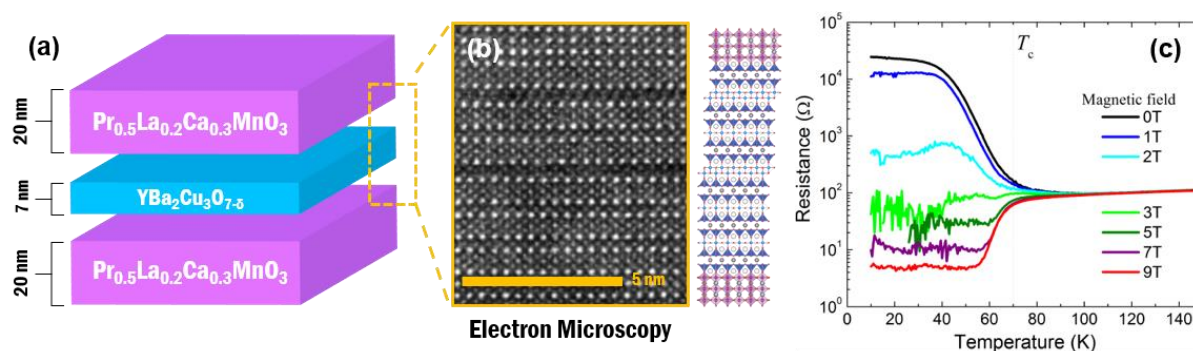


**Fig. 1:** (a) Schematic of a  $\text{PLCMO}_{20\text{nm}}\text{-YBCO}_{7\text{nm}}/\text{PLCMO}_{20\text{nm}}$  “superconducting sandwich” epitaxially grown on (001)-oriented  $\text{La}_{0.3}\text{Sr}_{0.7}\text{Al}_{0.65}\text{Ta}_{0.35}\text{O}_3$  (LSAT) substrates by pulsed laser deposition. (b) Cross-sectional transmission electron microscopy at the PLCMO-YBCO interfaces showing excellent lattice matching. (c) Magneto-transport data for trilayer in (a) in the presence of magnetic field. Data from ref [2].

### References

- [1] V.K. Malik et al. *Phys. Rev. B.* **85**, 054514 (2012)  
[2] B. Mallett et al. *Phys. Rev. B.* **94**, 180503(R) (2016)

# Magnonic Crystals: A Bottom-up Fabrication Approach Utilizing Polymer and Supramolecular Chemistry

Daniel Clyde<sup>1,4</sup>, Jenny Malmstrom<sup>2,4</sup>, David Ware<sup>1</sup>, Penny Brothers<sup>1,3,4</sup>

<sup>1</sup>*School of Chemical Sciences, University of Auckland.*

<sup>2</sup>*Department of Chemical and Materials Engineering, University of Auckland.*

<sup>3</sup>*Research School of Chemistry, Australian National University.*

<sup>4</sup>*The MacDiarmid Institute for Advanced Materials and Nanotechnology*

Magnonics, and the fabrication of magnonic crystals, is a new and emerging field of nanoscale science and technology. The goal of being able to produce devices that run on magnonics is driven by the increasing needs of efficiency and speed of the technological devices our society thrives on. Spin-waves, otherwise known as magnons (hence the term magnonics), are generated when a magnetic disturbance is introduced into a spin-aligned material.<sup>1</sup> This causes the aligned electron spins to precess, which in turn generates a detectable signal. Spin-waves require much less energy to transport a signal and travel at higher frequencies as opposed to electronic currents.<sup>2</sup> To transport magnons in a controlled manner, spin-wave guides are required as the signal carrier. However, the major drawbacks of magnonic crystals so far include damping of the spin-wave when carrying a signal, causing a loss of information, and so far have been difficult to miniaturize far enough to become advantageous enough to incorporate into devices.<sup>3</sup>

This research is focused on trying to develop ways in which magnonic crystals can be fabricated on the nanoscale, and will be investigating the effects of spin-wave production and damping using a variety of different conditions. The building blocks that have been selected for the fabrication of magnonic crystals are polyoxometalates (POMs) as the magnetically responsive material, and block copolymers (BCPs) as the structuring agent. POMs are magnetically diverse species, and with hundreds of unique POMs found in the literature, they have provided a range of different conditions to explore and investigate. The overall schematic showing the fabrication of these materials is shown in Fig. 1 illustrating the incorporation of the POMs into a polymer network and to further form micelles with POMs located in the core. With micelles housing the magnetic POMs, they have then been spin-coated onto a silicon wafer, where they have self-assembled to form a periodic array. The image on the right was taken with an atomic force microscope after successfully forming micelles and spin coating onto the silicon wafer substrate.

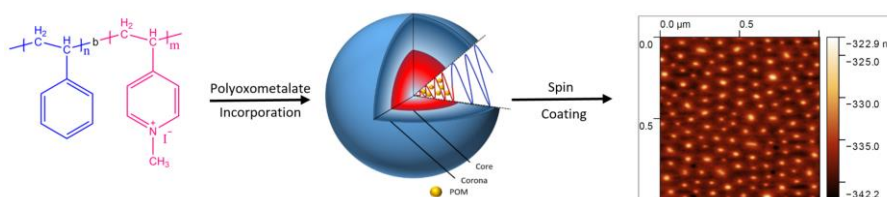


**Fig. 1:** Schematic representation of the steps taken in this research towards fabricating magnonic crystals.

## References

- Gomonay, O.; Jungwirth, T.; Sinova, J., Concepts of antiferromagnetic spintronics. *Physica Status Solidi-Rapid Research Letters* **2017**, *11* (4).
- Kruglyak, V. V.; Demokritov, S. O.; Grundler, D., Magnonics. *Journal of Physics D-Applied Physics* **2010**, *43* (26).
- Domingo, N.; Bellido, E.; Ruiz-Molina, D., Advances on structuring, integration and magnetic characterization of molecular nanomagnets on surfaces and devices. *Chemical Society Reviews* **2012**, *41* (1), 258-302.

## Intrinsic Anomalous Hall Effect in Chiral $D_{4h}$ Superconductors

M. D. E. Denys<sup>1</sup>, P. M. R. Brydon<sup>1</sup>

<sup>1</sup>*Department of Physics, University of Otago, PO Box 56, Dunedin 9054, New Zealand*

The polar Kerr effect has been observed in a number of unconventional superconductors, such as  $\text{Sr}_2\text{RuO}_4$  and the iron pnictides, providing evidence of an anomalous AC Hall conductivity. However, the origin of this effect is still controversial. The two major schools of thought are that the effect is either extrinsic, arising from impurity scattering [1,2], or intrinsic, due to the multi-band nature of the pairing [3,4]. We consider the intrinsic mechanism, and present preliminary results regarding the general conditions under which the anomalous AC Hall conductivity will appear in two dimensional models of superconducting materials belonging to the  $D_{4h}$  symmetry group. For example, this is relevant to  $\text{SrRuO}_4$ . Interpretations as to the physical origin of the effect are provided.

### References

- [1] R. M. Lutchyn *et al.*, Phys. Rev. B **80**, 104508 (2009).
- [2] E. J. Konig and A. Levchenko, Phys. Rev. Lett. **118**, 027001 (2017).
- [3] E. Taylor and C. Kallin, Phys. Rev. Lett. **108**, 157001 (2012)
- [4] M. Gradhand, *et al.*, Phys. Rev. B **88**, 094504 (2013).



## Deformation Studies of Mg-PSZ under Compressive Loading

T.R. Finlayson<sup>1</sup>, G.V. Franks<sup>1</sup>, J.R. Griffiths<sup>2</sup>, E.H. Kisi<sup>3</sup>, M.L. Sesso<sup>1,2</sup> and M. Stuart<sup>4</sup>

<sup>1</sup>The University of Melbourne, Melbourne, 3010, Australia

<sup>2</sup>La Trobe University, Bundoora, 3083, Australia

<sup>3</sup>The University of Newcastle, Callaghan, 2308, Australia

<sup>4</sup>Morgan Technical Ceramics, Pty., Ltd., 3168, Australia

Pure zirconia,  $ZrO_2$ , is not a useful material because phase transformations as it cools after processing at high temperature, are accompanied by dilatational and shear strains that lead to cracking. The addition of oxides such as MgO, stabilizes the high-temperature phases and the resultant “partially stabilized zirconia”, Mg-PSZ, is used in a variety of applications. There are two, little-understood features of the material. First, the transformation (which is martensitic) is time-dependent, causing creep under a constant stress (Fig. 1 [1]). Second, when the applied stress is removed, the creep strain reverses (Fig. 2 [2]). These effects occur under both tensile and compressive stresses, but at very different magnitudes. Partly motivated by a presentation at the International Conference on Martensitic Transformations (ICOMAT2017) held in Chicago in July, 2017 [3], we have studied Mg-PSZ in compression and simultaneously measured sample deformations (using strain gauges) and the accompanying microstructural changes using neutron diffraction at the ENGIN-X beamline on the ISIS, pulsed-neutron source at the Rutherford-Appleton Laboratory, Didcot, Oxfordshire, England. The advantage of such an experiment is that it provides simultaneous microstructural information both parallel to and perpendicular to the applied load on the compression sample. The results reveal two distinct stages of time-dependence, firstly, while the sample is under load and subsequently on the load removal.

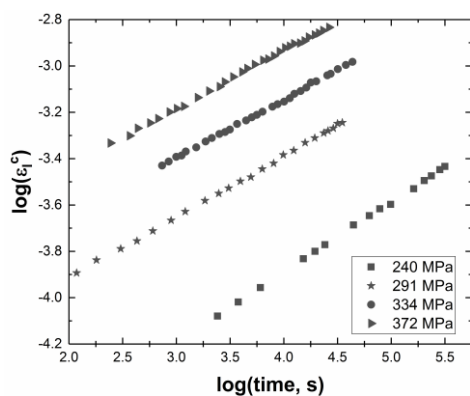


**Fig. 1:** Creep-in-tension data for Mg-PSZ (adapted from [1]).

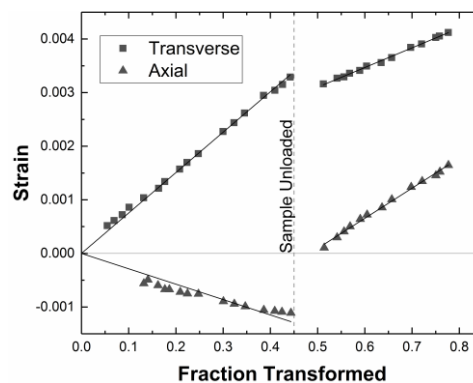


**Fig. 2:** Compression data for Mg-PSZ for an applied stress of 1200 MPa (adapted from [2]).

### References

- [1] T.R. Finlayson, A.K. Gross, J.R. Griffiths and E.H. Kisi, “Creep of Mg-PSZ at room temperature”, *J. Amer. Ceram. Soc.*: **77**, 617-624 (1994).
- [2] C.J. Wauchope, “Martensitic transformations in ceramics”, PhD Thesis (University of Queensland, 1996).
- [3] Christine Ulrich, *et al.*, in “Displacive Transformations in Non-Metallic Materials”: Session 1, ICOMAT2017 (11:35 am, 10 July, 2017).



## Modelling 1D High-Temperature Superconducting Quantum Interference Filters

M.A. Gali Labarias, K-H. Muller and E.E. Mitchell

*CSIRO Manufacturing, Lindfield, NSW, Australia*

Although the discovery of high temperature superconductivity in the cuprates occurred more than 30 years ago, there remains a lack of suitable theoretical models that can accurately describe the magnetic field performance of small, regular arrays of superconducting quantum interference devices (SQUIDs). The geometrical characteristics of superconducting quantum interference filters (SQIF), for example, play a crucial role in determining the voltage - magnetic flux response of the device [1,2,3]. The main reason for this is the inductive and super-current coupling between the SQUIDs that constitute the SQIF array. In contrast to low temperature superconductors (LTS), in high-temperature superconductors (HTS) the kinetic inductance, derived from the fluxoid term in the gauge invariant equation for the SQUID phases, cannot be neglected. This is because the kinetic inductance is proportional to the square of the London penetration depth and in HTS this penetration depth is much larger than in LTS. Furthermore, in SQIFs the kinetic inductance increases as the film thickness decreases.

In this talk I will focus on these issues and I will present a model that considers the kinetic inductance and the structural parameters of the array which enables us to simulate more accurately HTS SQIFs in one and two dimensions.

### References

- [1]. J. Oppenländer et al., Phys. Rev. B 63-02 (2001).
- [2]. J. R. Phillips et al., Phys. Rev. B 47-09 (1993).

## Delocalisation of *d*-electrons within Transition Metal Doped Clusters: Pushing the Limits of the Superatom Model

J. Gilmour<sup>1</sup> and N. Gaston<sup>2</sup>

<sup>1</sup>The MacDiarmid Institute for Advanced Materials and Nanotechnology, School of Chemical Physical Sciences, Victoria University of Wellington, PO Box 600, Wellington 6140, New Zealand  
<sup>2</sup>The MacDiarmid Institute for Advanced Materials and Nanotechnology, The Department of Physics, University of Auckland, Private Bag 92019, Auckland 1010, New Zealand

Superatomic clusters have long attracted interest in the fields of solid-state chemistry, materials science and condensed matter physics owing to their similarities to individual atoms. However, transition metals are generally treated as if they are purely magnetic dopants in these systems, unable to have their *d*-electrons meaningfully contribute to the formation of superatomic states. Here we demonstrate that this is not the case, illustrating that the lower the group of a transition metal and the higher its period, the more likely it is for its outermost *d*-electrons to delocalize, as is demonstrated in Fig 1. Using density functional theory methods, the electronic structure of a selection of 8, 20 and 40 valence electron clusters has been explored and their global structure characterised for a range of exchange correlation functionals. This work reinforces the contextual nature of transition metals within the superatomic framework and provides room for the development of new materials.

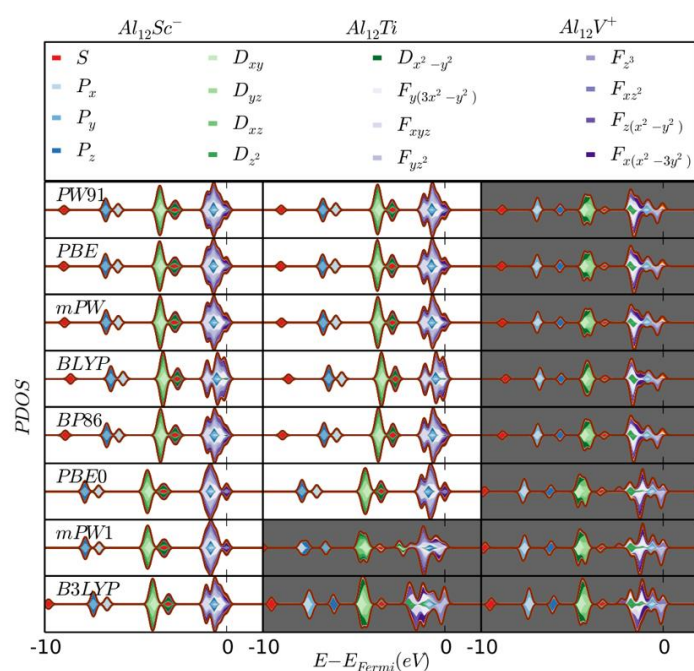


**Fig. 1:** Projected density of states (PDOS) image for the  $Al_{12}Sc^-$ ,  $Al_{12}Ti$  and  $Al_{12}V^+$  clusters for 8 common exchange correlation functionals used in the exploration of cluster materials. The positive PDOS values present the smeared projection values for the alpha spin orbitals whereas the negative values present the spin down orbitals. The grey face color indicates the plots which are not closed shell superatoms.

## Reinterpretation of physical property data for $\text{TmV}_2\text{Al}_{20}$

W.D. Hutchison<sup>a</sup>, G. A. Stewart<sup>a</sup>, R. White<sup>a</sup>, G.N. Iles<sup>b,c</sup>, J.M. Cadogan<sup>a</sup>,

T. Namiki<sup>d</sup> and K. Nishimura<sup>d</sup>

<sup>a</sup>*School of Science, The University of New South Wales, Canberra ACT 2600, Australia.*

<sup>b</sup>*Australian Centre for Neutron Scattering, Australian Nuclear Science and Technology Organisation, Kirrawee DC, NSW 2232, Australia.*

<sup>c</sup>*School of Science, RMIT University, Melbourne, VIC 3000, Australia*

<sup>d</sup>*Graduate School of Science and Engineering, University of Toyama, Toyama 930-8555, Japan*

Compounds of the  $\text{RM}_2\text{Al}_{20}$ -type (R = rare earth, M = transition metal) are of interest for the study of fundamental low temperature physical and magnetic properties. Members of this series crystallise in the cubic  $\text{CeCr}_2\text{Al}_{20}$  structure type with the space group  $\text{Fd}\bar{3}\text{m}$  (#227). Given that the rare earth site (cubic  $\bar{4}3\text{m} / \text{T}_d$  site symmetry) is at the centre of a polyhedron of 16 Al ions [1], members of the series are referred to as ‘caged rare earth compounds’. The relatively large lattice parameter (typically of the order of 15 Å) results in a large separation of the rare earth nearest neighbours and leads to weak R-R exchange interactions. Consequently, the magnetic ordering temperature is suppressed, typically to less than 2 K. In some cases magnetic order has not yet been observed. Investigations of  $\text{PrV}_2\text{Al}_{20}$  and  $\text{PrTi}_2\text{Al}_{20}$  revealed interesting phenomena associated with the non-magnetic ground state of the cubic  $\text{Pr}^{3+}$  site. These included the quadrupolar Kondo effect [2] and superconductivity behaviour [3].

The compound  $\text{TmV}_2\text{Al}_{20}$  is a hole analogue of  $\text{PrV}_2\text{Al}_{20}$  and was subsequently investigated at low temperatures in search of similar or related phenomena. A key outcome of this later work [4] was that the high quality, single crystal, heat capacity data were interpreted in terms of a cubic crystal field (CF) interaction with just the two parameters,  $x$  and  $W$ , of the Lea, Leask and Wolf [5] formalism. However an additional arbitrary broadening of the CF ground state was necessary to better match the experimental data at low temperature. In order to improve on these CF results, we carried out inelastic neutron scattering and electron paramagnetic resonance measurements which better define  $x$  and  $W$  for  $\text{Tm}^{3+}$  in  $\text{TmV}_2\text{Al}_{20}$  [6]. In this paper we show that in addition to this crystal field Hamiltonian, the single crystal magnetisation and specific heat data are better interpreted in terms of a model that involves partial Al flux substitution of an approximately 10% depleted Tm ‘cage’ site; this interpretation allows inclusion of ‘rattling’ contributions of caged Tm and Al ions in specific heat.

## References

- [1]. S. Niemann and W. Jeitschko, *Journal of Solid State Chemistry* **114**, 337-341, (1995).
- [2]. T. J. Sato *et al.*, *Physical Review B* **86**, 184419, (2012).
- [3]. M. Tsujimoto *et al.*, *Physical Review Letters* **113** 267001, (2014).
- [4]. Q. Lei *et al.*, *Journal of the Physical Society of Japan* **85** 034709, (2016).
- [5]. K. R. Lea *et al.*, *Journal of Physics and Chemistry of Solids* **23** 1381-1405, (1962).
- [6]. R. White *et al.*, *Determination of the Crystal Field Levels in  $\text{TmV}_2\text{Al}_{20}$ , in preparation.*

## Control of the persistent spin helix lifetime by crystal orientation

D. Iizasa<sup>1,2</sup>, M. Kohda<sup>1,3,4</sup>, U. Zülicke<sup>2</sup>, J. Nitta<sup>1,3,4</sup>, and M. Kammermeier<sup>2</sup>

<sup>1</sup>*Department of Materials Science, Tohoku University, Sendai 980–8579, Japan*

<sup>2</sup>*School of Chemical and Physical Sciences and MacDiarmid Institute for Advanced Materials and Nanotechnology, Victoria University of Wellington, Wellington 6140, New Zealand*

<sup>3</sup>*Center for Spintronics Research Network, Tohoku University, Sendai 980–8579, Japan*

<sup>4</sup>*Center for Science and Innovation in Spintronics (Core Research Cluster), Tohoku University, Sendai 980–8579, Japan*

In a semiconductor, the spin-orbit (SO) coupling enables a coherent control of the electron spin, while at the same time spin relaxation occurs via the SO coupling itself due to the interplay with impurity scattering. A way to overcome this problem is a collinear SO field with spin-preserving symmetry for an optimal ratio of linear Rashba and Dresselhaus SO strengths in a two-dimensional electron gas (2DEG) [1,2]. It allows the emergence of a long-lived helical spin density known as persistent spin helix (PSH). Recently, it was found that the PSH can be realized in general crystal orientations if and only if at least two Miller indices agree in modulus [3] (cf. Fig. 1), in addition to the well-established cases of [001], [110], and [111] oriented 2DEGs [4,5]. However, the usually accompanying cubic Dresselhaus SO field breaks the spin-preserving symmetry which limits PSH lifetime. Studies on such impact of the cubic SO field on the PSH lifetime are so far restricted to the well-established cases [4–6].

In this work, we unveil the robustness of the PSH damped by the cubic Dresselhaus field in zinc-blende semiconductor 2DEGs with general crystal orientation. It is shown that the interplay of orientation and magnitude of cubic field yields the most robust PSH state which can be well approximated by a [225] crystal orientation. It allows a 30% enhancement of the PSH lifetime compared to conventional [001] quantum wells as depicted in Fig. 2. Remarkably, the Rashba SO interaction is negligible in this situation.

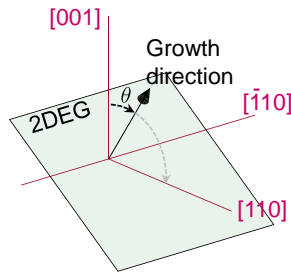


**Fig. 1:** PSH emerges at a growth direction with at least two identical Miller indices, here characterized by the polar angle  $\theta$  from [001] to [110].

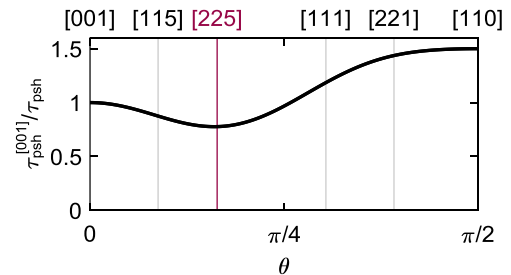


**Fig. 2:** PSH relaxation rate in terms of the relaxation rate at [001] in dependence of the crystal orientation.  $\tau_{\text{psh}}$  denotes the PSH lifetime.

### References

- [1] J. Schliemann, J. C. Egues, and D. Loss, *Phys. Rev. Lett.* **90**, 146801 (2003).
- [2] B. A. Bernevig, J. Orenstein, and S.-C. Zhang, *Phys. Rev. Lett.* **97**, 236601 (2006).
- [3] M. Kammermeier, P. Wenk, and J. Schliemann, *Phys. Rev. Lett.* **117**, 236801 (2016).
- [4] J. Schliemann, *Rev. Mod. Phys.* **89**, 011001 (2017).
- [5] M. Kohda and G. Salis, *Semicond. Sci. Technol.* **32**, 073002 (2017).
- [6] D. Iizasa, D. Sato, K. Morita, J. Nitta, and M. Kohda, *Phys. Rev. B* **98**, 165112 (2018).

## Magnonic Hydrogen Gas Sensing

M. Kostylev<sup>1</sup>, C.S. Chang<sup>1</sup>, S. Khan<sup>1</sup>, T. Schneider<sup>1</sup> and S. Watt<sup>1</sup>

<sup>1</sup>*Department of Physics and Astrophysics M019, The University of Western Australia,  
35 Stirling Hwy, Crawley 6009 WA, Australia*

Magnonics is an area of research that studies dynamic magnetic phenomena in magnetic materials. One fundamental type of the dynamics is precession of the magnetisation vector about its equilibrium direction in the materials. This gives rise to magnetisation oscillations (called “Ferromagnetic Resonance, (FMR)”) and waves (“called spin waves”). Quanta of these microwave-frequency excitations are magnons, which gave the name to the area.

We found that the FMR response of palladium-based ferromagnetic films [1] and nanostructures [2] is very sensitive to the presence of hydrogen gas in the sample environment. This led us to suggestion of a real-world magnonic hydrogen sensor. Importantly, being based on a novel sensing principle, our sensor is able to resolve hydrogen concentrations in the upper concentration range - between 20% and 100%. This range is very important for fuel-cell applications, but most of other sensor concepts loose sensitivity for these ultra-high gas concentrations.

In this talk, our latest results of investigation of the effect of hydrogen gas on the FMR and Inverse Spin Hall Effect [3] responses of Pd/Co bi-layer and PdCo and PdFe alloy films will be presented. These results include observation of an ultra-strong effect of the gas on the FMR peak frequency for a Pd<sub>73</sub>Co<sub>27</sub> alloy film and a finding that absorption of hydrogen by Pd results in a decrease in the spin diffusion length for this metal, as probed in the conditions of FMR in a Pd/Co bi-layer film.

### References

- [1] C.S. Chang, M. Kostylev, and E. Ivanov, Applied Physics Letters **102**, 142405 (2013).
- [2] C. Lueng, P. Lupo, P.J. Metaxas, M. Kostylev, and A.O. Adeyeye, Advanced Materials Technologies 1, 1600097 (2016).
- [3] S.Watt and M.Kostylev, arXiv:1909.10661 (2019).

## **Bulk Currents in Artificial Graphene with a Magnetic Field**

Z. E. Krix, O. P. Sushkov

*School of Physics, UNSW, Sydney, Australia*

We present calculations of the equilibrium current density for a patterned 2DEG with infinite strip geometry and a perpendicular magnetic field. A triangular lattice of anti-dots with lattice spacing 120 nm and potential maximum close to or above to Fermi level. Such a system is known as artificial graphene (AG). To compute the current density we numerically diagonalize the AG Hamiltonian over a set of Landau level basis states, this takes into account coupling between different Landau levels. Our calculations show that, at fields typical for quantum Hall measurements, the bulk current has two distinct components. One component is due to localized electrons in closed orbits around each anti-dot and scales weakly with potential modulation. The presence of a second component is the focus of this work. We show that there exist a set of extended streams of current which flow through the entire sample. These streams scale roughly in proportion to the potential strength and carry a current comparable to that carried by edge modes.

## Crystal structure and thermoelectric properties of *n*-type Bi<sub>2-x</sub>Ce<sub>x</sub>O<sub>2</sub>Se ceramics

H.Y. Hong, D.H. Kim, K. Park

*Faculty of Nanotechnology and Advanced Materials Engineering, Sejong University, Seoul 143–747, Korea*

Bi<sub>2</sub>O<sub>2</sub>Se consists of the tetragonal insulating [Bi<sub>2</sub>O<sub>2</sub>]<sup>2+</sup> and [Se]<sup>2-</sup> layers [1]. The oxide exhibits a low thermal conductivity and a large Seebeck coefficient [2]. Thus, Bi<sub>2</sub>O<sub>2</sub>Se is of particular interest as a potential *n*-type thermoelectric material. In this work, we prepared Bi<sub>2-x</sub>Ce<sub>x</sub>O<sub>2</sub>Se ( $x = 0 - 0.15$ ) samples by spark plasma sintering (SPS). For SPS, the prepared powders of Bi<sub>2-x</sub>Ce<sub>x</sub>O<sub>2</sub>Se ( $x = 0 - 0.15$ ) were placed in a graphite mold, heated up to 630 °C, and then kept at this temperature for 5 min under a pressure of 50 MPa in vacuum. The structural, optical, and thermoelectric properties of the Bi<sub>2-x</sub>Ce<sub>x</sub>O<sub>2</sub>Se as a function of Ce content were investigated by X-ray diffraction (XRD), XRD Rietveld refinement, scanning electron microscope (SEM), UV-visible spectroscopy, and thermoelectric property measurements. The major peaks of the calcined powders were matched with standard PDF # 25-1463 of Bi<sub>2</sub>O<sub>2</sub>Se, indicating a tetragonal structure with *I4/mmm* space group. Weak XRD peaks related to CeO<sub>2</sub> and Bi<sub>2</sub>O<sub>3</sub> in the calcined powders were detected. The sintered Bi<sub>2-x</sub>Ce<sub>x</sub>O<sub>2</sub>Se crystallized in a tetragonal structure. The electrical and thermal conductivities increased with increasing Ce content. The Seebeck coefficients of all the samples were negative, indicating that electrons are major carriers. The substitution of Ce for Bi is a promising approach for improving the thermoelectric properties of Bi<sub>2</sub>O<sub>2</sub>Se.

### References

- [1] J. Wu *et al.*, Nature Nanotechnol. **12**, 530–534 (2017)
- [2] X. Tan *et al.*, J. Am. Ceram. Soc. **101**, 4634–4644 (2018).

## Surveying the higher dimensions of the aperiodic composite nonadecane/urea

G.J. McIntyre<sup>1</sup>, M.-H. Lemée-Cailleau<sup>2</sup>, B. Toudic<sup>3</sup>

<sup>1</sup> *Australian Nuclear Science and Technology Organisation, Lucas Heights NSW 2234, Australia*

<sup>2</sup> *Institut Laue-Langevin, 6 rue Jules Horowitz, 38042 Grenoble Cedex 9, France*

<sup>3</sup> *Institut de Physique de Rennes, UMR URI-CNRS 6251, Université de Rennes 1 - 35042 Rennes Cedex, France*

A decade ago, few we observed for the first time that there exist phase transitions where the structural changes correspond just to degrees of freedom hidden in the internal (super)space of an aperiodic material, here the composite nonadecane/urea [1]. A key factor in the discovery of this type of transition [2] was the examination of the diffraction pattern in 3D, only possible at the time on a four-circle triple-axis neutron spectrometer, the analyzer used in zero-energy transfer to reduce the background and improve resolution. Despite the greater accessibility in reciprocal space compared with earlier experiments using a conventional triple-axis spectrometer, the weak intensity of the superlattice reflections limited the volume of reciprocal space that could be explored.

Modern neutron Laue diffractometers with large image-plate detectors permit rapid and extensive exploration of reciprocal space with high resolution in the two-dimensional projection and a wide dynamic range with negligible bleeding of intense diffraction spots [3]. Surveying nonadecane/urea with neutron Laue diffraction from 300 K to 4 K revealed further detail of the superspace-driven phase transition, notably an increase in misorientation in the plane perpendicular to the composite misfit axis, as well as a first-order transition to a new phase at lower temperature. Complementary monochromatic X-ray examination, again using a high-resolution image-plate detector, showed that this new phase corresponds to additional commensurate ordering of the guest alkane subsystem.

These observations shed light on how nature can use the degrees of freedom hidden in the internal superspace to form states that cannot be envisaged in the usual 3D real space.

### References

- [1] B. Toudic *et al.* *Science* 319, 69 (2008).
- [2] B. Toudic *et al.* *Euro. Phys. Lett.* 93, 16003 (2011).
- [3] G.J. McIntyre *et al.* *Physica B* 385-386, 1055 (2006).
- [4] S. Zerdane *et al.* *Acta Cryst.* B71, 293 (2015).



## Magnetism in alloys of the rare-earth nitrides

J. D. Miller<sup>1</sup>, M. al Khalfioui<sup>2</sup>, B. J. Ruck<sup>1</sup>, H. J. Trodahl<sup>1</sup>

<sup>1</sup>*School of Chemical and Physical Sciences, Victoria University of Wellington, P.O. Box 600, Wellington 6140, New Zealand*

<sup>2</sup>*Centre de Recherche sur l'Hétéro-Épitaxie et ses Applications (CRHEA), Centre National de la Recherche Scientifique (CNRS), Rue Bernard Gregory, F-06560 Valbonne, France*

The rare-earth mononitrides LN (L a lanthanide element) form the only epitaxy-compatible series of *intrinsic* ferromagnetic semiconductors. [1] The large variation in magnetic behaviours of the LN provides an opportunity to tune the properties of alloys with an eye to achieving compensated magnetisation or angular momentum states (net  $\mu = 0$  or net  $J = 0$ ). Alloys of GdN and SmN of the form  $Gd_xSm_{1-x}N$  have been grown and characterised using magnetisation and electrical transport. GdN is a spin-only magnetic moment that saturates at 7 Bohr magnetons/ion. In contrast, SmN has a ferromagnetic moment of 0.035 Bohr magnetons/ion. The vanishingly small moment of SmN results from a near cancellation of the spin and orbital moments, with spin-orbit coupling leading to the opposite alignment of these angular momenta. [2] Imbalance between the moments is dominated by the orbital contribution, which dictates that the spin magnetic moment is *antiparallel* to the net magnetisation. Thus, the spin magnetic moment in SmN aligns antiparallel to an applied magnetic field and there is an exchange - Zeeman conflict between neighbouring Gd and Sm ions in  $Gd_xSm_{1-x}N$  alloys. Magnetisation measurements taken well below the Curie temperature of GdN or SmN (Figure 1), magnetoresistance and AHE (not shown) show clear variation with composition, and the saturation magnetisation, the coercive and saturation fields are all strongly influenced by the Zeeman-exchange conflict.

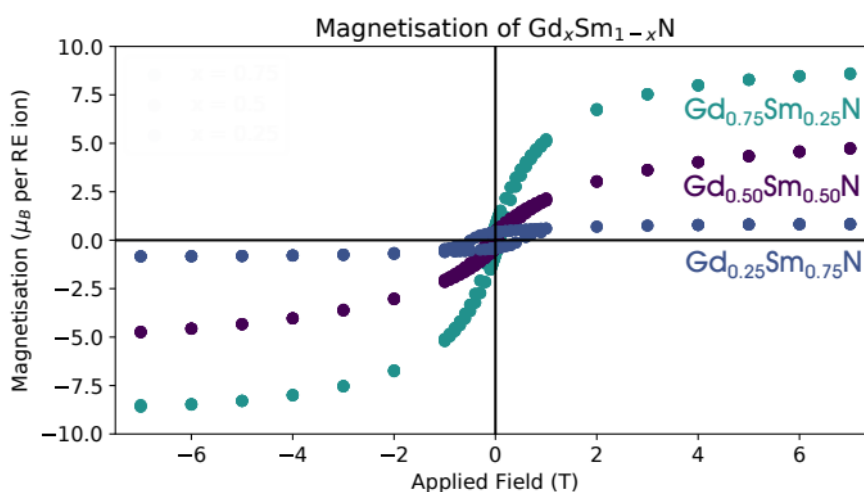


Fig. 1:

*Magnetisation Measurements of  $Gd_xSm_{1-x}N$  alloys showing the variation with Gd content*

## References

- [1] F. Natali et. al., Prog. Mat. Sci., vol. 58, 1316 (2013).
- [2] E. M. Anton et. al., Phys. Rev. B, vol. 87, 134414 (2013).

## Low-energy electron beam induced damage to organic molecules — limits to IPES application to organic molecules

G. Motta<sup>1</sup>, J. MacLeod<sup>1,2</sup>, J. Lipton-Duffin<sup>1,2</sup>

<sup>1</sup>*School of Chemistry Physics and Mechanical Engineering, Queensland University of Technology, Brisbane, Australia*

<sup>2</sup>*Institute for future environments, Queensland University of Technology, Brisbane, Australia*

A low-energy version of inverse photoemission spectroscopy (LEIPES) has been developed by Yoshida and co-workers which claims to solve the problems of damage to organic molecules due to electron beam irradiation. However, electrons with energies lower than 5 eV have been found to damage a wide range of organic molecules, even when the electron energy is lower than the ionisation energy of the target molecule (Stepanović et al. 1999). The mechanism responsible for this type of damage is called dissociative electron attachment. As the wavelength of the electrons becomes comparable to the lengths of the bonds present in the molecule, a resonance occurs thereby allowing the incoming electrons to attach to the molecule creating a transient molecular anion. Two possibilities arise: either the electron detaches from the molecule, or the anion dissociates into one or several fragments. This poses problems for surface analysis techniques which use low-energy electrons, since they can cause sample damage. However, studies performed on copper phthalocyanine, and tin phthalocyanine thin films using LEIPES showed no spectral changes even after several hours of continuous measurement (Yoshida 2015; Kashimoto et al. 2018). These results imply that our understanding of the interaction between low-energy electrons and organic molecular materials is still incomplete. I will report on our experiments to better understand low-energy electron damage in organic materials. We have found that irradiating trimesic acid on Ag(111) with a low-energy electron beam (2–4 eV) induces chemical changes in the molecules even below the energy threshold imposed on LEIPES. Understanding what kind of organic molecules are damaged by low-energy electron beams will allow us to properly assess the limits of IPES.

### References

1. Stepanović, M., Pariat, Y., and Allan, M. (1999), Dissociative electron attachment in cyclopentanone,  $\gamma$ -butyrolactone, ethylene carbonate, and ethylene carbonate-d<sub>4</sub>: Role of dipole-bound resonances, *J. Chem. Phys.*, 110, 11376–11382.
2. Kashimoto, Y., Yonezawa, K., Meissner, M., Gruenewald, M., Ueba, T., Kera, S., Forker, R., Fritz, T., & Yoshida, H. (2018), The evolution of intermolecular energy bands of occupied and unoccupied molecular states in organic thin films, *J. Phys. Chem. C*, 122, 1290–1297.
3. Yoshida, H. (2015), Principle and application of low energy inverse photoemission spectroscopy: a new method for measuring unoccupied states of organic semiconductors, *J. Electron Spectrosc. and Related Phenomena*, 204, 116–124.

## A menagerie of strongly correlated phases on the decorated honeycomb lattice

H. L. Nourse<sup>1</sup>, R. H. McKenzie<sup>1</sup>, B. J. Powell<sup>1</sup>

<sup>1</sup>*School of Mathematics and Physics, The University of Queensland, Brisbane, Queensland, Australia*

Decorated lattices are ubiquitous in nature and are often found in metal-organic frameworks (MOFs). We demonstrate that strongly correlated electrons on decorated lattices have rich phase diagrams. Because MOFs are highly tunable, decorated lattices presents a unique opportunity to design quantum materials to investigate fundamental questions within condensed matter physics, e.g., emergent quantum spin liquids, topological phases of matter, unconventional superconductivity, as well as the prospect of engineering new emergent phases of matter.

The menagerie of phases (see Table 1 for the decorated honeycomb lattice) occurs because of the unique geometrical structure of the molecules that decorate the lattice which act as important additional degrees of freedom (see Figure 1). As a salient example, an exotic spin-1 insulating phase (Hund's insulator) emerges on the decorated honeycomb lattice from a simple on-site Hubbard  $U$  because the molecular structure generates effective multi-orbital interactions that favors spin triplet formation. We specialize to the decorated honeycomb lattice as a concrete example but the phenomena generalizes to other decorated lattices.

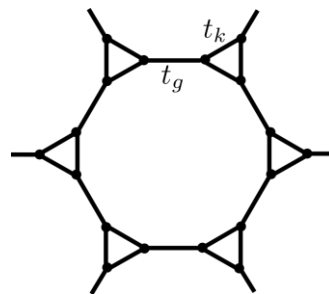


**Fig. 1:** The decorated honeycomb lattice, where  $t_k$  ( $t_g$ ) is the probability amplitude for an electron to move within (between) triangles.

Electrons unit cell	$t_k \gg t_g$ (Trimer limit)	$t_k \ll t_g$ (Dimer limit)
1		
2	Trimer Mott insulator	
3		Dimer Mott insulator
4	Band insulator	
5	Flat-band ferromagnet	Flat-band ferromagnet
6	Real-space Mott insulator	Band insulator / valence bond solid
7		
8	Hund's insulator	
9		Dimer Mott insulator
10		
11	Flat-band ferromagnet	Flat-band ferromagnet

**Table 1:** A summary of the insulating phases of the Hubbard model on the decorated honeycomb lattice.

## Substitutional Doping of Trirutiline Phases, $AB_2O_6$

S. Patel<sup>1,2</sup>, T. Söhnel<sup>1,2</sup>

<sup>1</sup>*School of Chemical Sciences, University of Auckland, Auckland, New Zealand*

<sup>2</sup>*MacDiarmid Institute for Advanced Materials and Nanotechnology, Victoria University of Wellington, Wellington, New Zealand*

Metal oxides of formula  $MSb_2O_6$  have garnered widespread interest in materials science research as they prove to be promising materials as semiconductor photocatalysts and ionic conductors. [1] Many of these compounds (e.g.  $M = Co, Zn, Ni, Fe$  etc.) are known to crystallize in a tetragonal trirutile phase [2], although  $CuSb_2O_6$  is known to exhibit a monoclinic distortion. [3] We are investigating several ternary compounds with general formula  $AB_2O_6$ , with substitutional doping of A ( $Cu_{1-x}Ni_xSb_2O_6$ ) and B ( $ZnSb_{2-x}Sn_xO_6$ ). Preliminary results have shown us that these materials show promising behavior as mixed ionic conductors due to oxygen vacancies being created through the substitutional doping.

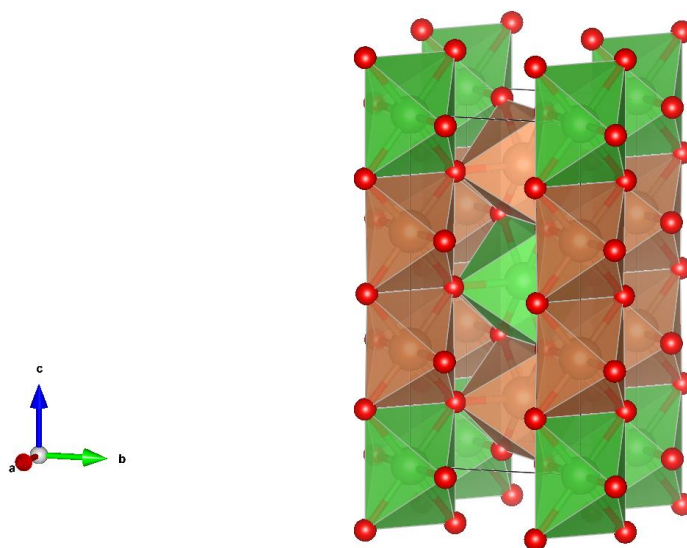


**Fig. 1:** *Tetragonal Trirutile Crystal Structure*

### References

- [1] Singh, J., Bhardwaj, N., Uma, S., Bull. Mater. Sci., (2013), 36, 287
- [2] Nikulin, AY, Zvereva EA, Nalbandyan VB, et al., Dalton Trans (2017), 46, 6059
- [3] Kang H.B., PhD thesis, University of Auckland (2017)

## Development of a spin-injection field effect transistor utilizing Rare-earth Nitrides

K. Pitman<sup>1,2</sup>, S. Granville<sup>2,3</sup>, B. Ruck<sup>1,2</sup>

<sup>1</sup>*School of Chemical and Physical Sciences, Victoria University of Wellington, Wellington, New Zealand*

<sup>2</sup>*Macdiarmid Institute for Advanced Materials and Nanotechnology, New Zealand*

<sup>3</sup>*Robinson Research Institute, Victoria University of Wellington, Wellington, New Zealand*

Energetically sustainable alternatives to our current computing technology are essential to minimize the effects of climate change. Hence, there is a need for a new type of transistor; one that has sustainable energy requirements and the potential to exceed the technological capabilities of electronic devices.

Spintronics is a potential alternative to our current electronics and has the capacity to integrate with current semiconductor technology [1]. Spintronics relies on the spin of the electron to allow for information transmission rather than electronic movement. The spin field-effect transistor was initially proposed by Datta and Das in 1990 and consists of two ferromagnetic electrodes that act as a spin injector and detector joined by a non-magnetic conducting channel [2].

However, the conductivity difference between the electrodes and conducting channel results in low spin injection efficiency, and an applicable spinFET is yet to be realised [3]. Rare-earth nitrides (RENs) consist of a Lanthanide 3- ion, and a Nitrogen 3+ ion. Gadolinium Nitride (GdN) is a REN semiconductor, is also ferromagnetic at low temperatures [4], and provides a potential solution to the mismatch in conductivity.

The fabrication of a spinFET utilising GdN as the ferromagnetic electrodes is presented as well as the measurement system employed to detect spin transport.

### References

- [1] S. A. Wolf et al., "Spintronics: A Spin-Based Electronics Vision for the Future", *Science*, vol. 294, pp 1488-1495, November 2001.
- [2] S. Datta and B. Das, "Electronic analog of the electro-optic modulator", *Appl. Phys. Lett.*, vol. 56, pp. 665-667, February 1990.
- [3] E. I. Rashba, "Theory of electrical spin injection: Tunnel contacts as a solution of the conductivity mismatch problem", *Phys. Rev. B*, vol. 62, pp 267-270, December 2000.
- [4] F. Natali, B. J. Ruck, N. O. V. Plank, H. J. Trodahl, S. Granville, C. Meyer, W. R. L. Lambrecht, "Rare-earth mononitrides", *Prog. Mater. Sci.*, vol. 58, pp. 1316-1360, October 2013.

# Topology from Interactions: Haldane-like Phase in the Extended Hubbard Model

Matthias Peschke<sup>1</sup>, Roman Rausch<sup>2</sup>

<sup>1</sup>*Department of Physics, University of Hamburg, Jungiusstraße 9, D-20355 Hamburg, Germany*

<sup>2</sup>*Department of Physics, Kyoto University, Kyoto 606-8502, Japan*

The extended Hubbard model with an attractive density-density interaction, positive pair hopping, or both, is shown to host a topological Haldane-like phase, with a doubly degenerate entanglement spectrum and interacting edge states. It is protected by a pseudogap of the dynamical spin excitations, whereby the spectral weight goes to zero at  $\omega=0$ . When the extended interaction terms combine in a charge-SU(2) symmetric fashion, a novel partially polarized pseudospin-ferromagnetic phase appears, in which spin excitations coexist with  $\eta$ -wave superconductivity and which still retains the topological features.

## References

- [1]. M. Peschke, R. Rausch, in preparation (2020)

## Preparation and structural characterisation of pure and Te-doped $\text{Cu}_2\text{OSeO}_3$

R. Rov<sup>1,4</sup>, J. S. Flores<sup>2</sup>, E. P. Gilbert<sup>3</sup>, S. Yick<sup>2</sup>, C. Ulrich<sup>2,3</sup>, T. Söhnel<sup>1,4</sup>

<sup>1</sup> School of Chemical Sciences, University of Auckland, Auckland 1142, New Zealand

<sup>2</sup> School of Physics, University of New South Wales, Sydney NSW 2052, Australia

<sup>3</sup> Australian Nuclear and Science Technology Organisation (ANSTO), Australia

<sup>4</sup> MacDiarmid Institute of Advanced Materials and Nanotechnology, Victoria University of Wellington, New Zealand

$\text{Cu}_2\text{OSeO}_3$  is a multiferroic materials that shows the formation of skyrmions at low temperatures. A skyrmion is a topologically protected particle-like magnetic spin structures on the order of 10-100 nm. Recent studies have also shown that the skyrmions can be manipulated through applications such as an external electric fields and heat. This offers the potential for development for a much more stable, energy efficient and faster storage in memory devices. The magnetic skyrmions pack into a hexagonal lattice with the skyrmion lattice only stable in a narrow magnetic field-temperature range [1,2]. Here we present the preparation of pure and Te-doped  $\text{Cu}_2\text{OSeO}_3$  single crystals with chemical vapour transport, the structural characterisation with X-ray and neutron single crystal diffraction, small angle neutron scattering and magnetisation measurements. Mapping of the magnetic field-temperature phase diagram showed that tellurium doping resulted in an enlarged stability range for the skyrmion phase had been achieved [3].

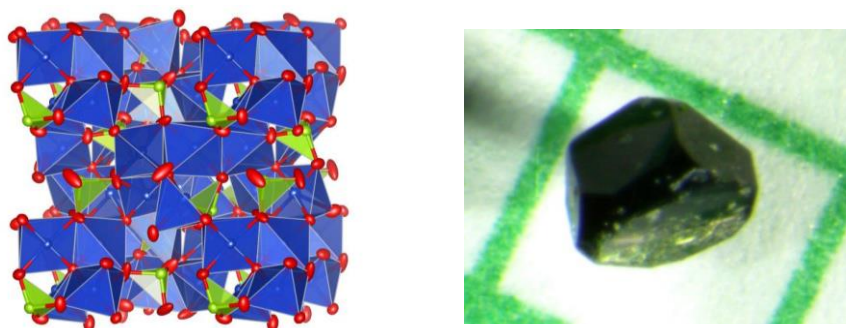


**Fig. 1:** Crystal structure of  $\text{Cu}_2\text{OSeO}_3$  at 300 K (left; Cu blue, Se yellow, O red atoms), single crystal of  $\text{Cu}_2\text{OSeO}_3$  grown with chemical vapour transport (right).

### References

- [1] S. Seki, J.-H. Kim, D. Inosov, R. Georgii, B. Keimer, S. Ishiwata, Y. Tokura, *Phys. Rev. B* **85**, 220406 (2012).
- [2] A. Fert, N. Reyren, V. Cros, *Nature Rev. Mat.* **2**, 17031 (2017).
- [3] R. Rov, Master's Thesis, *University of Auckland* (2019).

## Exploring the Pyrophosphate Series $K_2Cu_{1-x}Fe_xP_2O_7$

R. Silk<sup>1</sup>, M. Avdeev<sup>2</sup>, J. S. Flores<sup>3</sup>, C. Ulrich<sup>3</sup>, T. Söhnel<sup>1,4</sup>

<sup>1</sup>*School of Chemical Sciences, University of Auckland, Auckland, New Zealand*

<sup>2</sup>*Australian Nuclear and Science Technology Organisation (ANSTO), Australia*

<sup>3</sup>*School of Physics, University of New South Wales, Sydney NSW 2052, Australia*

<sup>4</sup>*MacDiarmid Institute of Advanced Materials and Nanotechnology, Wellington, New Zealand*

Phosphate materials are of great interest to materials science. Metal phosphate compounds are known to exhibit conductive properties for battery use [1], photocatalytic abilities to decompose other compounds [2], the ability to conduct protons [3], etc. High temperature sintering techniques were used to produce the diphosphate series  $K_2Cu_{1-x}Fe_xP_2O_7$ . The material forms two different modifications, a tetragonal ( $P-42_1m$ ) and an orthorhombic modification ( $Pbnm$ ) as shown in Figure 1. The crystal structure was determined through the use of powder X-ray diffraction (PXRD). PXRD patterns show a shift in peaks to lower angles with increasing iron content, which is consistent with an increase of lattice constant parameters. The presence of additional phases such as  $KPO_3$  can also be observed. UV-Vis measurements show how the transitions change with increasing amounts of iron and different modifications. Tauc plots revealed that the material has a direct band gap of approximately 3 eV. IR measurements revealed that water had been absorbed by the material and there a slight shift in peak position with increasing iron content. First magnetic measurements did not show any long-range ordering down to 2 K, the compounds remained paramagnetic. The  $K_2CuP_2O_7$  and  $K_2Cu_{0.75}Fe_{0.25}P_2O_7$  samples show short-range antiferromagnetic contribution across both modifications.

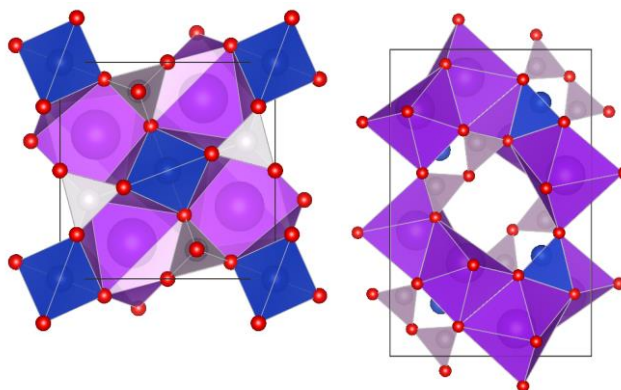


**Fig. 1:** Crystal structure of  $K_2CuP_2O_7$  with tetrahedral space group  $P-42_1m$  (left) and orthorhombic space group  $Pbnm$  (right).

### References

- [1] X. Lei, H. Zhang, Y. Chen, W. Wang, Y. Ye, C. Zheng, ... Z. Shi, *J. Alloys Comp.* **626**, 280 (2015).
- [2] M. Zhou, X. Jiang, M. Xia, H. Huang, Z. Lin, J. Yao, Y. Wu, *J. Alloys Comp.* **689**, 599 (2016)
- [3] Y. Jin, Y. Shen, T. Hibino, *J. Mat. Chem.* **20**, 6214-6217 (2010).



## Exploring the Novel Pyrovanadate Series $K_2Mn_{1-x}CoV_2O_7$

M. Smith<sup>1</sup>, M. Avdeev<sup>2</sup>, J. S. Flores<sup>3</sup>, C. Ulrich<sup>3</sup>, T. Söhnel<sup>1,4</sup>

<sup>1</sup>*School of Chemical Sciences, University of Auckland, Auckland, New Zealand*

<sup>2</sup>*Australian Nuclear and Science Technology Organisation (ANSTO), Australia*

<sup>3</sup>*School of Physics, University of New South Wales, Sydney NSW 2052, Australia*

<sup>4</sup>*MacDiarmid Institute of Advanced Materials and Nanotechnology, Wellington, New Zealand*

Materials with the Melilite-type structure have been intensively studied throughout the years due to their interesting piezoelectric, electrochemical, luminescent, magnetic, and structural properties [1,2]. Many oxides with the general formula  $A_2BC_2O_7$  crystallise into the melilite family of minerals, where A is a large cation from group one or two; B is typically a first-row transition metal with four-fold coordination; and C is a smaller cation like Si, V, P, or Ge [1-4]. The Pyrovanadate ( $A_2BV_2O_7$ ) compounds  $K_2MnV_2O_7$  and  $K_2CoV_2O_7$  exist in the melilite group, with the tetragonal space group  $P\bar{4}2_1m$ , consisting of alternating layers of  $K^+$  ions in between  $MV_2O_7^{2-}$  sheets comprised of connected  $MO_4$  and  $VO_4$  tetrahedra (Figure 1) [1,2]. The crystal structure  $K_2Mn_{1-x}CoV_2O_7$  was determined from the rietveld refinement of powder X-ray diffraction (PXRD) patterns. Refinement of PXRD patterns showed a systematic shift in reflections with increasing cobalt content, consistent with an increase of lattice constant parameters. UV-Vis measurements show how the addition of cobalt leads to an additional electronic transition whose intensity increases with increasing cobalt concentration. Tauc plots revealed that the material has a direct band gap of approximately 2 eV. Photoluminescent measurements of the cobalt doped species revealed promising results for white light emitters due to electronic transitions across the cobalt tetrahedra and pyrovanadate units. First magnetic measurements indicate a long-range antiferromagnetic ordering at just over 2 K for  $K_2CoV_2O_7$ .

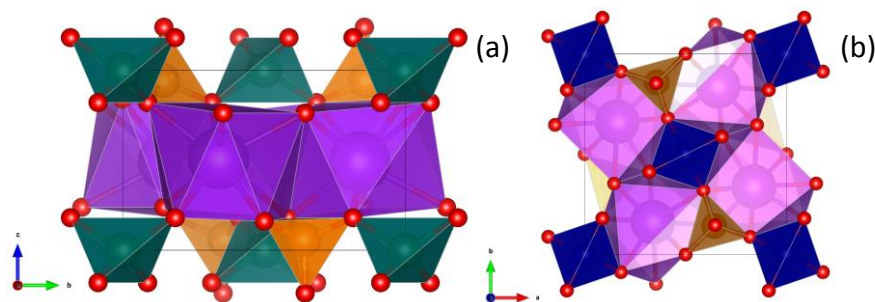


Fig. 1: Crystal structure of the  $P\bar{4}2_1m$  tetragonal systems (a)  $K_2MnV_2O_7$  and (b)  $K_2CoV_2O_7$ .

### References

- [1] H. B. Yahia, E. Gaudin, J. Darriet, J. Z. Naturf. B **62**, 873 (2007).
- [2] H. B. Yahia, R. Essehli, I. Belharouak, E. Gaudin, E. Mat. Res. Bull. **71**, 7 (2015).
- [3] V. Ramesh, Nuclear Magnetic Resonance: Volume 45; Royal Society of Chemistry (2016).
- [4] M. Sale, M. Avdeev, Z. Mohamed, C. D. Ling, P. Barpanda, Dalton Trans. **46**, 6409 (2017).

## Characterising the local crystal field interaction for RFeO<sub>3</sub> (R = Er, Ho)

G. A. Stewart<sup>1</sup>, T. Frankcombe<sup>1</sup>, G.N. Iles<sup>2</sup>, Z. Yamani<sup>3</sup>

<sup>1</sup>*School of Science, The University of New South Wales, Canberra, ACT 2600, Australia*

<sup>2</sup>*Dept of Physics, RMIT University, Melbourne, VIC 3000, Australia*

<sup>3</sup>*Canadian Nuclear Laboratories, Chalk River, Ontario, K0J 1J0, Canada*

There is renewed interest in orthorhombic ferrites RFeO<sub>3</sub> (R = rare earth) as a potential source of useful *multiferroic* materials [1]. The low temperature magnetic anisotropy of the ferrites is influenced by the anisotropic crystal field (CF) interaction at the R site. On the basis of recent low temperature inelastic neutron scattering (INS) investigations of HoFeO<sub>3</sub> [2], we hoped to interpret the data in terms of the CF interaction acting at its Ho<sup>3+</sup> site. However, the local symmetry is low (monoclinic, C<sub>s</sub>(m)) and Ho<sup>3+</sup> is a non-Kramers ion whose ground multiplet (J = 8) is necessarily split into 2J + 1 = 17 singlet states [3]. Against this, the INS analyses have identified just 5 of these (0, 0.61, 10.1, 15.1 and 22 meV) where the lowest two energy states constitute a *quasi-doublet*. In support of our INS results, a near identical set of low-lying singlet levels has been confirmed for Ho<sup>3+</sup> in isostructural HoCrO<sub>3</sub> via a detailed interpretation of low temperature specific heat data [4]. However, the situation is more encouraging for the neighbouring case of ErFeO<sub>3</sub> where Er<sup>3+</sup> (J = 15/2) is a Kramers ion and reasonably consistent energy levels have been determined for all 8 Kramers doublets using optical spectroscopy [5].

In this on-going work we are searching for the CF parameters of both Er<sup>3+</sup>:ErFeO<sub>3</sub> and Ho<sup>3+</sup>:HoFeO<sub>3</sub>:

- (i) employing two different lattice charge summations (a simple point charge model and a charge distribution computed using the PAW version of VASP [6]) to compute within-rank, Stevens, CF parameter ratios B<sub>nm</sub>/B<sub>n0</sub> (n = 4, 6; m = even integer with -n ≤ m ≤ n),
- (ii) conducting grid searches over the remaining parameters B<sub>20</sub>, B<sub>22</sub>, B<sub>2-2</sub>, B<sub>40</sub>, B<sub>60</sub> for Er<sup>3+</sup> in ErFeO<sub>3</sub> (simultaneously converting them for Ho<sup>3+</sup> in HoFeO<sub>3</sub>), and
- (iii) comparing CF levels predicted for Er<sup>3+</sup> in ErFeO<sub>3</sub> and Ho<sup>3+</sup> in HoFeO<sub>3</sub> with the known experimental values.

Early matches to the ErFeO<sub>3</sub> data have been achieved with the point charge model approach but not yet for HoFeO<sub>3</sub>. The most recent results will be presented at Rotorua.

### References

- [1] D. H. Ryan, Quentin Stoyel, Larissa Veryha, Kai Xu, Wei Ren, Shixun Cao and Zahra Yamani, IEEE Trans. Magn. 53 (2017) 3101505
- [2] G. A. Stewart, G. N. Iles, R. A. Mole, Z. Yamani and D. H. Ryan, Crystal field excitations of Ho<sup>3+</sup> in HoFeO<sub>3</sub>, Handbook of 41<sup>st</sup> Annual Condensed Matter and Materials meeting, Wagga Wagga, Australia (2017)
- [3] U. V. Valier, J. B. Grubers and G. W. Burdick, Magneto-optical spectroscopy of the rare earth compounds: development and application, Sci. Res. Publishing Inc (2012).
- [4] T. Chatterji, F. Demmel, N. Jalarvo, A. Podlesnyak, C. M. N. Kumar, Y. Xiao and T. Brückel, J. Phys.: Condens. Matter 29 (2017) 475802
- [5] D. L. Wood, L. M. Holmes and J. P. Remeika, Phys. Rev. 185 (1969) 689 - 695
- [6] G. Kresse and D. Joubert, Phys. Rev. B 59 (1999) 1758-1775

## **Prediction of the spin triplet two-electron quantum dots in Si: towards controlled quantum simulations of magnetic systems**

Dmitry Miserev<sup>1</sup>, O. P. Sushkov<sup>2</sup>.

<sup>1</sup>*Department of Physics, University of Basel, Klingelbergstrasse 82, CH-4056 Basel, Switzerland*

<sup>2</sup>*School of Physics, University of New South Wales, Sydney, Australia*

Ground state of two-electron quantum dots in single-valley materials like GaAs is always a spin singlet regardless of what the potential and interactions are. This statement cannot be generalized to the multi-valley materials like n-doped Si. Here we calculate the spectrum of a two-electron Si quantum dot analytically and numerically and show that the dot with the lateral size of several nm can have the spin triplet ground state which is impossible in the single-valley materials. Predicted singlet-triplet level crossing in two-electron Si quantum dots can potentially establish the platform for quantum simulation of magnetic many-body systems based on the triplet quantum dots. We suggest several examples of such systems that open a way to controlled quantum simulations within the condensed matter setting.

## Computational and Spectroscopic Studies on Magnetically Frustrated $M'M''_3\text{Si}_2\text{Sn}_7\text{O}_{16}$ ( $M' = \text{Fe, Co}$ ; $M'' = \text{Fe, Mn}$ ) Structures

J. Vella<sup>1,2</sup>, T. Söhnel<sup>1,2</sup>, C. Ling<sup>3</sup>

<sup>1</sup> School of Chemical Sciences, University of Auckland, Auckland 1142, New Zealand

<sup>2</sup> MacDiarmid Institute of Advanced Materials and Nanotechnology, Wellington, New Zealand

<sup>3</sup> School of Chemistry, The University of Sydney, Sydney, NSW 2006, Australia

The magnetically frustrated Kagomé structure found within  $\text{Fe}_4\text{Si}_2\text{Sn}_7\text{O}_{16}$  (and select transition-metal doped series) has been thoroughly studied, particularly through diffraction, Mössbauer spectroscopy and magnetic susceptibility methods<sup>1,2</sup>. While it is understood that multiple exchange mechanisms are competing to produce this exotic magnetism, the exact nature and relative strengths of these competing mechanisms has yet to be explored.

This work presents an investigation of the electronic and magnetic structures of select  $M'M''_3\text{Si}_2\text{Sn}_7\text{O}_{16}$  ( $M' = \text{Fe, Co}$ ;  $M'' = \text{Fe, Mn}$ ) compounds, using hard and soft X-ray spectroscopy coupled with Density Functional Theory calculations. The first step of successfully reproducing these compounds' band structures and ground state magnetic structures was followed by calculation of relative exchange energies, to determine dominant mechanisms electron density, and bonding analyses in an attempt to find the anisotropy responsible for the formation of the canted and frustrated magnetic supercell present in these compounds. These investigations have pointed towards a super-exchange mechanism as a potential driving force alongside direct exchange interactions (Fig.1).

Additional work on replicating/predicting X-ray absorption spectra (NEXAFS) of these materials through computational methods will also be presented.

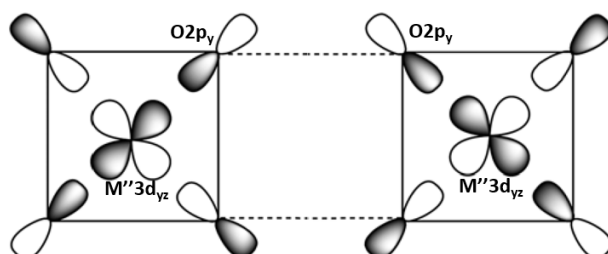


**Figure 1.** Proposed super-exchange pathway which competes with direct exchange mechanisms, taken with modification<sup>3</sup>.

### References

- [1] C. D. Ling, M. C. Allison, S. Schmid, M. Adveev, J. S. Gardner, C. W. Wang, D. H. Ryan, M. Zbiri, T. Söhnel, *Phys. Rev. B*, **96**, 180410 (2017)
- [2] M. C. Allison, M. Avdeev, S. Schmid, S. Liu, T. Söhnel, C. D. Ling, *Dalton Transactions*, **45** (23), pp.9689-9694 (2016)
- [3] J. B. Goodenough, *J. Phys. Chem. Solids*, **6** (2–3): 287. (1958)

## Topological superconductivity from the 2D Hubbard model

Sebastian Wolf and Stephan Rachel

*School of Physics, University of Melbourne, Parkville, VIC 3010, Australia.*

Topological superconductivity constitutes one of the most fascinating and active fields of experimental and theoretical condensed matter research. Topological superconductors host non-Abelian anyons as quasiparticles, either bound to vortex cores or localized at sample edges, which can be combined into topological qubits. Promising candidate materials include doped TIs (e.g.  $\text{Cu}_x\text{Bi}_2\text{Se}_3$ ) or doped Weyl semimetals (e.g.  $\text{MoTe}_2$  and  $\text{WTe}_2$ ) which have in common that strong spin-orbit coupling is present.

In order to understand how the interplay of spin-orbit effects of the band structure with the electron-electron interactions can lead to topological superconductivity, we employ the asymptotically exact weak coupling renormalization group. We study the Rashba-Hubbard model on the square lattice as a paradigm for spin-orbit coupled superconductivity. In the absence of spin-orbit coupling spin-singlet pairing dominates the phase diagram. We find that due to spin-orbit coupling, in most of the phases there is significant mixing of spin-singlet and spin-triplet pairing.

## Photoluminescence of *Coscinodiscus sp.* Diatoms

J. Wu<sup>1</sup>, G. J. Smith<sup>1</sup>, K. G. Ryan<sup>2</sup>, G. V. M. Williams<sup>1</sup>

<sup>1</sup>*School of Chemical and Physical Sciences, Victoria University of Wellington, Wellington, New Zealand*

<sup>2</sup>*School of Biological Sciences, Victoria University of Wellington, Wellington, New Zealand*

Diatoms are a type of algae that have porous, nanostructured cell walls (frustules) composed of amorphous silica. As a result of this frustule structure, diatoms have been found to “capture” light [1]. This has motivated our research to establish how light is captured, how this energy is dissipated as heat, and if the thermal energy generated is sufficient to purify water by vaporization/distillation [2]. This technique has the potential to relieve the crisis of a scarcity of potable water worldwide.

In this presentation, we report the results from photoluminescence and diffuse absorption measurements on *Coscinodiscus sp.* diatoms. It is known that diatoms photoluminesce in the blue-green region of the spectrum. This has been attributed to defects in the silica structure and/or to organic molecules embedded in or on the surface of the frustules [3].

Using diffuse absorption and 3-dimensional photoluminescence (combined emission and excitation) spectroscopies, we find that, some of the luminescence may be consistent with it originating from members of the  $\beta$ -carboline family of organic molecules. This tentative assignment was made on the basis of the luminescence spectral positions under neutral/acidic and alkaline conditions.

### References

- [1]. J. Romann et al., Nature, Scientific Reports, 5, 17403 (2015).
- [2]. J. Fang et al., Journal of Materials Chemistry A, 5(34), 17817-17821 (2017).
- [3]. E. De Tommasi et al., Nature, Scientific Reports, 8, 16285 (2018).

## Development of whitlockite $\beta$ - $\text{Ca}_3(\text{PO}_4)_2$ phosphors

H. Zhou<sup>1,3</sup>, S. Huang<sup>2</sup>, T. Söhnel<sup>1,3</sup>

<sup>1</sup>*School of Chemical Science, University of Auckland, Auckland 1142, New Zealand*

<sup>2</sup>*Department of Chemicals and Materials Engineering, University of Auckland, Auckland 1142, New Zealand*

<sup>3</sup>*MacDiarmid Institute of Advanced Materials and Nanotechnology, Wellington, New Zealand*

LEDs are the new generation of artificial light, the building block of which is based on the inorganic phosphors coated on the surface of P-N junction of the semiconductor. The activator ions of the phosphors “qualitatively” determine the luminescence property, while the crystal host “quantitatively” affects the luminescence spectra. The host structure influences the luminescence feature in three aspects, unspherical distribution of the crystal field splitting the energy states (crystal-field splitting effect), ligand polarizability that red-shifting the spectral feature (nephelauxetic effect) and the phonon interaction from the surrounding crystal (Stoke shift).[1, 2] Phosphate phosphors are attracting large interest of research because of its outstanding thermal stability and good optical property. Whitlockite  $\beta$ - $\text{Ca}_3(\text{PO}_4)_2$  structure have good photoluminescence tunability. By substituting the six-coordinated Ca4 or Ca5 sites with other cations, modification of the  $\beta$ - $\text{Ca}_3(\text{PO}_4)_2$  as phosphors host will improve the phosphors fluorescence. Here, a series of  $\text{Eu}^{2+}$ -doped  $\text{Na,Al-Ca}_3(\text{PO}_4)_2$  phosphors are being studied.

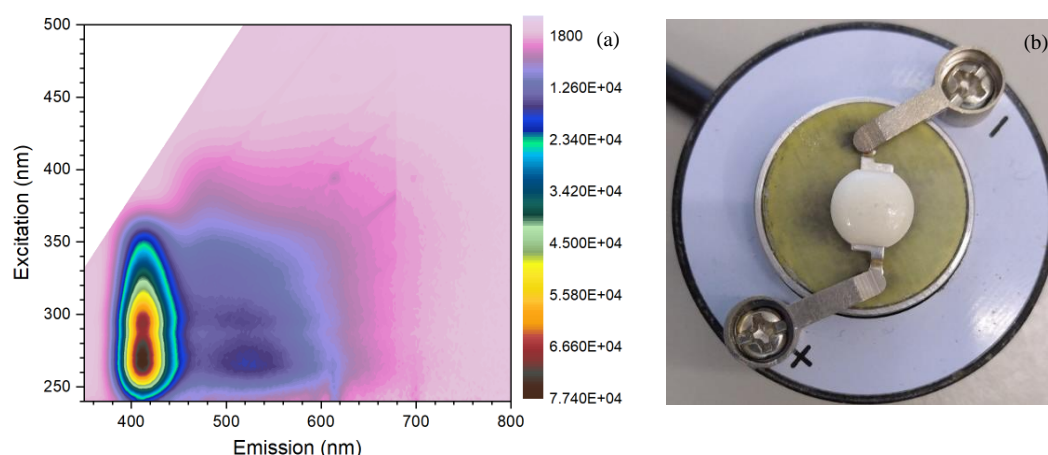


**Fig. 1:** (a) 3D emission spectra of  $\text{Eu}^{2+}$ -doped- $\text{Na,Al Ca}_3(\text{PO}_4)_2$  phosphors. (b) LED assembled by the  $\text{Eu}^{2+}$ -doped- $\text{Na,Al Ca}_3(\text{PO}_4)_2$  phosphors

### References

1. George, N.C., K.A. Denault, and R. Seshadri, *Phosphors for Solid-State White Lighting*. Annual Review of Materials Research, 2013. **43**(1): p. 481-501.
2. Tanner, P.A., Y.Y. Yeung, and L. Ning, *What factors affect the 5D0 energy of  $\text{Eu}^{3+}$ ? An investigation of nephelauxetic effects*. The Journal of Physical Chemistry A, 2013. **117**(13): p. 2771-2781.

# Nonlinear optical response of the $\alpha$ -T<sub>3</sub> model due to the nontrivial topology of the band dispersion

L. Chen<sup>1</sup>, J. Zuber<sup>2</sup>, Z. Ma<sup>3</sup>, C. Zhang<sup>2</sup>

<sup>1</sup> Department of Applied Physics, Beijing University of Civil Engineering and Architecture, Beijing 102616, China

<sup>2</sup> School of Physics, University of Wollongong, New South Wales 2522, Australia and

<sup>3</sup> School of Physics, Peking University, Beijing 100871, China

We study the electronic contribution to the nonlinear optical response of the  $\alpha$ -T<sub>3</sub> model. This model is an interpolation between a graphene ( $\alpha=0$ ) and dice or T<sub>3</sub> ( $\alpha=1$ ) lattice [1]. Using a second-quantised formalism we calculate the first and third order responses for a range of  $\alpha$  and chemical potential values as well as considering a band gap in the first-order case. Conductivity quantisation is observed in the first order, whilst Higher-order Harmonic Generation (HHG) is observed in the third order response with the chemical potential determining which applied field frequencies both quantisation and HHG occur at. We observe a range of experimentally accessible critical fields between  $10^2$ - $10^6$  V/m with dynamics depending on  $\alpha$ ,  $\mu$  and applied field frequency (see Figure 1). Our results suggest an  $\alpha$ -T<sub>3</sub> could be an ideal candidate material for use in tunable terahertz devices.

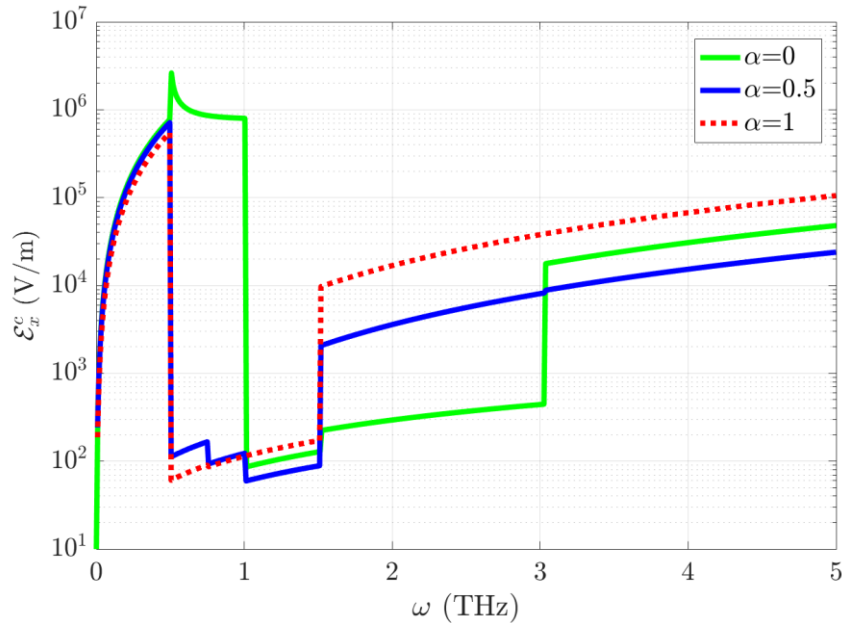


**Fig. 1:** Critical field for  $a=0.142\text{nm}$  (inter-atomic distance),  $\tau_1=\tau_2=3\text{eV}$  (hopping amplitudes between adjacent sites),  $\mu=1\text{meV}$  (chemical potential),  $\varepsilon=0\text{eV}$  (band gap) and  $T=0\text{K}$  (temperature).

## References

[1]. J.P. Carbotte *et al.*, Phys. Rev. B **99**, 115406 (2019).



## Quantum size effects in topological-insulator nanostructures

L. Gioia<sup>1,2</sup>, M. Kotulla<sup>2</sup>, U. Zülicke<sup>2</sup>, M. Governale<sup>2</sup>

<sup>1</sup>*Department of Physics and Astronomy, University of Waterloo, Waterloo, Canada*

<sup>2</sup>*School of Chemical and Physical Sciences and MacDiarmid Institute for Advanced Materials and Nanotechnology, Victoria University of Wellington, Wellington, New Zealand*

The interplay between band inversion and size quantization creates a rich phenomenology of novel electronic properties in nanostructures made from topological insulators. As paradigmatic examples, we have investigated the size dependence of quantized energies and electron-bound-state properties in quantum wells [1], quantum rings [2], and spherical nanoparticles [3]. Analytical results are obtained for the wave functions of the single-electron eigenstates in rings and nanoparticles, allowing us to obtain also analytically the electronic ring-interferometer transmission function and the matrix elements for optical transitions in a nanoparticle. We discuss distinctive confined-topological-insulator quantum-size effects, including oscillations of the band gap as a function of system size [1,3], unconventional Aharonov-Bohm oscillations of the quantum-ring conductance [2], and oscillatory optical-transition amplitudes [3]. See Fig. 1 for an illustration. Our theory can be extended to describe other nanostructures, such as nanowires [4], and also provides a unified perspective on multi-band models for charge carriers in semiconductors and Dirac fermions from elementary-particle physics.

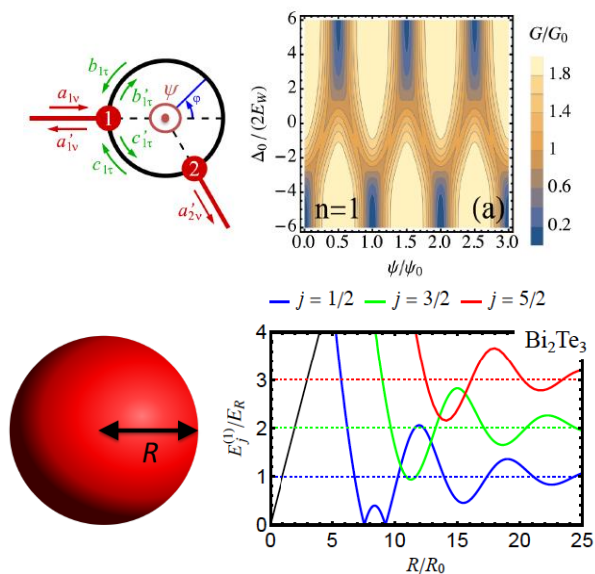


**Fig. 1:** Left: Unconventional Aharonov-Bohm oscillations of the ring conductance  $G$  distinguish the topological regime ( $\Delta_0 < -2E_w$ ) from the normal regime ( $\Delta_0 > -2E_w$ ) [2]. Right: Oscillatory nanoparticle-radius dependence of the lowest topological bound-state energy levels labeled by total-angular-momentum quantum number  $j$  [3].

### References

- [1] M. Kotulla, U. Zülicke, New J. Phys. **19**, 073025 (2017).
- [2] L. Gioia, U. Zülicke, M. Governale, R. Winkler, Phys. Rev. B **97**, 205421 (2018).
- [3] L. Gioia, M. G. Christie, U. Zülicke, M. Governale, A. J. Sneyd, Phys. Rev. B **100**, 205417 (2019).
- [4] B. Bhandari, M. Governale, F. Taddei, U. Zülicke, K.-I. Imura, in preparation.

## Participant List

<b>Name</b>	<b>Affiliation</b>
Andrew Chan	University of Auckland, New Zealand
Aydin Cem Keser	University of NSW, Australia
Ben Mallett	University of Auckland, New Zealand
Chris Ling	The University of Sydney, Australia
Clemens Ulrich	University of NSW, Australia
Daisuke Iizasa	Tohoku University, Japan
Dana Goodacre	University of Auckland, New Zealand
Daniel Clyde	University of Auckland, New Zealand
Daniel Gregg	ANSTO, Australia
Daniel Teis	Scitek
David Cavanagh	University of Otago, New Zealand
Dimi Culcer	University of NSW, Australia
Eva Anton	Victoria University of Wellington, New Zealand
Gabriele Motta	Queensland University of Technology, Australia
Garry McIntyre	ANSTO, Australia
Giulia Novelli	ANSTO, Australia
Glen Stewart	University of NSW Canberra, Australia
Henri Menke	University of Otago, New Zealand
Henry Nourse	University of Queensland, Australia
Holger Fehske	University Greifswald, Germany
Huihua Zhou	University of Auckland, New Zealand
Jack Zuber	University of Wollongong, Australia
Jackson Allen	University of Wollongong, Australia
Jackson Miller	University of Auckland, New Zealand
James Carter	Nano Vacuum
James Gilmour	Victoria University of Wellington, New Zealand
James Storey	Victoria University of Wellington, New Zealand
Janez Bonca	J. Stefan Institute, Slovenia
Jeffrey Tallon	Victoria University of Wellington, New Zealand
Jiazun Wu	Victoria University of Wellington, New Zealand
Joe Trodahl	Victoria University of Wellington, New Zealand
John Cashion	Monash University, Australia
Joseph Vella	University of Auckland, New Zealand
Julie Karel	Monash University, Australia
Kira Pitman	Victoria University of Wellington, New Zealand
Kyeongsoon Park	Sejong University, Korea
Marc A. Gali Labarias	CSIRO, Australia

Mark Smith	University of Auckland, New Zealand
Martin Kaupp	Technical University of Berlin, Germany
Martin Spasovski	University of Auckland, New Zealand
Mathew Denys	University of Otago, New Zealand
Matthew O'Brien	University of NSW, Australia
Michael Kammermeier	Victoria University of Wellington, New Zealand
Michael Nielsen	University of NSW, Australia
Mikhail Kostylev	University of Western Australia, Australia
Narendirakumar Narayanan	Australian National University, Australia
Nazli Rad	Scitek
Oleg Sushkov	University of NSW, Australia
Oleg Tretiakov	University of NSW, Australia
Park Choon Mahn	Dong-A University, Korea
Pascal Henkel	Justus Liebig University Giessen, Germany
Peter A Jacobson	University of Queensland, Australia
Peter Prelovsek	J. Stefan Institute, Slovenia
Peter Schwerdtfeger	Massey University, New Zealand
Philip Brydon	University of Otago, New Zealand
Ridwone Hossain	University of Wollongong, Australia
Roger Lewis	University of Wollongong, Australia
Roman Rausch	Kyoto University, Japan
Rosanna Rov	University of Auckland, New Zealand
Ruth Knibbe	University of Queensland, Australia
Ryan Silk	University of Auckland, New Zealand
Sadamichi Maekawa	RIKEN, Japan
Samuel Yick	University of NSW, Australia
Sebastian Wolf	University of Melbourne, Australia
Simon Granville	Victoria University of Wellington, New Zealand
Sneh Patel	University of Auckland, New Zealand
Stephan Rachel	University of Melbourne, Australia
Susant Kumar Acharya	University of Canterbury, New Zealand
Taka Kaneko	Ezzi Vision
Tane Butler	Victoria University of Wellington, New Zealand
Tehreema Nawaaz	Victoria University of Wellington, New Zealand
Thomas Sanders	University of Wollongong, Australia
Tilo Söhnel	University of Auckland, New Zealand
Timothy Daniel Christopher	University of Auckland, New Zealand
Trevor Finlayson	University of Melbourne, Australia
Ulrich Zuelicke	Victoria University of Wellington, New Zealand
Vedran Jovic	GNS, New Zealand
Vishakya Jayalatharachchi	Queensland University of Technology, Australia
Wayne Hutchison	University of NSW Canberra, Australia

William Holmes-Hewett  
Wojciech Grochala  
Zeb Krix

Victoria University of Wellington, New Zealand  
University of Warsaw, Poland  
University of NSW, Australia